



TECHNISCHE
UNIVERSITÄT
WIEN

Master Thesis

Two-Photon Structured Hydrogels based on Hyaluronic Acid for Applications in Tissue Engineering

Performed at the Institute of Applied Synthetic Chemistry
Technische Universität Wien



Under the supervision of

Univ.Prof. Dipl.-Ing. Dr.techn. Robert Liska

and

Projektass. Dipl.-Ing. Dr.techn. Stefan Baudis

by

Elise Zerobin, BSc

Witthauergasse 19/12, 1180 Wien

Vienna, March 13, 2017



*"For a long time, I have considered even the craziest ideas about atom nucleus...
and suddenly I discovered the truth"*

Maria Göppert-Mayer¹

1906-1972

Danksagung

An erster Stelle möchte ich mich bei dir bedanken, Robert, dass du mir die Möglichkeit gegeben hast, meine Diplomarbeit in deiner Arbeitsgruppe durchzuführen. Durch deine fachliche Kompetenz und Bemühen, immer ein offenes Ohr für deine Mitarbeiter zu haben, machst du diese Arbeitsgruppe zu etwas ganz Besonderem. Dank deiner Förderung habe ich einen sehr tiefen Einblick in die Welt des tissue engineering bekommen und mein bereits bestehendes Interesse in den Gebieten der Medizin und Chemie vertiefen dürfen.

Außerdem bedanke ich mich bei dir, Stefan für die kompetente Betreuung dieser Arbeit. Du hast mit deinen produktiven Denkanstößen und motivierenden Worten wertvollen Beitrag zu dieser wissenschaftlichen Arbeit geleistet.

Ein herzliches Dankeschön gebührt auch demjenigen, der mich überhaupt erst in die Welt der Polymerchemie eingeführt hat. Dir, Christian bin ich sehr dankbar, dass du bereits während meiner Bachelorarbeit, mein Bestreben, ein Teil dieses Instituts zu bleiben, forciert hast. Anno dazumal wurde der Grundstein für unsere, bis heute bestehende Tarockrunde gelegt. Für zahlreiche und abwechslungsreiche Abende bedanke ich mich auch bei euch, Paul und Robert. Ihr habt mir das Gefühl gegeben, in den eigenen vier Wänden in Oberösterreich den Klinger Franz zu rufen.

Des Weiteren ein herzliches Dankeschön an das Triumph4Rat[®]- Hofi und Schnöll, die in dieser intensiven Lebensphase einen großen Platz in meinem Herzen eingenommen haben. Auf eure Ehrlichkeit kann man sich immer verlassen.

Danke auch an das gesamte Team des FBMC. Ich bin froh, Teil einer so abwechslungsreichen und einzigartigen Arbeitsgruppe zu sein. Vor allem bedanken möchte ich mich bei Daniel B., für deine höchst-interessanten, medizinischen Geschichten, bei Gernot, für deine ehrliche Meinung, bei Hansi, für deine unheimliche Hilfsbereitschaft, bei Markus L., dafür, dass ich den ein oder anderen Lachkrampf durchstehen musste, bei Markus K., für deine bodenständigen Ratschläge, bei Mia, für deine moralische Unterstützung, bei Konzi, für die vielen interessanten Diskussionen und natürlich bei Yazgan, mein Licht am Ende des Tunnels.

Im speziellen möchte ich auch meinen Brüdern, Martin und Flo danken, die mir schon mein gesamtes Leben lang eine unheimlich große Stütze sind. Auch Antonia und Lisi möchte ich für ihre Unterstützung und Herzlichkeit danken. Ihr seid die besten Familienmitglieder, die man sich wünschen kann.

Zuletzt gebührt ein enormer Dank meinen Eltern, die mir immer alle Freiheiten und jede erdenkliche Möglichkeit gegeben haben, meine Träume zu verwirklichen. Danke dafür, dass ihr mir dieses Studium ermöglicht habt. Euch widme ich diese Arbeit.

Abstract

Hydrogels are an important class of biomaterials, widely used in tissue engineering. With these hydrogels, scientists aim to replace injured or removed functional tissue, because these materials show physicochemical similarity to extracellular matrix (ECM). Their permeability for nutrients, as well as their high water content are accounting for their application in soft tissue regeneration. Cells require amongst other factors, defined structural properties of hydrogels, to properly attach and proliferate within a matrix. Consequently, 3D fabrication of scaffolds can be realized by Additive Manufacturing Techniques, such as Two-Photon Polymerization (2PP). Macromolecules with natural origin, having photopolymerizable groups (precursors) can be fabricated via 2PP with high spatial resolution. The applied near-infrared laser offers high transparency towards biological tissues, being able to realize high penetration depth and little photo-damage of native matrices. Despite research has introduced a variety of different state of the art precursors [meth(acrylates)], these are potentially irritant and cytotoxic, when used as scaffolds to mimic ECM.

Within this thesis, recently developed photopolymerizable precursors, based on hyaluronic acid (HA) were synthesized via an enzymatic transesterification reaction using divinyl adipate. Compared to their cytotoxic counterparts [meth(acrylates)], vinyl ester modified HA precursors (HAVE) show promising biocompatibility. The introduction of thiols into the precursor formulation enables effective crosslinking under high conversion using the concept of thiol-ene chemistry. The slow homopolymerization rate of HAVE can thereby be overcome and multifunctional thiols can be used to study their effect on hydrogel matrices. The contribution of HAVE macromers on viscoelastic properties of hydrogels was investigated via photorheology. Based on the characteristics of the storage modulus, the effect of macromer size, degree of substitution, macromer content and type of thiol component on the crosslinking density, as well as on the reactivity of the formulation was investigated. Synthesized HAVE macromers, with different chain length and number of polymerizable groups on the HA backbone allow the fabrication of hydrogels with tailored mechanical properties. Additionally, a new approach was studied, to use HAVE in combination with collagen as interpenetrating network. Finally, cells were encapsulated via 2PP in the presence of HAVE macromers and their survival was studied.

Kurzfassung

Hydrogele spielen eine große Rolle im Bereich der Biomaterialien, wobei diese bereits weitgehend für die Geweberekonstruktion (tissue engineering) genutzt werden. Beschädigtes oder entferntes Gewebe kann mithilfe dieser Hydrogele ersetzt werden, da diese Materialien ähnliche physikochemische Eigenschaften zu extrazellulärer Matrix zeigen. Wegen ihrer Durchlässigkeit für Nährstoffe und ihrem hohen Wassergehalt werden sie besonders oft zur Weichgeweberegeneration verwendet. Damit Zelladhäsion und -proliferation innerhalb einer Matrix entsprechend stattfinden kann, sind nebst anderen Faktoren definierte strukturelle Eigenschaften dieser Hydrogele notwendig. Über generative Fertigungsverfahren, vor allem Zwei-Photonen-Polymerisation (2PP), können Gewebestrukturen mit diesen Anforderungen hergestellt werden. 2PP erlaubt im Speziellen die hochauflösende Fertigung von photopolymerisierbaren Makromolekülen (Präkursoren) basierend auf natürlichen Polymeren. Aufgrund der hohen Transparenz von biologischem Gewebe bezüglich des verwendeten gepulsten Nah-Infrarot-Lasers können hohe Eindringtiefen bei gleichzeitig geringem Schaden der umgebenden Matrix erreicht werden. Obwohl bereits eine Vielzahl an unterschiedlichen Präkursoren (z.B. Meth(acrylate)) entwickelt wurden, weisen diese gewisse Nachteile wie Zytotoxizität innerhalb der extrazellulären Matrix auf.

Innerhalb dieser Arbeit wurden neu entwickelte Präkursoren basierend auf Hyaluronsäure (HA) über eine enzymatische Umesterung mit Divinyladipat synthetisiert. HA-Präkursoren, die mit Vinylester modifiziert wurden (HAVE), weisen verglichen mit Meth(acrylaten) eine höhere Biokompatibilität auf. Eine effektive Vernetzung von HAVE kann durch die Zugabe von Thiolen zu der Präkursorformulierung erreicht werden (Thiol-En-Chemie). Die langsame Homopolymerisation der HAVE wird somit über die Einführung von multifunktionellen Thiolen überwunden. Unterschiedliche Thiole und deren Effekt auf die Hydrogelmatrix konnten somit untersucht werden. Mittels photorheologischer Studien wurde außerdem der Beitrag von HAVE-Makromolekülen auf die viskoelastischen Eigenschaften der Hydrogele untersucht. Anhand des Verlaufes des Speichermoduls wurde der Einfluss von Makromergröße, Substitutionsgrad, Makromergehalt und Art des Thiols auf die Vernetzungsdichte und die Reaktivität der Formulierung untersucht. Über die Synthese von HAVE ist es möglich, die mechanischen Eigenschaften von Hydrogelen anhand ihrer Kettenlänge und Nummer der polymerisierbaren Gruppen anzupassen. Zusätzlich wurde ein neues Konzept vorgestellt, bei dem HAVE in Kombination mit Kollagen als interpenetrierendes Netzwerk verwendet wurde. Außerdem wurden mit 2PP Zellen in eine HAVE-Hydrogelmatrix eingebettet und deren Überleben untersucht.

Table of Contents

Introduction		1			
Objective		30			
General Part		32			
Experimental Part		82			
Summary		101			
Materials and Methods		105			
Abbreviations		108			
Appendix		110			
References		139			
			Gen.	Exp.	App.
1	State of the Art	32			
2	Synthesis	35	82		
2.1	Preparation of Low-Molecular Weight HA	35	83		
2.2	Synthesis of Tetrabutylammonium Salt of HA	40	85		
2.3	Synthesis of HA Vinyl Ester	43	87	111	
3	Characterization of Hydrogel formulations by Photorheology	46	91		
3.1	Storage Stability	51	92	112	
3.2	The Effect of Thiol Component	54	93	113	
3.3	Variation of Parameters	58	94		
3.3.1	The Effect of Macromer Content	58	94	126	
3.3.2	The Effect of Degree of Substitution	61	95		
3.3.3	The Effect of Macromer Chain Length	63	96	128	

3.4	Hydrogel Network considering Vinyl-Groups per Macromer Chain	66	97	130
3.5	Collagen as additional Matrix Compound	69	98	139
3.5.1	Preliminary Tests	71	98	
3.5.2	The Influence of Collagen on HAVE hydrogels	74	99	
4	Proof of Concept	79	100	

Introduction

1 Tissue Engineering

Since Vacanti and Langer² founded the field of Tissue Engineering (TE) in the early 1990s, the know-how in this sector has steadily improved. TE is a discipline with great potential, providing treatment for injured or malfunctioning tissue. Tissues in living organisms are very complex systems because they provide specific functions and ensure survival. The functions of these tissues (e.g. skin, blood vessels, cartilage, livers and bone) need to be mimicked as good as possible, where the fundamental principles of TE need to be considered. They are based on scaffolds, cells and signals, which are displayed in the triad shown in Figure 1.

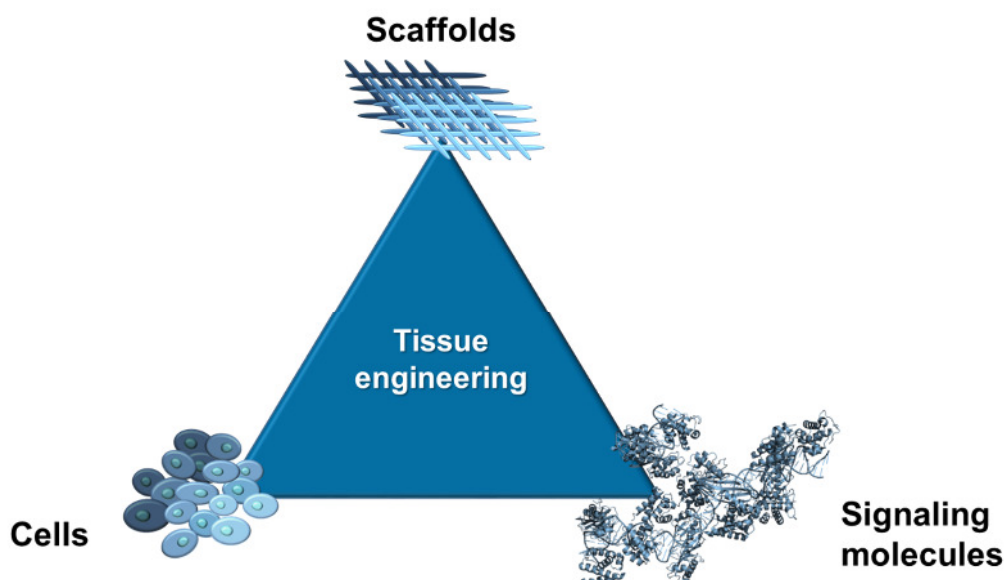


Figure 1: Basic principles of tissue engineering

Scaffolds primarily provide a 3D network for cells to grow and proliferate. Furthermore, this substrate serves as a delivering system for **signaling molecules** like cytokines and growth factors. Due to their porous structure and mechanical properties, scaffolds are a key component for the development of functional tissues. Besides scaffolds and signaling molecules, **cells** take another key role in TE. With a proper matrix for cells to migrate and proliferate, cell survival can be supported and will facilitate the development of biological functions. Close cooperation among clinicians, chemists, material engineers and biologists is required to realize the replacement of functional tissue by connecting the principles of above-named engineering disciplines with life

sciences. Tissue in general can be engineered by combining cells with biocompatible matrices to obtain tissues similar to the original material. Figure 2 shows examples of synthetic polymers, already extensively used in TE, including polyethylene glycol (PEG), polyvinylalcohol (PVA), polyurethane (PU), polyhydroxyethyl methacrylate (PHEMA), polyvinylpyrrolidone (PVP), polyacrylic acid (PAA), polyacrylamide (PAAm), polyimide (PIM) and polyoxazoline (POx).^{3,4}

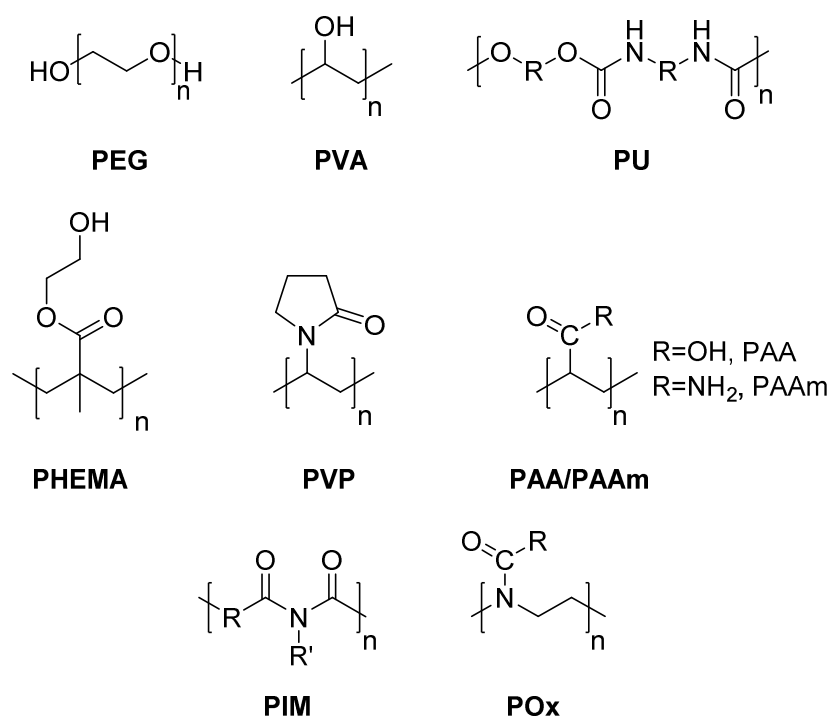


Figure 2: Examples of synthetic polymers used in the field of tissue engineering

Besides synthetic polymers, naturally occurring polymers, such as hyaluronic acid (HA), chondroitin sulfate, collagen, gelatin, alginate, agar, cellulose, chitosan, elastin, or fibrinogen were already modified for being used in the field of TE.⁵ Some examples of natural polysaccharides are depicted in Figure 3. Both, synthetic and naturally derived polymers need to meet biological requirements given by cells to ensure their survival. As some of these polysaccharides, especially HA and collagen, are naturally present in the extracellular matrix (ECM) of the human body (see Figure 4), they are in the focus of research. The ECM is a 3D polymer network consisting of fiber-forming proteins such as collagen, proteoglycans, elastin, fibronectin, laminin and glycoproteins.⁶ All tissues and organs in the human body contain ECM, forming matrices with varying degree of stiffness. Particularly, the structure and composition of macromolecules depend on the localization and function of the scaffold inside the body and differ from tissue to tissue.

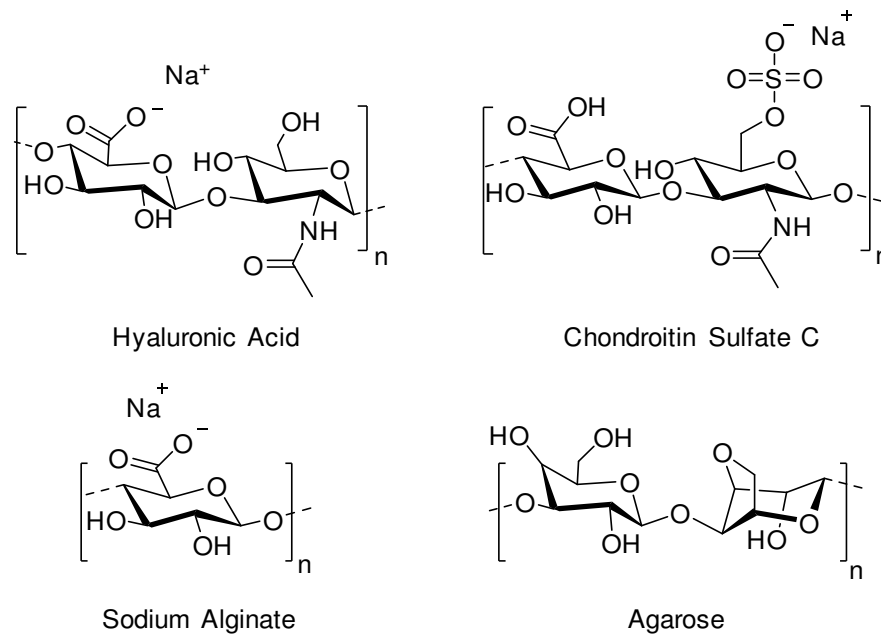


Figure 3: Examples of polysaccharide units, which can be used for tissue engineering

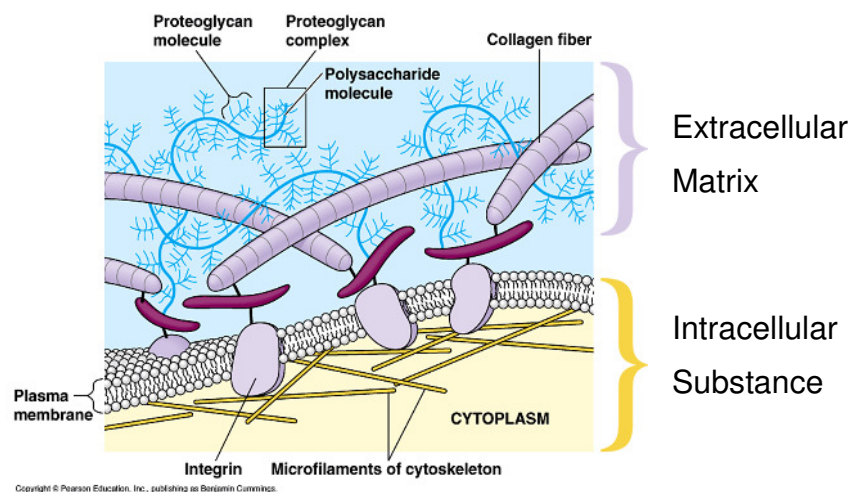


Figure 4: Schematic structure of ECM ⁷

Molecules of the ECM, like proteoglycans, are highly acidic and hydrated molecules, which are associated with other proteins to construct molecular interconnected aggregations, building a highly complex 3D network. As the cells are used to natural polymers of the ECM, these polymers are in focus of research to develop artificial ECM components. Compared to synthetic polymers, endogen matrix components have the advantage, that immunological response of the body is minimized, when natural polymers are used as substrates for TE. As this discipline, also focuses on the recovery of injured tissue, a minimal activation of the immune system is desirable for a complication-less healing progress. Proper functions of tissue *in vivo* are amongst others guided by the biomechanical properties of scaffolds. Especially particular

applications in the field of TE require high mechanical performance of artificial tissues. When using natural polymers for TE, one drawback can be their low mechanical strength, resulting in difficulties in handling.⁸ Hence, most of them are too soft and brittle to be used on their own as materials for TE. For this reason, material properties need to be engineered, depending on the demands of replaced tissue.

For this reason, the interconnection of molecules which form the 3D network can be changed. These connections are called crosslinks and are formed during the polymerization process of network building blocks. Functional groups of di- or multi-functional monomers react with each other to form these continuous 3D structures. By adjusting the polymerization mechanism, it is possible to adjust the network structure and their mechanical properties like proposed in literature.⁹ Not only the reaction mechanism but also the crosslinking density can determine the characteristics of a polymer network. The crosslinking density is therefore a versatile tool to determine the network architecture by the number of functional groups on the monomer. Depending on these factors the mechanics of a polymer network can be adjusted and chemically or physically crosslinked networks can be formed. These networks can be used in TE to build scaffolds with desired mechanical and chemical properties.

2 Hydrogels for Tissue Engineering

Hydrogels are crosslinked 3D networks which are able to absorb large amount of water, demonstrating effective cell culture platforms.^{10,11,12} Hence these hydrophilic materials do not dissolve, when immersed in water, hydrogels keep their 3D structure providing an optimal scaffold matrix forming a new type of materials, called biomaterials. As they are in direct contact with tissue, they should fulfill following requirements when used in TE.¹³

- Biodegradable and bioactive
- Structural similarity to desired type of tissue
- Provide temporary mechanical support that allows tissue growth
- Supply of suitable environment for the regulation of cell behavior (e.g. adhesion, proliferation, migration, differentiation)

The human body consists of different types of tissues depending on the localization inside the body. Mechanical properties of biomaterials range from stiff matrices, like bones and relatively soft materials, like the vitreous body of the eye. This thesis focuses on soft tissues and therefore deals with hydrogels as potential tissue regeneration material. Hence, hydrogels can provide cells a highly hydrated tissue-like environment, they have been used already extensively as scaffolds for TE.^{5,14,15} Alike hydrogels, tissue itself contains high amount of water. Accordingly, they can imitate the function of extracellular matrix by keeping the ability for nutrients to diffuse between tissue layers. The high water-content of the hydrogels is the consequence of the presence of multiple hydrophilic moieties inside the monomers. Carboxyl-, amide-, amino- and hydroxyl groups ensure the hydrophilicity of the polymer. Hydrogels can be classified into the origin of their building blocks. Either synthetic or natural monomers can be used for the formation of hydrogels. As previously discussed, natural polymers are especially interesting for hydrogel formation. Consequently, HA is described in detail in the following chapter.

3 Hyaluronic Acid and modifications thereof

With a chain length of several thousand repeating units, HA is a high molecular weight glycosaminoglycane (GAG). Together with covalently linked proteins, these GAGs assemble the so called proteoglycans, representing one of the two major classes of ECM macromolecules. The second class are fibrous proteins, having structural and adhesive function.¹⁶ GAGs and proteoglycans in a broader sense, fill the majority of the ECM¹⁷ and the content of HA within the ECM differs from tissue to tissue. Still the rather high concentration of HA in soft tissue leads to the formation of viscoelastic solutions in tissue. The high water-binding capacity of the polymer is a reason, why HA acts as a lubricant and shock absorber in joints. GAGs are carbohydrate chains, consisting of repeating disaccharide units. In the case of HA, D-glucuronic acid is β -1,4 linked with D-N-acetylglucosamine (Figure 5).

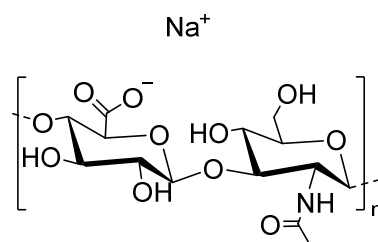


Figure 5: Structure of hyaluronic acid

In solution these long polymer chains can build various different conformations due to the presence of hydrogen bridges.¹⁸ Studies showed that the hydrogen bonds, especially between the amide and the carboxylate group are responsible for the type of secondary structure of HA chains in solution.¹⁹ These hydrogen bridges can vary depending on the glycosidic angle between the D-glucuronic acid- and D-N-acetylglucosamine units. These forces imply a physically bonded network structure and contribute to mechanical properties of soft tissue. Several advantages arise, when using natural polymers, especially HA as a component for biomaterials for TE. As an endogenic compound HA induces less inflammatory response in the human body, than exogenic substances.²⁰ Furthermore, HA is easy to isolate and has a variety of modification possibilities. In the medical sector HA has been used in eye surgeries since 1976 and the clinical testing for the improvement of the cure of arthritic joints is steadily rising.²¹ Industrially HA can be obtained from two different production processes. First by the extraction of animal tissues and second via bacterial fermentation. Animal tissues, such as rooster combs and bovine synovial fluid can be

used for the extraction of HA because it is naturally produced by the HA-synthase in living organisms. In contrast to the extraction of HA from tissue directly, HA can also be received by bacterial expression in *Streptococcus* strains with high molecular weight and high purity.

After isolation, HA is not yet applicable for biomedical applications. The polymer itself shows relatively short half-life *in vivo*,²² which leads to degradation of HA in living organisms. Consequently, viscoelastic properties are lost, which are crucial to ensure e.g. lubrication for joints, if HA is used as a replacement for the intervertebral disc. This gives motivation for the modification of the polysaccharide units of HA. By modifying the backbone, the mechanical properties can be improved with the goal to maintain tissues functions. Recent reviews²³⁻²⁵ give an overview of the common modifications of the HA backbone developed for biomedical applications. For human and veterinary patients, a wide range of materials based on HA have evolved already, for example intra-articular viscosupplements, dermal fillers, corneal- and dermal wound repair.

HA in particular shows very soft and flexible consistence and structural properties sometimes need to be adjusted depending on the demands of TE. Therefore, the introduction of functional groups by modification of HA, can be used to form crosslinked hydrogels, to determine physical properties of HA networks. For example articular joints, exposed to large stresses need to show high mechanical strength.²⁶ These external impacts also lead to plastic deformation, due to the viscoelastic character of crosslinked hydrogels. In the end, a compromise must be found. Besides different crosslinking methods, the crosslinking density of a network also defines hydrogel properties. By directing the mesh size of a matrix, tissue regeneration can be improved because the crosslinking density plays an important role in cell differentiation.²⁷ Figure 6 gives an overview on how HA modification leads to HA-macromers, which can be further crosslinked, either physically or chemically, to form HA hydrogel networks.¹⁵

As HA on its own only shows few crosslinking possibilities, the backbone must be modified beforehand. Figure 6 shows, how chemical modification results in so called HA macromers (precursors), used for further crosslinking. The present chapter focuses on hydrogels and the formation thereof, by different crosslinking methods. According to the type of interaction between the chains, either physical or chemical, HA hydrogels can be roughly divided into two categories. Chemical Hydrogels are irreversibly covalently crosslinked networks, whereas physical hydrogels are reversible networks,

held together by molecular forces. An overview of HA crosslinking methods is given in Figure 7.

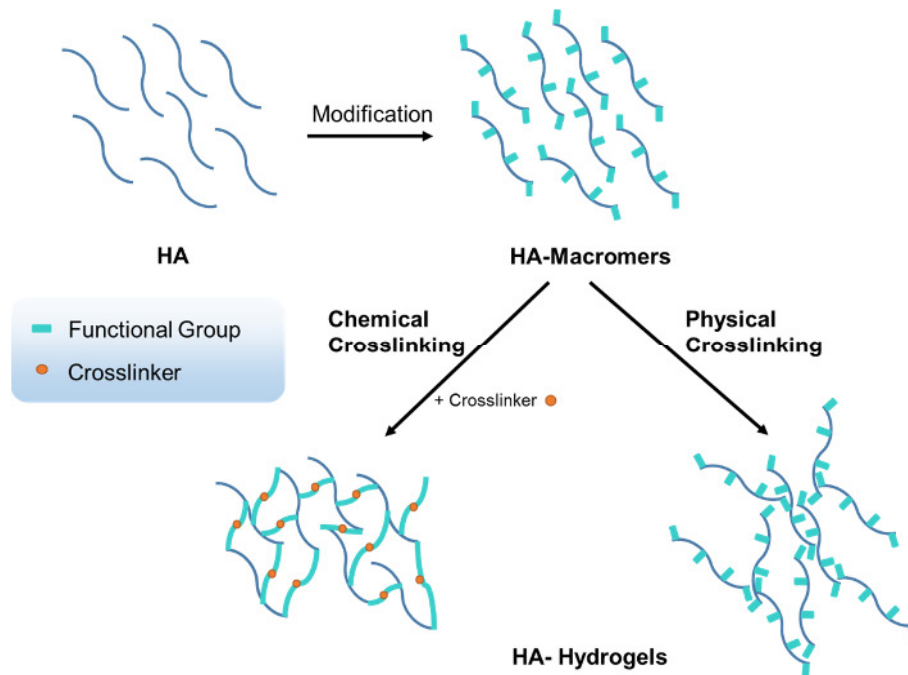


Figure 6: Modification of HA and subsequent crosslinking possibilities for the formation of hydrogels

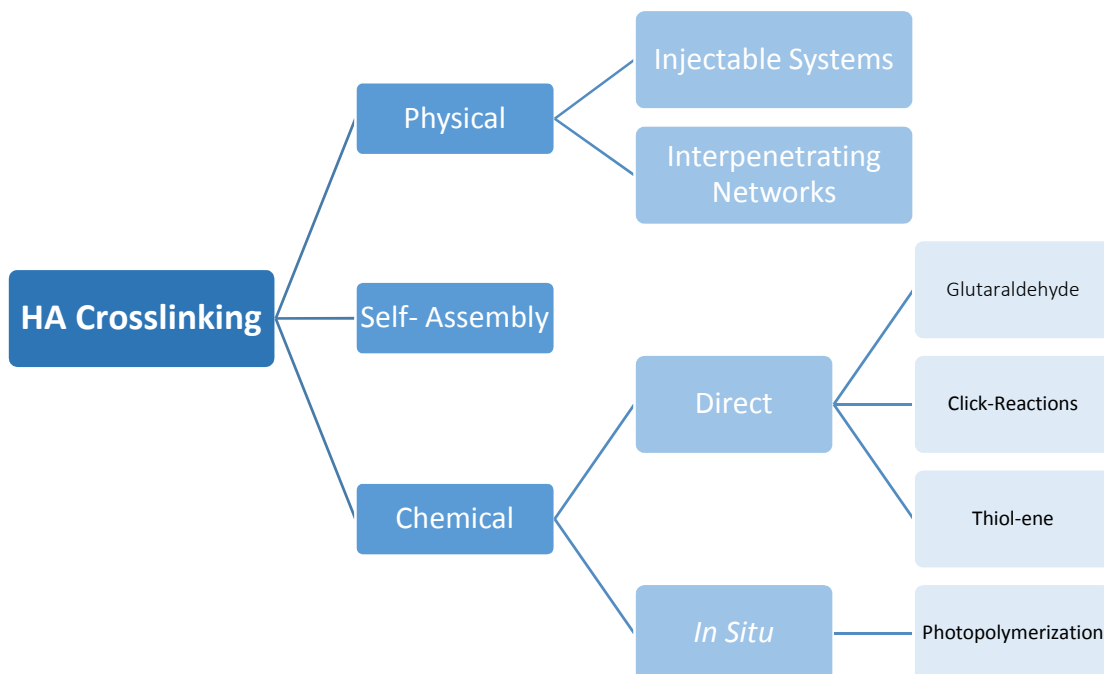


Figure 7: Crosslinking methods for HA hydrogels

Functional groups on the HA backbone, which are accessible for the modification of HA are the primary hydroxyl- and the carboxylic group of the sugar moieties. Following section gives an overview on some modifications of HA and their crosslinking.

3.1 Physical crosslinking

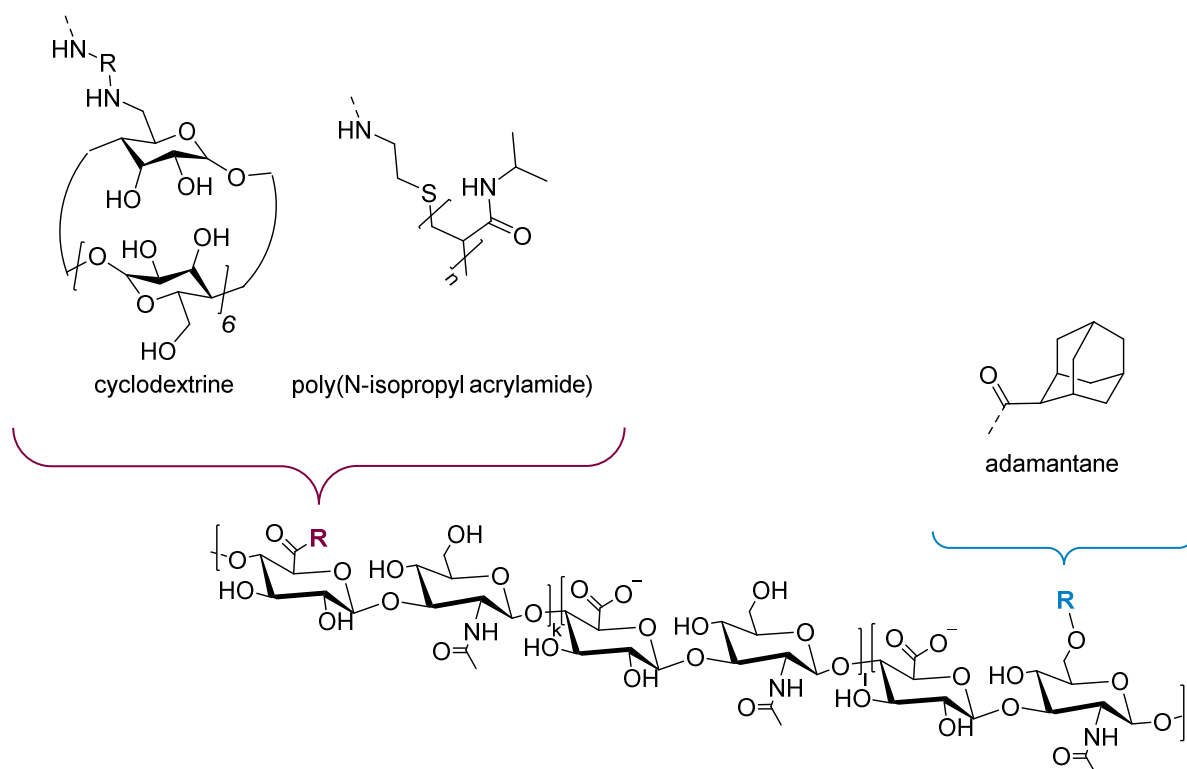


Figure 8: Modification possibilities of HA for physical crosslinking methods

Following section deals with the possibilities to crosslink HA via physical interactions between polymer chains. These physical crosslinks may not be permanent, but are sufficient to form hydrogels, insoluble in aqueous media, where the persistent interactions between the chains avoid dissolution of the physical network. For example amphiphilic derivatives were already investigated, by grafting hydrophobic chains onto HA backbones.^{28,29} The associated polymers form a gel and show strong elastic behaviour compared to initial viscous behaviour of HA solutions. Compared to chemical crosslinks, physical crosslinks can be reversible and do not require additional matrix compounds, like crosslinking catalysts. Furthermore, physical crosslinking does not result in the production of heat during the crosslinking process, which could damage incorporated cells and surrounding tissue.³⁰

3.1.1 Injectable Hydrogels

In recent years hydrogels have already been used as materials for drug delivery systems.³¹ Hydrogels, which are rapidly crosslinking *in situ* by chemical reaction or through physical interaction at the site of interest are especially convenient. These systems are known under the term of “injectable hydrogels” because the hydrogel precursor solution is loaded in a syringe and injected at the target location (see Figure 9). At this location, the hydrogel is formed as consequence to an external stimulus, such as temperature, pH or ionic strength.

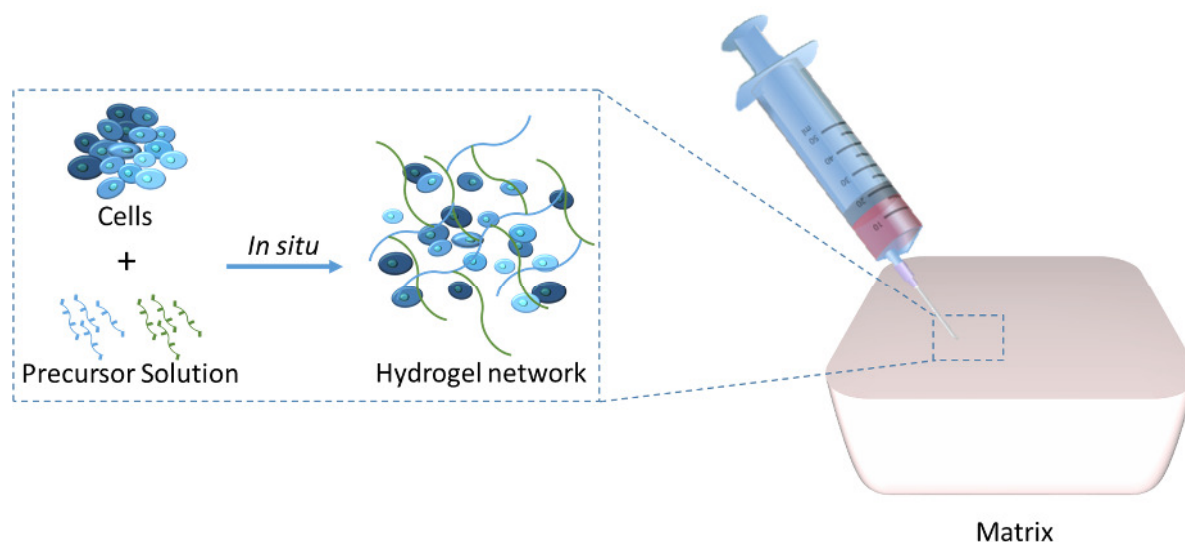


Figure 9: Scheme of *in situ* network formation of injectable hydrogels

These hydrogels can overcome the obstacle, when therapeutics show low solubility in aqueous solutions. By using injectable delivery systems, higher amounts of drug reach the target location and overall less material is needed for the treatment.³⁰ One specific example of injectable hydrogels for example are thermo-responsive hydrogels, studied by Lee et al.³² They used a copolymer based on HA and poly(N-isopropyl acrylamide) (PNIPAAm) and investigated the characteristic behavior in aqueous solutions. It was found, that below the lower critical solution temperature (LCST), PNIPAAm chains hydrate and form expanded structures. These expanded shapes help to dissolve the copolymer below 32 °C. Above the LCST, PNIPAAm chains change to compact conformation, due to reduced H-bridges inside the sidechains. Due to this effect, self-assembling of macromolecules was examined, by measuring an increase of viscosity. Furthermore, it was shown, that long chain PNIPAAm grafted HA showed higher increase of viscosity than short chain copolymer samples. With this system, physical crosslinking can be used to solidify hydrogels, right after their implantation into the

dorsal surface of a rabbit. Injectable thermo-responsive polymers with defined drug release kinetics were developed by this technique.

3.1.2 Interpenetrating Networks

Another type of physically crosslinked hydrogels are based on Interpenetrating Networks (IPNs). IPNs in general consist of two polymers, each of them in network form, whereas the two polymers are usually crosslinked in the presence of each other.³³ Examples are the crosslinking of PVA in the presence of unmodified HA.³⁴ Ionic bonds between the two types of polymers lead to a tightly bonded hydrogel structure under certain conditions. Researchers found a correlation between pH, dissociation of ionic bonds and swelling ratio of the IPN. Also HEMA-modified dextran was polymerized in presence of HA to produce IPNs as biomaterials for bioprinting.³⁵

3.2 Self-Assembly

Self-assembled macromolecules can be classified in-between physically and chemically crosslinked hydrogels. For instance host-guest systems such as β -cyclodextrin (host) and adamantane (guest) were recently introduced, to produce stimuli-responsive hydrogels by so-called “dual crosslinking” (see Figure 10).³⁶ First a physical assembly of pendant groups is performed *ex-vivo*. This leads to gels with thixotropic properties, emerging shear-thinning properties for the system. This means, viscosity is decreased significantly after application of shear forces (e.g. injection by a syringe). At the end of the needle, the hydrogel is reformed immediately. Additionally, Rodell et. al performed a secondary covalent crosslinking at the place of injection. For the self-assembly, HA was either modified by amidation to produce host molecules or by esterification to lead to guest molecules. Due to its hydrophobic inner core, β -cyclodextrin was used as a host, which surrounds the guest molecule (adamantane) and therefore increases solubility of the drug to be delivered.

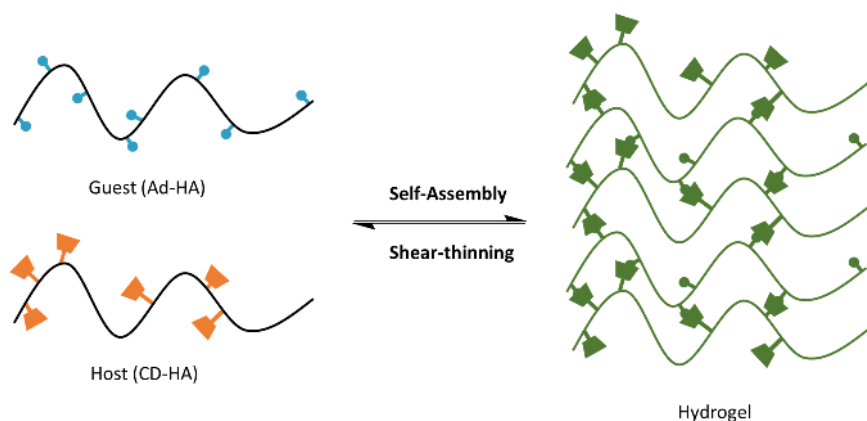


Figure 10: Network formation by using Adamantane- (Ad-HA) and β -cyclodextrin (CD-HA) modified HA³⁶

Based on the degree of modification, material concentration and the ratio of host-to-guest moieties, hydrogel properties can be designed. By using self-assembly and afterwards covalent crosslinking of materials inherently dynamic networks with shear-thinning behavior can be produced. The combination of physical and covalent crosslinking demonstrates a promising method to produce advanced drug delivery systems with unique properties for medical applications, such as soft tissue reconstruction.

Since physical or self-assembled hydrogels are held together by molecular entanglements and/or ionic-, H-bonding or hydrophobic forces, these types of gels are rarely homogeneous. Clusters and domains, between e.g. hydrophobic- associated domains can create inhomogenities. These can be circumvented by the chemical covalent crosslinking of macromers which is described in following section.

3.3 Chemical Crosslinking

Physical bonding can sometimes show certain disadvantages, for example some hydrogels lose initial mechanical strength or dissipate when exposed to external stimuli, like physiological buffer.³⁷ By using chemical crosslinks, irreversible formed hydrogels can be produced and dissipation of the gel can be avoided. Chemical crosslinking of HA is extensively reported in literature³⁸ and includes crosslinking via carbodiimides, di-epoxides, hydrazides and divinyl sulfones. Figure 11 shows a few examples for possible modifications of HA used for chemical crosslinking. An extensive overview on most reported HA macromers are depicted in literature.^{39,40}

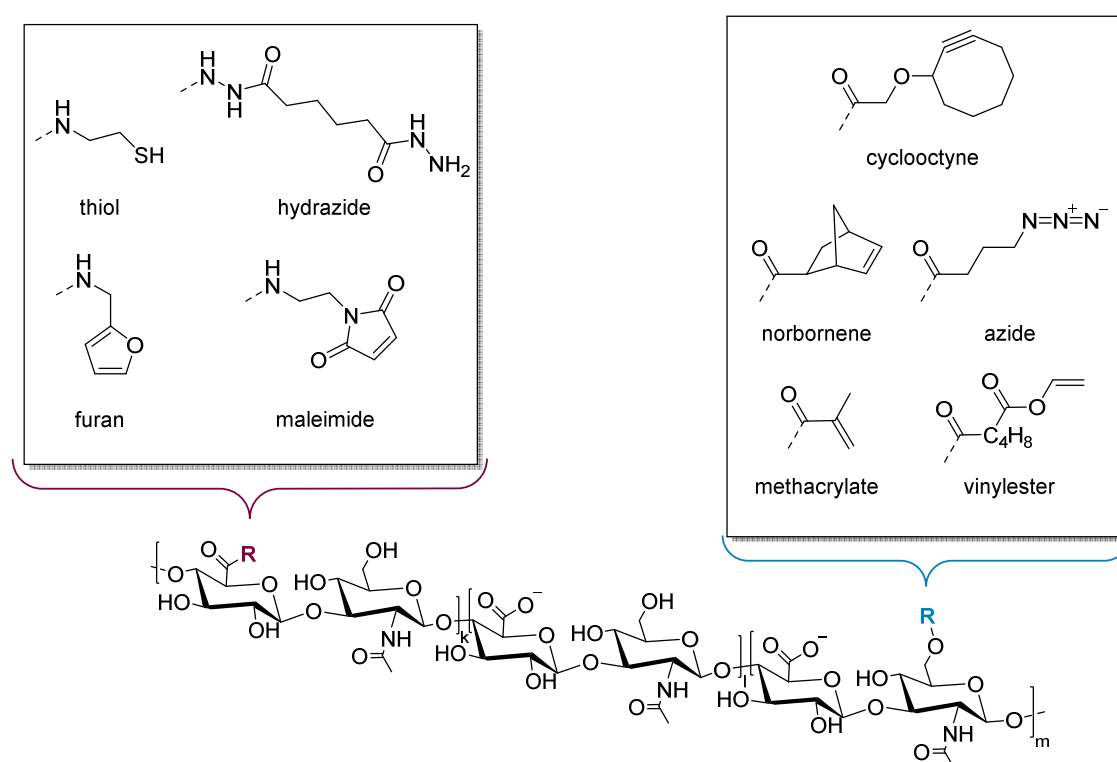


Figure 11: Modification possibilities of HA for chemical crosslinking methods

3.3.1 Direct chemical crosslinking

3.3.1.1 Crosslinking with Glutaraldehyde

Bulpitt and Aeschlimann⁴¹ for example developed an *in situ* polymerizable HA for articular cartilage applications. The amidation of HA with carbodiimides is a versatile tool, to functionalize the HA backbone. Due to its water solubility EDC is widely used as a carboxyl activating agent and therefore reacts with the carboxyl group of HA forming very reactive intermediates. As seen in Figure 12 the nucleophilic attack of an amine then results in the amide modified HA.

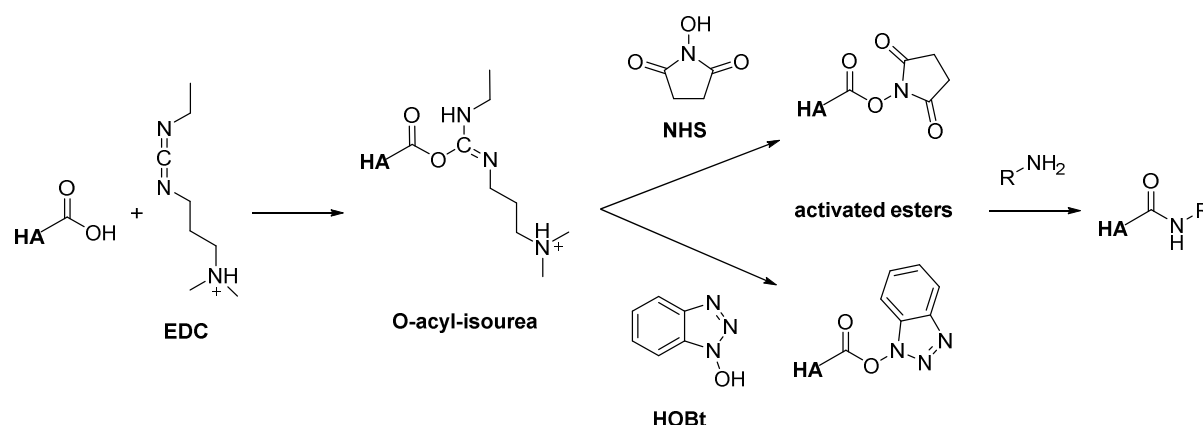


Figure 12: Amidation of HA with EDC by Bulpitt et al.⁴¹ and Schante et al.³⁹

The major advantage of using EDC is the ability to perform amidation reactions in aqueous media by using the native form of sodium-HA without previous modification. Moreover, this method prevents the degradation of the HA backbone and therefore maintains its high molecular weight responsible for its substantial viscoelastic properties. Thereafter the crosslinking of modified HA was performed by using a set of commercially available crosslinkers, like bifunctional esters and glutaraldehyde. Similar to this, hydrazide modified HA was synthesized in literature.^{42,43} Therefore hydrazides with different backbone lengths were used for the development of drug delivery systems. Modified HA was then crosslinked with macromolecular aldehydes to form biomaterials for the controlled release of therapeutic agents at wound sites. Glutaraldehyde has been already extensively used for TE,⁴⁴ although it is reported to be a toxic compound, that even at low concentration shows cell-growth inhibition.⁴⁵

3.3.1.2 Click-Chemistry

Click-Reactions are another possibility for the crosslinking of HA. They are known for their easy and selective way of covalently binding two molecular building blocks under high yield and with little or no by-products.⁴⁶ The widely used and well established **azide/alkyne cycloaddition**, catalyzed by Cu^{I} (CuAAC) fulfills these reaction conditions.⁴⁷ The catalysis by Cu^+ ions offers high specificity and quick kinetics, as described in literature.⁴⁰ Crescenzi et. al. already used this method to synthesize drug delivery systems on the basis of HA.⁴⁸

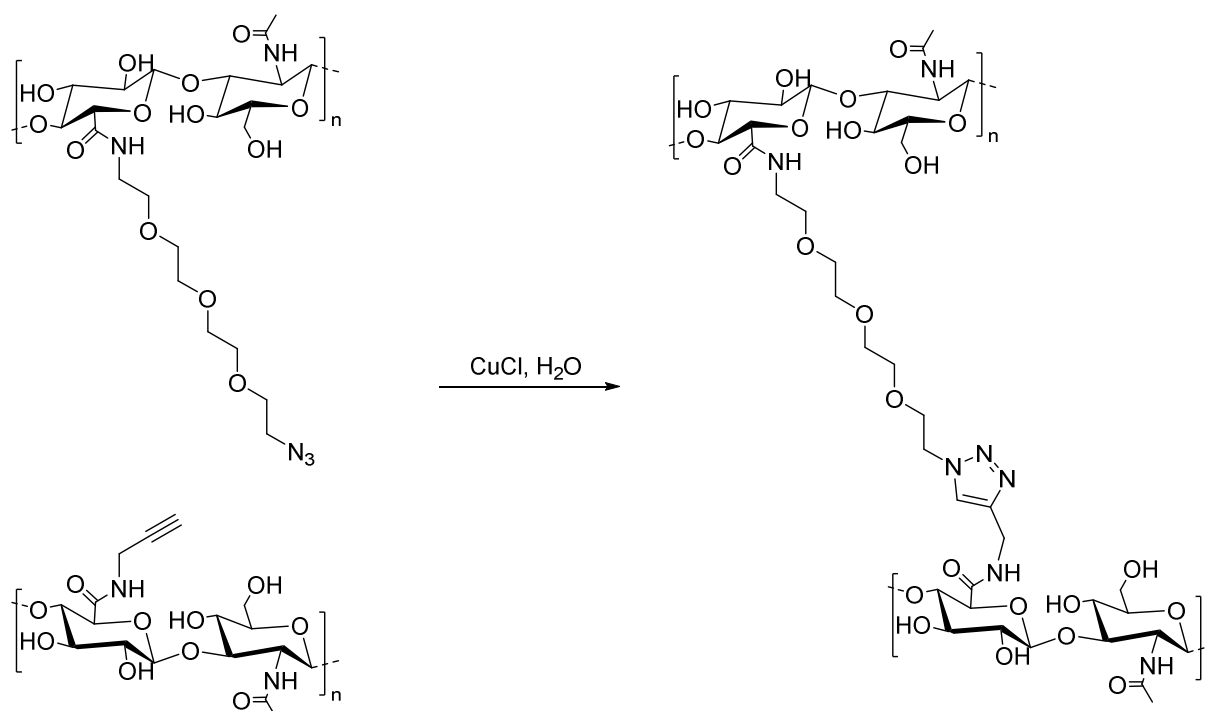


Figure 13: Chemical crosslinking of HA macromers via azide/alkyne cycloaddition⁴⁸

However, under physiological conditions, the cytotoxicity of the Cu catalyst can be a concerning issue, if traces remain in biological tissue. Since non-catalyzed azide/alkyne reactions have been known since 1893,⁴⁹ there are ways to circumvent the use of Cu and make use of Click-Reactions for biological systems.⁵⁰ Consequently Cu-free strain-promoted azide-alkyne cycloadditions (SPAAC) were performed for instance to produce PEG hydrogels.⁵¹ Similar to this, Takahashi et. al.⁵² prepared hydrogels upon mixing solutions of HA with azide- and cyclooctyne functionalities. They furthermore investigated biodegradation *in vitro* and *in vivo* on basis of the hydrolysis of formed ester linkages.

When talking about cycloadditions, **Diels-Alder reactions** were also examined for the chemical crosslinking of HA macromers. By the modification of HA's carboxylic group furan functionalities can be introduced.⁵³ Crosslinking with bismaleimide PEG leads to hybrid hydrogels which are tuned to mimic properties of the ECM. Further research showed, that Young's modulus can be directed by variation of the degree of substitution of furan functionalities of the HA backbone.⁵⁴ Another possibility to realize chemically crosslinked polymers can be the use of thiol-ene chemistry. These reactions are categorized into two types, whereas one is an interdisciplinary field between current Click-Reactions and the second type will be discussed in subsequent section.

3.3.1.3 Thiol-Ene Reactions

Reactions between thiols and reactive carbon-carbon double bonds, or simply "Enes", were already mentioned in the early 1900s.⁵⁵ Thiol-ene reactions are a useful tool to design material properties of hydrogels, especially by the possibility to modify the properties via synthetic cues. These reactions are insensitive to ambient oxygen or water and can be employed to an enormous range of both thiols and Enes. Additionally, these chemo-selective reactions occur under very mild conditions (aqueous media, room temperature, physiological pH values), which is advantageous for the field of TE. There are two major types of thiol-ene reactions. First, the Michael-type Addition reaction, where thiols can act as nucleophiles and induce an addition onto typical Michael Acceptors (enes). Besides these reactions, the second type of thiol-ene reactions is the radical induced addition, providing particular advantages described below. Recently published reviews give an overview on hydrogels for biomedical applications using thiol-ene chemistry.^{56,57} Thiols are permanently present in biological systems and offer a wide range of possibilities to produce biopolymer networks. For example thiol modified HA, crosslinked with polyethylene glycole diacrylate led to a system where the release of growth factors for wound repair can be investigated.⁵⁸ Also two different kinds of thiolated HA derivatives were compared by Shu et. al. concerning their reactivity to acrylate- and amide derivatives of PEG.⁵⁹

Nevertheless, there are some points to be considered when using thiols for TE. Bad odor, a short shelf life and potential cytotoxic reagents must be excluded when aiming applications *in vivo*. The mechanism of these type of reactions follows a step-growth like manner between double bonds and multifunctional thiols. A polymer network will be formed only if one of both monomers contain more than two reactive functionalities.

State-of-the-art-monomers are acrylates and methacrylates but also thiol-ene chemistry of vinyl esters (VEs) has been reported.⁶⁰ The reactivity of acrylates, methacrylates and VEs vary, because of the way these monomers are reacting with radicals. The mechanisms and reactivity of the radicals are shown in Figure 14 comparing acrylates and VEs.

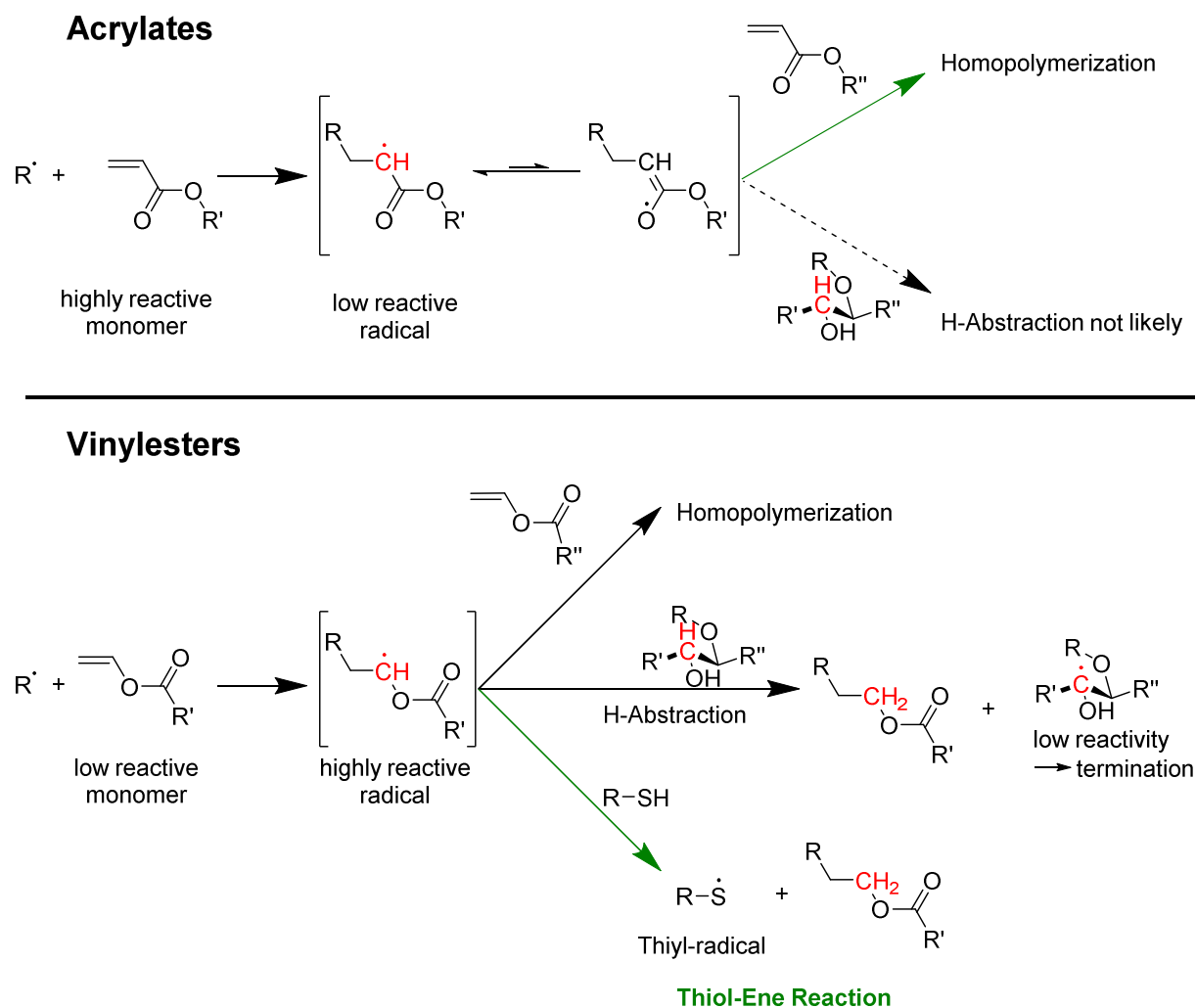


Figure 14: Reaction mechanisms of acrylates compared to vinyl esters including reactive intermediates⁶⁰

As can be seen in Figure 14 acrylates are highly reactive monomers, because the reaction of a radical with the acrylate leads to a very well resonance stabilized radical. For this reason, side reactions like H-abstractions, which lower the reactivity, are not very likely. Still the homopolymerization of acrylates happens to a great extent, due to the high reactivity of the acrylate monomer. In case of the quite low reactive VE monomers, the resulting radical is not resonance stabilized, which makes it very reactive. Therefore, side reactions like H-abstraction are very likely and lead to termination of the polymerization process. By introducing thiols into the system, it is

possible to direct the H-abstraction to a substrate, which generates radicals that do not terminate the polymerization, but yield in highly reactive thiyl radicals. This thiyl radicals react with further VE monomers resulting in a homogeneous network formation. Compared to the free radical polymerization, thiol-ene chemistry is not dependent on an oxygen free environment, because peroxy radicals are also capable of propagating the chain reaction, by abstracting a hydrogen from the thiol, generating the reactive thiyl radical species.⁶¹ Consequently oxygen inhibition and low conversions do not occur. Talking about network formation in general, the mixing of two reactive solutions usually leads to crosslinking immediately upon mixing.⁶² This effect can be disadvantageous, when spontaneous crosslinking consequently leads to inconsistent gels, due to insufficient control of the reaction. These problems can be circumvented by photopolymerization.

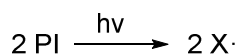
3.3.2 *In situ* chemical crosslinking

3.3.2.1 Photopolymerization

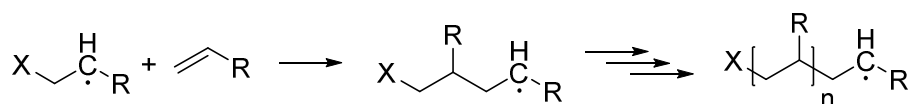
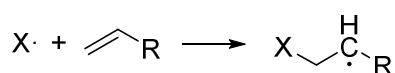
Photopolymerization is a technique, which has gained increasing interest in recent years.⁶³ Photopolymerization in general is the irreversible transformation of a liquid polymerizable formulation into a solid, which is triggered by light.⁶⁴ This selective triggering enables the formation of hydrogels under mild conditions. Network formation is therefore occurring only if the precursor solution is irradiated with light. Consequently, photopolymerization is a very controlled process with minimal invasion to surrounding matter. Hydrogel properties hence can be directed and modified by irradiation of defined areas. Compared to these disciplines in biomedicine, where the geometric dimensions of hydrogels are not primarily important, the main advantage of photopolymerization is the ability to cure solvent-free formulations within a fraction of a second with high spatial control. Furthermore, it is a more energy efficient process than thermally induced polymerization.⁶⁵ Photopolymerization can circumvent the disadvantages, which derive from mixing reactive solutions, change in pH, ionic strength and temperature. Moreover, by photopolymerization it is possible to combine the benefits of aforementioned Click-Reactions with radical-induced thiol-ene reactions. By crosslinking via light, it is possible to homogenize solutions completely, before exposure to radiation and therefore initiation of the polymerization process. In consequence, radicals are generated by the photoinitiator (PI) and following propagation reactions occur, like the addition of radicals to the double bonds of

monomers. Accordingly, additional monomers react with the propagating radical and form growing polymer chains until no more monomer is present. Termination processes, like recombination, disproportionation or oxygen inhibition can also stop the chain growth, but must be avoided because they lead to incomplete curing and decreased mechanical performance of the resulting polymer. The photopolymerization mechanism is demonstrated in Figure 15.

Initiation



Propagation



Termination

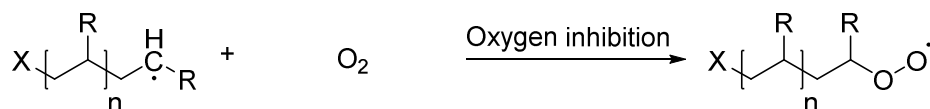
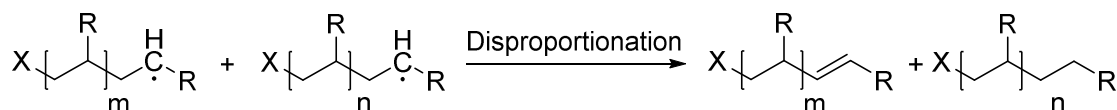
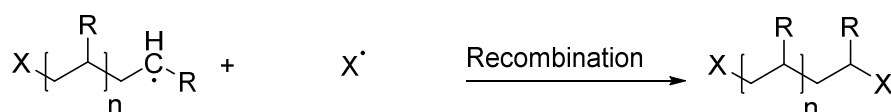
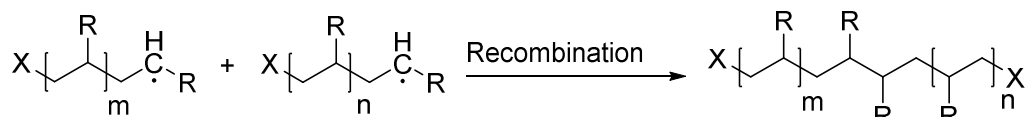


Figure 15: Mechanism of photopolymerization

There are 2 types of PIs: Type I PIs undergo unimolecular reaction and in contrast to this, Type II PIs undergo a bimolecular reaction. The cleavage of the Type I PIs proceeds from an excited triplet state and results in the formation of two radicals. Usual Type I PIs are aryl ketones, which decompose by alpha cleavage between the alpha carbon and the carbonyl. The resulting benzoyl radical initiates the polymerization. The second class of PIs, namely Type II PIs undergo a bimolecular reaction and therefore need the presence of another species (co-initiator) to form radicals.⁶⁶ These ketones do not undergo cleavage after being excited to triplet state. Generally, Type I PIs are

more efficient in the production of radicals and have higher decomposition rates due to the reason that the solvent cage effect influences the bimolecular reaction of the Type II PI system.⁶⁷ Accordingly, Type I PI cleave more efficiently, they do not produce high amount of singlet oxygen species and are therefore less cytotoxic. In addition to that, the poor activity of Type II PIs in aqueous solutions exclude them for the use in the biomedical sector. The focus in this thesis is therefore laid on the in Figure 16 depicted Type I PIs (Li-TPO and I2959).

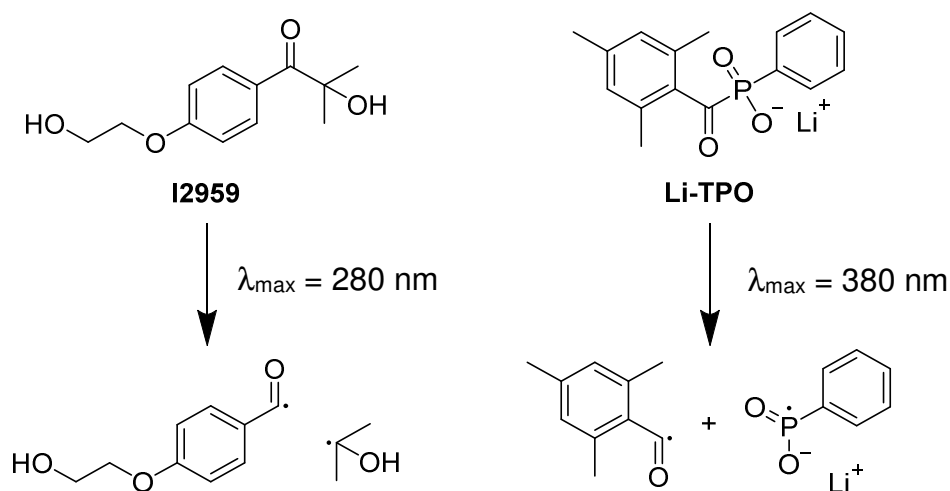


Figure 16: Alpha cleavage of water soluble Type I PIs I2959 and Li-TPO and their maximum absorption values (λ_{\max}) for the $\pi\text{-}\pi^*$ transition

A lot of organo-soluble PIs were introduced. However, water soluble PIs are required for biological applications due to the natural environment of cells. Usually Irgacure 2959[®] (I2959) is used, when water solubility is required.⁶⁸ One drawback is the low water-solubility of I2959, which was removed by further development and improvement of already known mono acylphosphineoxide (MAPO)⁶⁹ salts as PIs. Benedikt et al.⁷⁰ described the synthesis of the MAPO salt lithium phenyl (2,4,6-trimethylbenzoyl)phosphinate (Li-TPO) and performed biocompatibility studies. Figure 16 shows the two relevant PIs, I2959 and Li-TPO and their dissociation upon irradiation.

The cytocompatibility of the most commonly used PI, namely I2959, compared to Li-TPO was already investigated in literature.⁷¹ Beside the reactivity of a PI, the cytotoxicity is a major factor for applications in TE. In general the cytotoxicity corresponds with the hydrophobicity of the PI by reason of improved permeability of hydrophobic molecules through phospholipid bilayers of cellular membranes.⁷² Although I2959 is the most commonly used PI, there are some arguments, which

question the use of I2959 in biomedicine. This PI has an absorption spectrum that is poorly matched with those wavelengths of light, which are considered to be benign to cells (visible light). Out of this reason I2959 does not cleave effectively and the rate is limited, at which the polymerization is initiated. Basically, polymerization in the presence of cells is difficult to realize. Contrary to this, acylphosphineoxide PIs commonly offer absorption spectra at wavelengths adequate for cell encapsulation (above 400 nm). Yet commercially available initiators of this class show low solubility in water. Literature examined the influence of various initiator concentrations of I2959 and Li-TPO on cell survival of human neonatal fibroblasts in PEG-diacrylate gels.⁷¹ As radicals are highly reactive and often cytotoxic researchers performed experiments with similar number of radicals produced during PI cleavage, to effectively compare cell survival rates. By adjusting PI concentrations and illumination times, similar photon absorption was evoked. Further studies about Li-TPO⁷⁰ introduced excellent LC50 values (53.1 mmol/L) and very high polymerization rates and double bond conversions via UV-VIS irradiation measurements. They also compared the biocompatibility of two different bisacylphosphine oxide PIs with I2959. Although Li-TPO has higher absorption bands in the UV spectrum, it showed best biocompatibility results of all tested PIs. Both studies showed several advantages of Li-TPO over I2959, like successful visible light polymerization, very good water solubility and polymerization- as well as cell survival rates. These findings make Li-TPO a very promising candidate to be used as PI in combination with cells.

Not only the PI, but also the type of monomer modification is a crucial factor when it comes to cell survival. Several studies have been investigated in literature, where methacrylate modified HA was used to produce biocompatible hydrogels via photopolymerization. For example glycidyl methacrylate modified HA (GM-HA) was synthesized for the application of these hydrogels as wound healing components (see Figure 17).⁶²

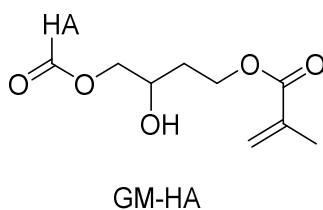


Figure 17: Glycidyl methacrylate modified HA for wound healing components

Rheological oscillatory shear stress experiments were performed to analyze hydrogel properties and the relation between degree of crosslinking density and gel stiffness. Furthermore, firm gels were obtained, by increasing concentrations of initiator, I2959 and co-monomer (N-vinylpyrrolidinone). The investigation of biocompatibility was performed by testing the cytocompatibility of human aortic endothelial cells with crosslinked and uncrosslinked GM-HA hydrogels. Moreover, the response of endothelial cells to the GM-HA gels in subcutaneous implants in rats was studied, where small inflammatory responses were found

Scaffolds for bone tissue regeneration were also introduced in literature in combination with methacrylate modified HA.⁷³ Mechanical properties of these HA hydrogels and their swelling ratios were examined. The modification of HA was performed by reacting the carboxylic acid of HA with 2-aminoethyl methacrylate. Afterwards the hydrogel was tested as a drug delivery carrier and therefore loaded a drug with high osteogenic activity. Besides biocompatibility, the release kinetics of this drug were examined and correlated to hydrogel loading concentrations. Another example of using methacrylate modified HA was investigated by Seidi et al.⁷⁴ The exposure of methacrylated HA precursors to gradients of UV light resulted in hydrogels with elastic modulus gradients. These stiffness gradients were tested for the application of HA hydrogels for interface TE. In general the influence of the degree of methacrylation on HA hydrogel properties was studied by Bencherif et.al..⁷⁵

Not only homopolymerization, but also the photocrosslinking of HA in combination with crosslinking agents, like thiols, was studied in literature. As described in section 3.3.1.3 thiol-ene chemistry can be a versatile tool to produce *in situ* photocrosslinked hydrogels with variable mechanical performance.⁷⁶ For instance Marklein et al.⁷⁷ described the production of porous 3D hydrogels with tunable elastic moduli on the basis of methacrylated HA in combination with the Michael Addition of dithiols. Seeding of the hydrogels with mesenchymal stem cells led to the observation of spreading and proliferation of cells in a mechanical dependent manner. Partly peptide functionalized PEG-DA macromers were also fabricated in literature via Michael Addition of cysteine residues of peptides onto PEG-DA. Through this, hydrogels with varying mechanical properties were produced by mixing methacrylate modified HA in combination with varying concentrations of peptide modified PEG-DA.⁷⁸

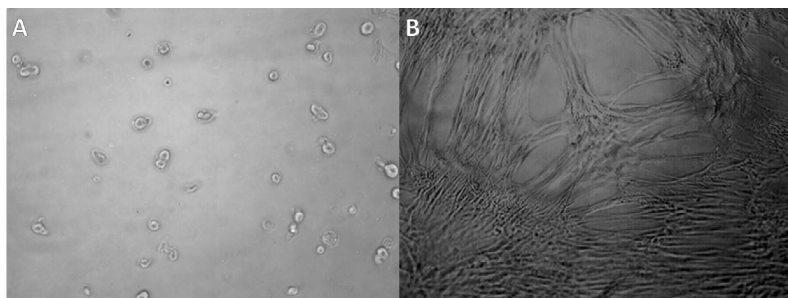


Figure 18: Fibroblasts cultured on HA-based hydrogels, containing RGD peptides (B) and no peptides (A) results on various cell adhesion properties⁷⁸

This study revealed, that the introduction of peptides onto macromer backbones showed dramatic changes in terms of cell adhesion and proliferation. Not only methacrylate- but also norbornene modified HA was used in combination with thiols for the production of photopatterned hydrogels.⁷⁹ Several hydrogels with varying mechanical properties were studied. Orthogonal secondary crosslinking reactions of unreacted norbornene- modified HA with mono- and di-thiols were performed and the compressive modulus of the hydrogels examined.

Although methacrylates already showed reasonable results for biomedical applications, there are some drawbacks, especially when acrylates are used in TE. The high reactivity of acrylates towards amino- or thiol groups of proteins and DNA makes these derivatives potential cytotoxic.⁸⁰ When acrylate moieties are coming in contact with biological tissue, the Michael-Addition of biomolecules occurs (see Figure 19).

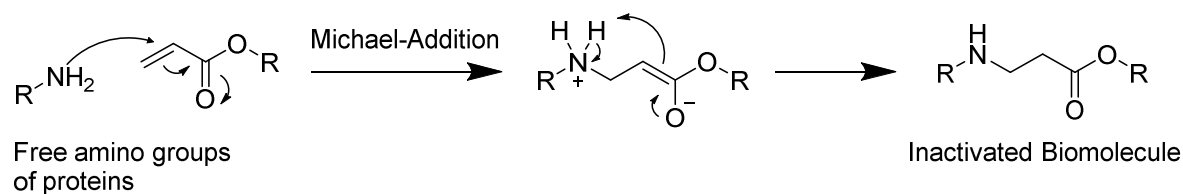


Figure 19: Mechanism of the Michael-Addition of nucleophiles to acrylates, leading to inactivated biomolecules

Proteins for example contain free amino groups and can be denatured by above-mentioned Michael-Addition, which leads to the change of protein conformation *in vivo*. These side reactions are irreversible and lead to dysfunctions in the bioprocess and need to be avoided when working in the field of TE. The growing demand for finding alternative low-toxic photo-reactive groups for the modification of HA led to the introduction of VEs. Recent studies^{80,81} showed the significant better performance of VEs concerning cytotoxicity, compared to methacrylates and acrylates. The lethal

concentration (LC_{50}) at which 50% of the tested cells survive, is significantly higher for VEs than for the reference compounds (see Figure 20).

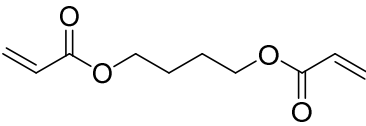
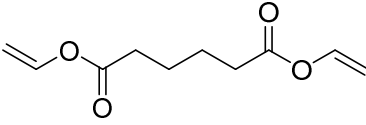
Monomer	LC_{50} [mM]
 acrylates	<0.63
 vinyl esters	>10

Figure 20: LC_{50} values for vinyl esters compared to acrylates⁸⁰

Considering these results, VE modification seem to be an appropriate possibility to achieve biocompatible hydrogels for TE.

4 Additive Manufacturing Techniques

The field of Additive Manufacturing Techniques (AMTs) has improved tremendously over the last decade, particularly in the field for regenerative medicine, to fabricate artificial scaffolds for soft tissues and therefore provide a suitable environment for living cells.^{82,8384} of can be realized by rapid prototyping techniques. These 3D environments facilitate cell adhesion and proliferation, especially to realize the development of functional tissues. Literature recently provided an extensive overview about AMT for scaffolds, which were developed during the last decade.⁶⁵ Special focus is hereby laid on lithography based AMTs for regenerative medicine (see Figure 21).

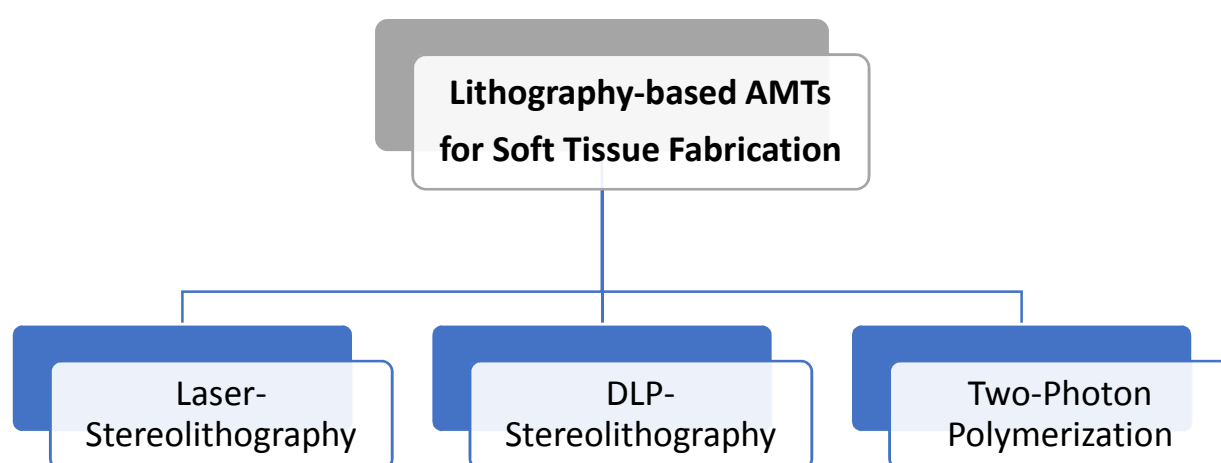


Figure 21: Lithography-based Additive Manufacturing Techniques (AMTs) include Laser-based Stereolithography (SLA), Digital Light Processing-based Stereolithography (DLP-SLA) and Two-Photon-Polymerization (2PP)

There is a broad field of different techniques with loads of alternative technologies, which require different types of feedstock. Thermally induced AMTs, which derive from a solid feedstock were already introduced in literature to realize biocompatible scaffolds, whereas the precision and the complexity of the pore geometry is still a big drawback.⁸⁵⁻⁸⁸ Contrary to these systems, lithography-based AMTs, derived from liquid feedstocks, are promising alternatives, where high resolutions can be achieved. Laser-based Stereolithography (SLA), Digital Light Processing-Stereolithography (DLP-SLA) and Two-Photon Polymerization (2PP) are examples of those techniques, used for soft tissue fabrication. The functional principle of SLA, DLP-SLA and 2PP are depicted in Figure 22. The basic working principle of SLA is based on an UV-laser light source, where the light beam is deflected, according to the geometry of a CAD-file (CAD= computer-aided design).

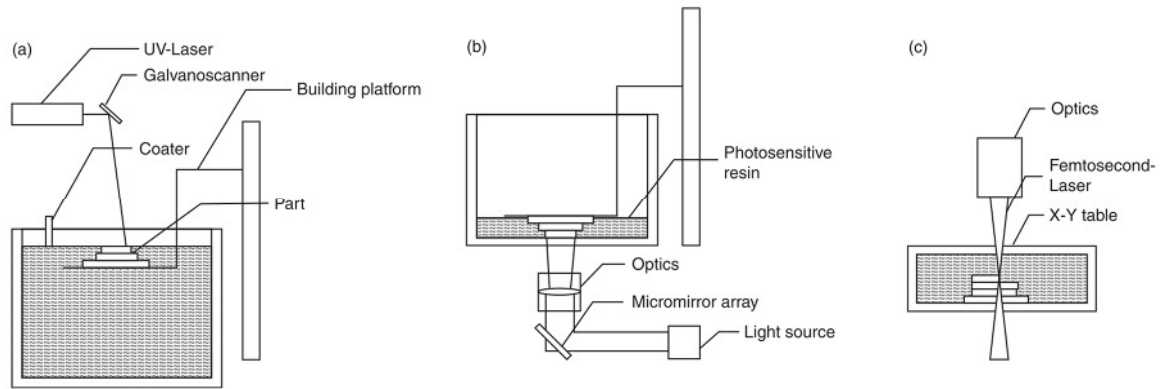


Figure 22: Lithography-based Additive Manufacturing Techniques⁶⁵ (a) Laser-based Stereolithography, (b) Digital Light Processing-based Stereolithography and (c) Two-Photon Polymerization

In general, the photosensitive material is polymerized on the surface of the formulation, where layer-by-layer polymerization occurs by scanning a selected sample area by the coherent laser beam. As described in literature⁸⁹ SLA was already used for the processing of materials with elastic modulus ranging from 0.4 to 8000 MPa to print complex 3D scaffolds with a size of 5×5 mm with a feature size of down to $20 \mu\text{m}$. In contrast to SLA, DLP-SLA uses an optical system to project a whole cross-section of an aimed structure onto the bottom of a transparent vat. Appropriate lenses focus the image on the bottom of the vat where the photosensitive material solidifies (Figure 22). Afterwards the building platform is lifted in z-direction and liquid formulation fills up the empty space. Bottom-exposure shows the advantage, that less material is needed for the polymerization process, compared to the top-exposure technique (SLA). As the light source does not need to be coherent, the building speed, which is the rate of layer-by-layer curing of the formulation, can be increased drastically. Through this, DLP-SLA reaches building speeds up to 10-20 mm/h, by still maintaining a feature size down to $40 \mu\text{m}$.

As layer-by layer manufacturing techniques are based on a top- or bottom exposure, some disadvantages arise, like limited resolution⁹⁰ due to materials surface tension⁹⁰ and oxygen inhibition⁹¹. These drawbacks can be eliminated by using one recently developed AMT, known as 2PP. This lithography based technique is especially interesting when it comes to 3D processing of cell matrices.⁹² Reasons for this are the ability to print 3D patterns under very mild conditions, directly within the sample volume and writing with high spatial resolution. The principle of 2PP is based on the induction of photochemical reactions by a multiphoton absorption of laser radiation (see Figure 23).

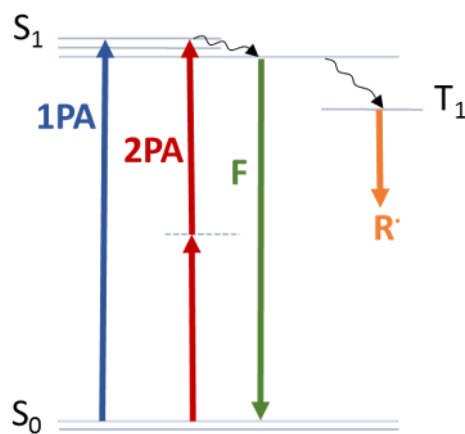


Figure 23: Two Photon Absorption (2PA) compared to One Photon Absorption (1PA) and following relaxation processes; fluorescence (F) and radical formation ($R\cdot$)

In contrast to one photon absorption (1PA), two photon absorption (2PA) is a non-linear absorption process, because the probability of simultaneous absorption of two photons at the same time, scales as the square of the incident light intensity. Therefore, light sources with a very high photon density in the focal point are required. Ultra-short laser pulses (femtosecond-lasers) can provide these high peak intensities, while still operating at average laser powers.⁹³ Accordingly, the PI is excited by these highly focused Ti:Sapphire lasers with high energy output. Photons emitted in the near infrared (NIR) have a wavelength of 800 nm. As two photons with this specific wavelength have the same energy than one photon with 400 nm, which would be emitted by a UV laser, the effective 2PP in presence of cells can be enabled. Furthermore, deep penetration of tissue itself is possible as absorption of tissue at these wavelengths is not occurring. The PI absorbs two photons at the same time and initiates the polymerization. The mechanism of radical generation by the electronic transitions of the PI are depicted in detail in the Jablonski diagram in Figure 23.⁹² The consumption of the energy of one (for 1PA) or of two photons (for 2PA) by the PI molecule leads to the excitation of the electrons from the ground- (S_0) to the excited singlet state (S_1). The relaxation afterwards then can occur via fluorescence (F) or via inter system crossing to an excited triplet state (T_1). From this state, radicals ($R\cdot$) can be produced by further loss of energy and the polymerization can be initiated.

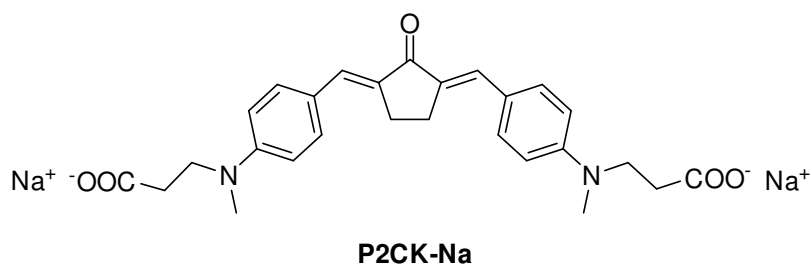


Figure 24: Newly developed two photon active, water-soluble photoinitiator

2PA is only occurring when the PI molecule shows high 2PA cross-section, resulting in a high probability of reaching the excited state.⁹⁴ Typical PIs with high 2PA cross-sections are planar conjugated π -systems with strong donor/acceptor groups. Only a few PIs were developed for water borne systems. By the introduction of carboxylic sodium salts onto known core structures, water solubility of PIs was increased. One promising chromophore of this type is P2CK, depicted in Figure 24. This chromophore is used in this work for the fabrication of hydrogels via 2PP.⁹⁵ 2PA only occurs in the focal point of the laser beam because of the increased electron density at this site. Subsequent intra- and inter-molecular charge transfer interactions between excited PI and monomer initiate the polymerization process. Figure 25 shows the polymerization in the small focal volume, leading to excellent spatial control with very high resolution in the sub- μm range.⁹⁶

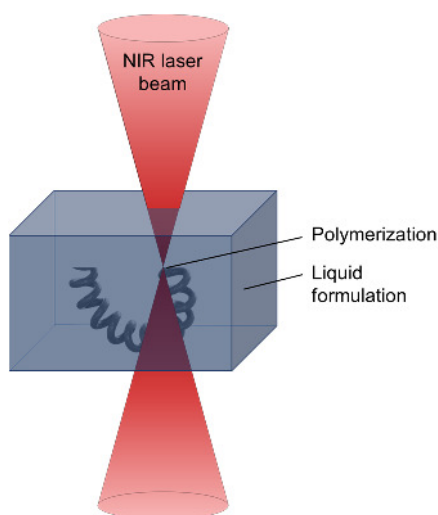


Figure 25: 2PP in the focal point of a NIR laser inside a photo curable formulation

The long wavelength of the NIR laser offers various advantages, like the possibility of deeper tissue penetration and less damage of surrounding tissue. Therefore, 2PP is a process especially suitable for various biological applications. Compared to other AMTs, which use an additive stacking process, where formulations are polymerized

layer-by-layer, the 2PP process has the advantage of being able to polymerize a formulation around pre-suspended cells inside a matrix volume. Through this technique spatially defined immobilization of cells inside a hydrogel matrix can be realized.⁹⁷ 2PP printing in presence of whole organisms⁹⁸ and bone tissues with adequate tough properties have already been printed with multiphoton lithography.⁹⁹ In conclusion, 2PP is a technology very well suited to produce a variety of 3D scaffolds for the field of TE. The high resolution and the increasing writing speed depict the advantages to alternative methods for the engineering of biocompatible hydrogels.

Objective

Hydrogels are physically or chemically crosslinked networks, representing an important class of biomaterials for tissue engineering (TE). A variety of hydrogel monomers have already been developed as supplements for soft tissue scaffolds, which can also be manufactured by material printing to fabricate well-defined hydrogel structures. Especially natural polysaccharides, such as hyaluronic acid (HA) shows promising performance in the field of TE, being a major component of the extracellular matrix (ECM). To create hydrogels with defined properties, low-toxic, photo-crosslinkable macromer precursors are required. Modification of these natural polymers, especially with methacrylate- and acrylate functionalities led to macromers with several disadvantages. Primarily cytotoxicity and low reactivity of introduced polymerizable groups arose demand for alternative precursors. Former studies established vinyl ester (VE) functionalities based on HA to be used as biocompatible substitutes. Although, extensive research showed promising results for these newly developed hydrogel precursors, a few issues are still pending. Previous work on HA macromers was performed, where the polymer backbone was extensively degraded, compared to the native form of HA. These very low molecular weight (MW) HA macromers, which also possessed a very high number of functional groups, led to undesirable brittle hydrogels.

Accordingly, the following hypothesis is established within this thesis. Controlled degradation of the starting material should be performed to adjust the MW of HA precursors. Consequently, HA macromers with a MW lower than commercial available HA, but still higher than previously studied within this research group should be developed. Mentioned precursors with increased MW should introduce following advantages, such as inter- and intra-molecular hydrogen bonds, leading to physical associated gels. These can already serve as a stable matrix for cells, before chemical network formation is performed via photopolymerization. By this, sedimentation or agglomeration of embedded cells is avoided. In addition, high-MW HA does not lead to activation of inflammation-promoting receptors inside the ECM which would occur for macromers with very low MW. The new precursors should lead to more flexible and elastic hydrogels, in contrast to the brittle and stiff gels obtained in previous studies. Furthermore, the effect of decreased number of polymerizable functionalities on the network density should be examined. Particularly, the reactivity of the precursors, as

well as the mechanical properties of the resulting hydrogels should be studied via photorheology measurements. Moreover, the effect of macromer content, chain transfer agent and additional natural polymers on network properties should be investigated. Finally, network formation of the newly developed hydrogel precursors in the presence of cells should be examined by two photon polymerization (2PP).

General Part

1 State of the Art

The importance of hyaluronic acid (HA) in the field of TE is steadily rising, especially since the modification of the polymer backbones enables new characteristics and therefore makes biomedical applications accessible. Recent reviews describe the advances of the most common modifications of HA in the field of biomedicine.^{11,18,23-25} Especially due to the high reactivity of acrylates, they are already extensively used as modification of HA for TE. The research group of Liska focused on biocompatible hydrogels and introduced modifications of HA, including acrylates (ACs), methacrylates (MAs), thiols (SHs) and vinyl esters (VEs) (Figure 26).¹⁰⁰

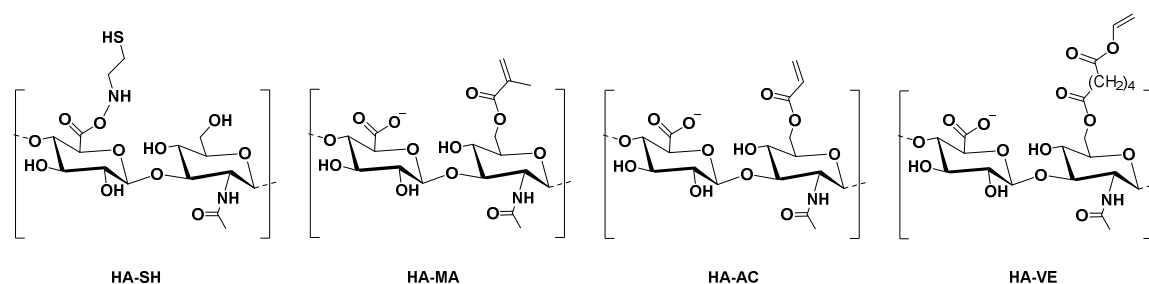


Figure 26: Chemical structures of HA derivatives: HA modified with thiol (HA-SH), methacrylate (HA-MA), acrylate (HA-AC) and vinyl ester functionalities (HA-VE)

HA-SH hydrogels have already been tested for clinical applications such as wound healing scaffolds.¹⁰¹ Reversible hydrogel formation by the formation of disulfide linkages could be obtained under physiological conditions. Furthermore, long-term cell viability of fibroblasts and their proliferation after cell encapsulation was examined.

Not only acrylates, methacrylates and thiols but also VE are in the focus as functional groups for the production of polymerizable hydrogels, especially since VE as low-toxic monomers were introduced for the use as artificial tissues.⁸¹ Generally, there are different approaches for the synthesis of VE. Husár et al.⁸⁰ described the synthesis of VE in the presence of Pd(II) salts. This method transforms simple carboxylic acids into VE by dissolving them in excessive amount of vinylacetate. Since HA is not soluble in vinylacetate and these Pd catalyzed reactions are quite expensive and sensitive to moisture they do not seem to be a suited method for the synthesis of VE.

Already in the 90ies, modifications of polysaccharides with VE moieties were introduced by literature, using lipase catalyzed transesterification reactions.¹⁰² Wang et. al.¹⁰³ showed a simple and selective method for the modification of the anticancer nucleoside analog cytarabine. They could use acrylic resin of the lipase *Candida Antarctica* (CAL-B) to ensure transesterification with the sugar moiety under mild conditions. They successfully modified the primary hydroxyl group of the sugar with divinyl adipate (DVA) to yield VE functionalities on the sugar unit. Accordingly, the approach to modify of the primary hydroxyl group of HA by this method seems reasonable. As DVA is commercially available and was already used for the production of biomaterials,¹⁰⁴ this reagent was selected for the transesterification reaction with HA. The influence of different degrees of substitution (DS) on the HA backbone on the photoreactivity and the influence of macromer content on the gel stiffness was shown. Cell compatibility assays based on resazurin showed increased cell viability for HA-VE than for HA-AC and HA-MA.

Tomášiková¹⁰⁵ followed the research of Qin and investigated the effect of several different DS on the mechanical properties of the hydrogels during gelation. Furthermore, influence of macromer chain length was evaluated. Results of photorheometric studies showed, that increasing DS leads to higher photoreactivity and higher crosslinking densities, which has a direct influence on the mechanical properties of the hydrogel. Figure 27 clearly shows the increase of the maximum storage modulus by increasing the macromer content of HA-VE and the DS.

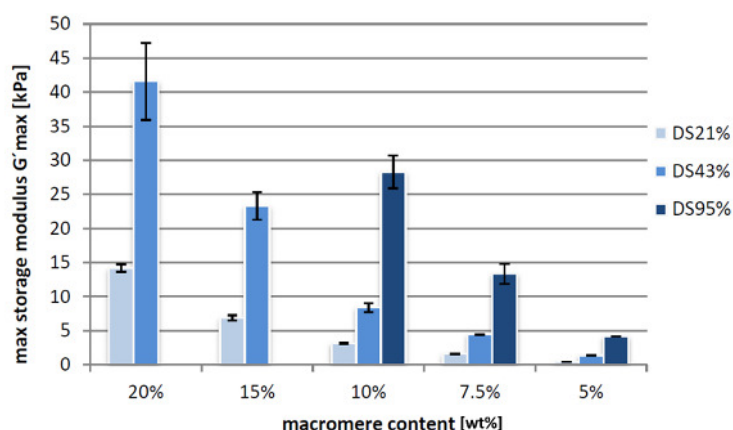


Figure 27: Photorheological results of HA-VE with different DS and different macromer content¹⁰⁵

Thiol-ene chemistry was introduced to increase VE reactivity. As research showed, that the homopolymerization of VE is less favourable than the crosslinking of VE with thiols,¹⁰⁶ a water-soluble di-functional thiol, DL-dithiothreitol (DTT) was added to the formulation, as this specific one was already used in literature for the photopolymerization of HA.¹⁰⁷ Former research focused on very small HA fragments (~20 kDa), resulting in very stiff and brittle hydrogels due to the lack of elasticity for the network of the small macromer chains. Characterization of these hydrogels depicted a trend, where increasing macromer size showed an increase of photoreactivity and crosslinking density of hydrogels. This can be explained by the junction of HA backbones resulting in the formation of additional crosslinks and faster network formation. Consequently high-MW HA with decreased degree of substitution of photopolymerizable groups should be proposed within this thesis.

2 Synthesis

2.1 Preparation of Low-Molecular Weight HA

Native, high-molecular HA is produced on the surface of various cell types in the epidermis and in connective tissue of the human body showing a molecular weight (MW) between $4 \cdot 10^2$ and $2 \cdot 10^4$ kDa¹⁰⁸ or even $2 \cdot 10^6$ kDa in synovial fluid.¹⁰⁹ The majority of the ECM consists of proteoglycans and within these macromolecules, the content of HA differs from tissue to tissue.¹⁷ Viscoelastic solutions are formed, already at rather low concentrations of HA in soft tissue, contributing to the role as lubricant and shock absorber in joints. The structure in the dissolved state was ever since extremely difficult to determine and caused extensive research. Conformation and interactions of HA chains with surrounding matter in the dissolved state are still topic of controversial discussions.¹¹⁰ For example intramolecular hydrogen bonds, like shown in Figure 28, influence amongst other forces the conformation of HA.¹¹¹

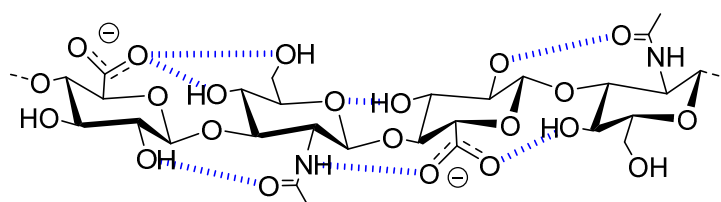


Figure 28: Different intramolecular hydrogen bonds between HA molecules

These characteristics make it difficult to handle solutions of high MW HA and hard to fabricate hydrogels with appropriate mechanical properties, suitable for TE. Accordingly, commercially available HA, with a MW of 1.6 MDa needs to be degraded to achieve macromer chain lengths suitable for further processing. For the field of TE the size of the macromer chain is eminently important because cell surface receptors regulate immunological responses in the human body and these responses can stand in correlation with HA macromer size. Toll-like receptors distinguish between endo- and exogenic substances by recognizing pathogen- and damage-associated molecular patterns, such as ECM-fragments.^{110,112,113} Love et.al described, that HA with a MW higher than 10 kDa is desirable for products used in ophthalmology, orthopedic and TE and low-MW HA can be utilized in biomedicine for producing substances that induce the expression of pro-inflammatory mediators.¹¹⁴ For this reason, an appropriate degradation method

needed to be developed. There are many ways reported, how HA can possibly be degraded.¹⁸ Ranging from thermal¹¹⁵ or ultrasonic influence¹¹⁶ up to enzymes (hyaluronidases)¹¹⁷, free radicals¹¹⁸ or by pH-dependent¹¹⁹ degradation. Especially acidic and basic hydrolysis of the glycosidic bond was already investigated in literature.¹²⁰ Tomášiková¹⁰⁵ and Qin¹⁰⁶ used the acidic degradation of HA to produce low-MW HA with a MW of about 20 kDa. These HA macromers led to very brittle hydrogels, as a result of which they did not perform well for desired applications. Therefore, the synthesis of HA precursors should be performed, where the HA chain length should exhibit the values from previous studies. In order to synthesize macromers suiting the new approach, a degradation study was performed, to investigate the degradation time necessary for achieving a desired MW. Commercially available HA (1.6 MDa) was degraded by acidic hydrolysis at a pH of 1 (see Figure 29). Gel permeation chromatography (GPC) measurements were performed, to monitor the MW immediately during degradation, as the degradation depends on a lot of different factors, like pH, temperature and stirring speed.

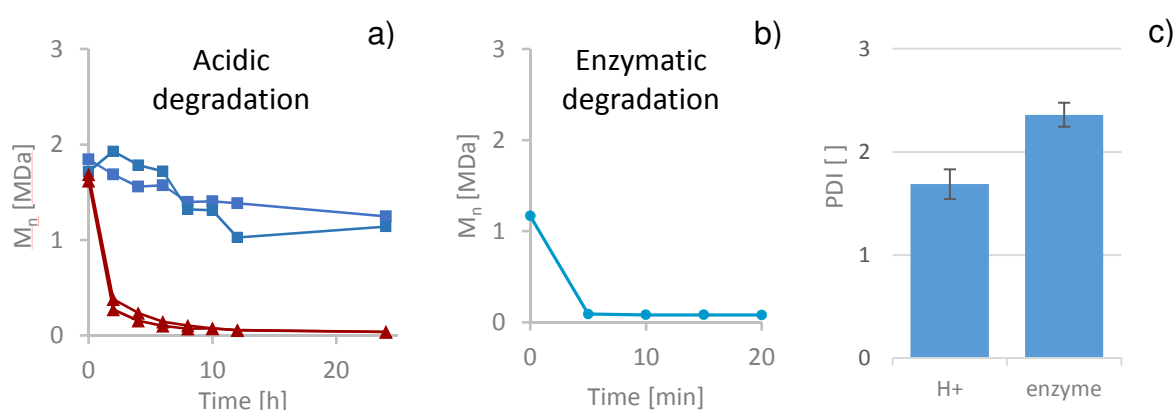


Figure 29: a) Acidic degradation at 60 °C (—■—) and 23 °C (—▲—), b) enzymatic degradation, c) average PDI values for acidic- and enzymatic degradation

HA was dissolved in water over night by mechanical stirring until a homogeneous solution was received and the pH was adjusted to 1 using a pH-meter by dropwise addition of concentrated HCl. To investigate the effect of temperature, the degradation was performed at room temperature (23°C) and 60 °C both in a duplicate experiment. After the pH was set to 1 the degradation was continued for 24h. During this period, the pH value was monitored and samples of the aqueous solution were drawn, whereupon the viscosity of the solution significantly decreased with time. The samples were neutralized by the addition of NaOH and

GPC measurements were performed. As can be seen in Figure 29 the degradation at elevated temperatures proceeds faster than the hydrolysis at room temperature and reaches a MW of around 100 kDa in a time scale of 6h.

An alternative degradation method was investigated, with the goal to avoid very small HA fragments due to excessive and uncontrolled degradation. Therefore, an enzymatic cleavage of the HA backbone was performed. Hyaluronidase is an enzyme that hydrolyzes the polymer at the β -1,4-N-acetylglucosaminide bond.¹²¹ This enzyme not only degrades HA but should lead to homogeneous chain sizes due to the catalysis of a trans-glycosylation reactions. This rises the idea of using an enzymatic digestion for the selective degradation of HA, to achieve homogeneously cleaved polymer chains. Hyaluronidase (HASE) (Type I -S) from bovine testes was used. HA was dissolved in PBS buffer and HASE in acetate buffer, which contained bovine serum albumine (BSA), due to stabilization effects regarding HASE. After homogeneous solutions were achieved, the enzyme solution was added to the HA solution to start the degradation. Due to optimum performance of the enzyme, the degradation study was performed at 37 °C and the MW of HA monitored via GPC. As previous experiments with an activity of HASE of 100 and 10 U/mg led to inconsistent GPC measurements, due to unsuitable column size, the activity was further diluted to 5 U/mg. Before each GPC measurement, the drawn sample was heated to 98 °C for 10 min, to inactivate the enzyme and separate BSA from the reaction solution via centrifugation. Figure 29a) shows MW values received from GPC measurements. As can be seen in Figure 29b) the enzymatic degradation for an enzyme activity of 5 U/mg occurred very fast and therefore the MW could not be controlled properly. To determine the homogeneity of the cleaved polymer chains, the PDI was used to investigate the molecular weight distribution. The PDI values for the enzymatic degradation and the acidic degradation of HA were received by GPC and are depicted in Figure 29c). Against the expectation of the enzymatic degradation leading to a narrower MW distribution, Figure 29c) depicts the opposite result. The PDI of the enzymatic degradation is significantly higher, resulting in a broader MW distribution, which is not desired for this thesis. The mechanism of the enzymatic digestion is still a very complex process and requires further investigation to produce narrow molecular weight distributions. As for now experiments showed that the acidic degradation

led to lower PDI values and therefore yielded in more narrow MW distributions compared to the enzymatic degradation.

For this reason, acidic degradation was chosen as a method to decrease the MW of native HA, according to procedure at 60 °C as described above. In contrast to the degradation at room temperature the degradation at 60 °C accelerates the degradation process, which increases efficiency for the laboratory scale. Furthermore, the increased temperature leads to the separation HA chain segments, as a result of the weakening of hydrogen bonds. By reasons of this separation, viscosity also decreases significantly.³⁸ The aim of the degradation was to achieve different HA batches with different MW ranging from relatively low- to very high MW. Acidic degradation of the first batch (77, 100, 150 kDa) was performed by stirring a 1 wt% aqueous solution of HA at a pH of 1. After monitoring the degradation via GPC, the appropriate MW was received by withdrawing one third of the solution after 5.5 h of degradation. Two more samples were drawn after 7.5 h and 9.5 h yielding in three different MW values. The second batch (150, 540 kDa) was degraded by the same method (pH of 1) except the concentration of the solution was 0.2 wt%. After neutralization and dialysis, HA batches were lyophilized. Table 1 shows various MW received after mentioned degradation steps. ¹H-NMR spectra of degraded HA in D₂O were measured and an exemplary spectrum is depicted in Figure 30.

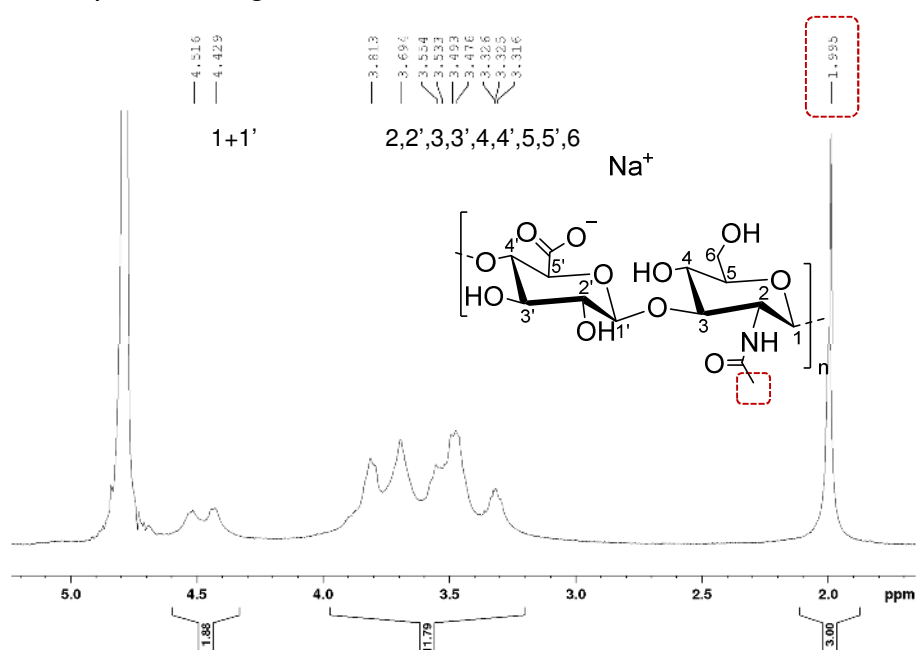


Figure 30: ¹H-NMR (D₂O) of degraded HA (150 kDa)

The well separated singlet at 2.0 ppm represents the methyl signal of the acetamido group, which was later used as reference signal to determine the degree of substitution (DS) for the synthesized macromer. Signals from 4.4-4.6 ppm represent the protons at the anomeric C-atoms (C₁, C_{1'}) and signals from 3.3-3.9 ppm can be interpreted as the ring-protons of the HA backbone and the CH₂ signal of the primary OH group. Although a 400 MHz spectrometer and 512 scans were used to evaluate the protons of HA, the spectrum shows some inconsistent values for the ring protons. As described in literature¹²² dissociation of OH-groups lead to varying H-bonds, which control the molecule's stiffness. Named factors would result in different proton mobilities, which would lead to these divergences from exact values for the protons.

Table 1: Resulting number average of molecular weight (\overline{M}_n) and the corresponding polydispersity index (PDI) and the yields of the acidic degradation of native HA after specific degradation times (t)

t [h]	Yield [%]	\overline{M}_n [kDa]	PDI []
24	96 ^a	22	2.33
9.5		77	2.38
7.5	69 ^{*,b}	100	2.13
5.5		150	2.46
6	70 ^b	180	1.91
3	80 ^b	540	1.80

** one batch*

^a Dialysis with a MWCO of 3.5 kDa

^b Dialysis with a MWCO of 50 kDa

The yields in Table 1 were determined after dialysis, whereas the molecular weight cutoff (MWCO) of the dialysis tubes for HAVE with 22 kDa was 3.5 kDa and for all other HAVES 50 kDa. For this reason, the yield is influenced by the MWCO, in such a manner, that it is decreasing, when the MWCO is set to higher values, due to increased loss of smaller HA fragments. Furthermore, the PDI is rising with increasing time of degradation (except value for 5.5h)

2.2 Synthesis of Tetrabutylammonium Salt of HA

In order to improve the solubility of HA in DMSO, the tetrabutylammonium (TBA) salt was generated via an ion exchange of the existing Na-salt of HA.¹²³ The reaction was carried out in DMSO to be able to perform the later modification of HA described in Section 2.3.

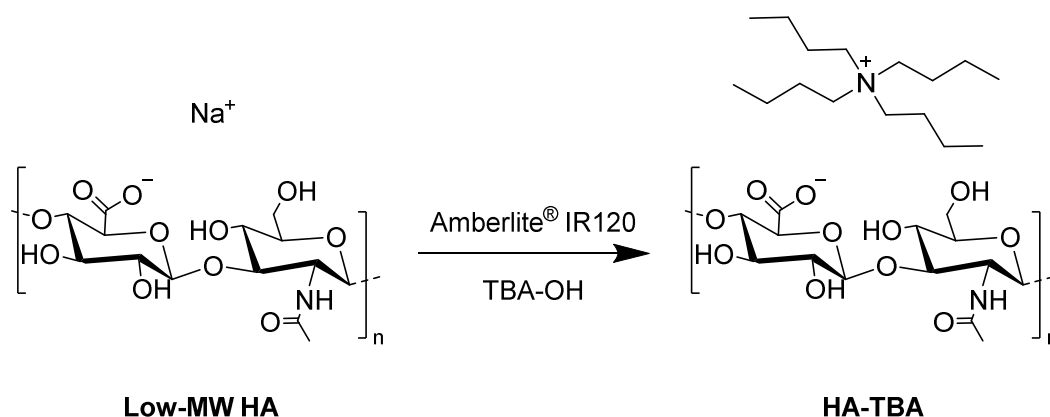


Figure 31: Synthesis of the tetrabutyl ammonium salt of HA (HA-TBA) using the ion exchange resin Amberlite® IR120, followed by neutralization of the reaction mixture with TBA-OH

Previously degraded HA was dissolved in demineralized water to obtain a 1 and 3 wt% solution, respectively. 5 mass equivalent of highly acidic ion exchange resin Amberlite® were added and the slurry was stirred for 4 h at room temperature. The ion exchange resin was removed by suction filtration, the resin was washed with demineralized water and the filtrate neutralized by addition of a 40% aqueous solution of tetrabutylammonium hydroxide (TBA-OH). After reducing the volume of the solution by evaporation in vacuo, the HA-TBA solution was lyophilized for at least 24 h. Quantitative amounts of HA-TBA were received as a slightly pink solid. The yields are given in Table 2. The successful synthesis of the TBA salt was confirmed by ¹H-NMR measurements of the lyophilized product. Figure 32 compares the spectrum of HA-Na salt (bottom) with the spectrum of HA-TBA (top).

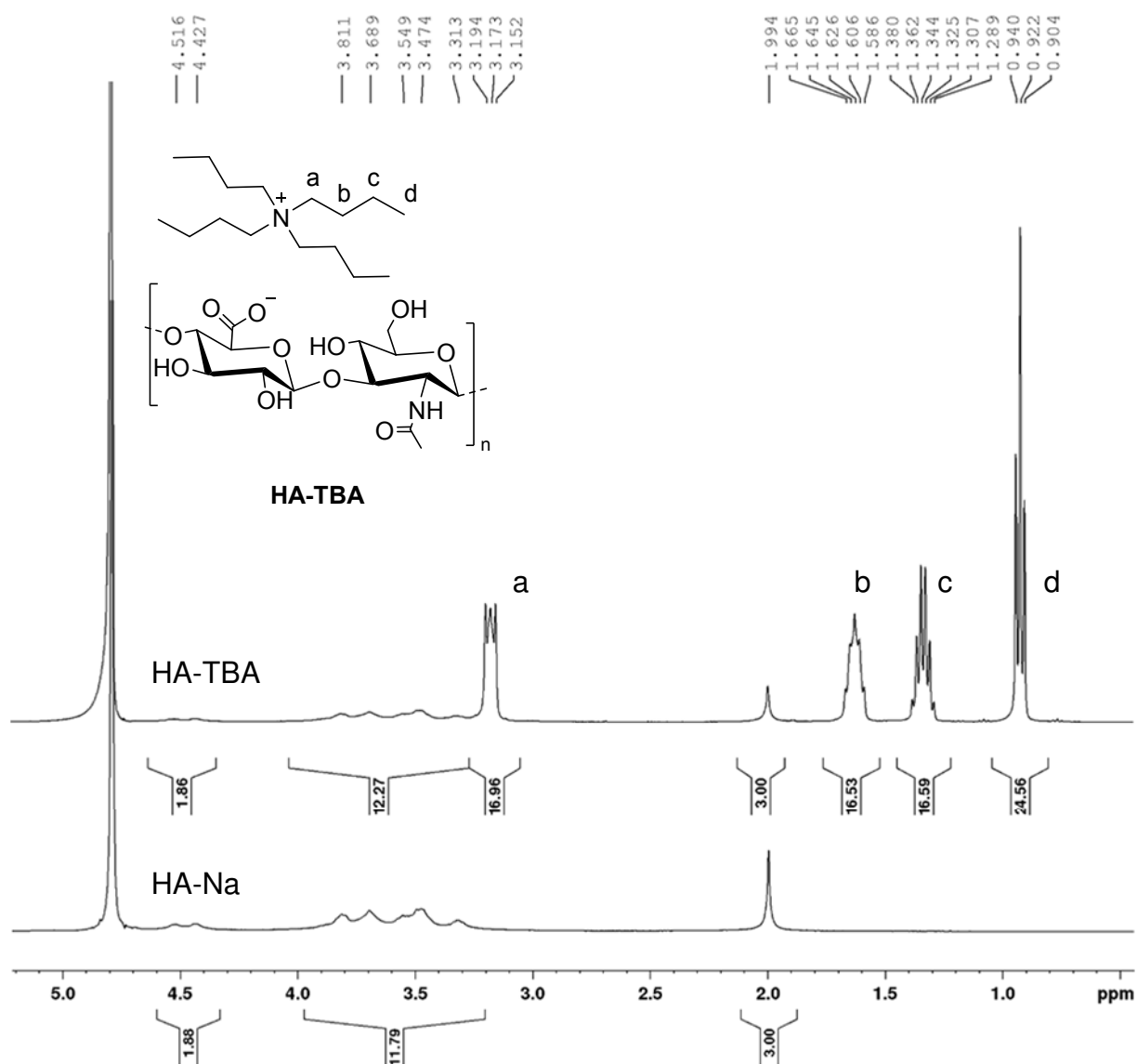


Figure 32: ¹H-spectrum (D₂O) of HA-TBA compared to HA-Na (MW = 150 kDa)

The additional 4 signals (marked with a-d) of the TBA can be clearly seen, whereas characteristic CH₃ signals are located at 0.9 ppm, whereas the CH₂ signals (marked with a-c) are more down-shifted. As the integrals show, hydrogens derived from TBA have double the desired value than it would be for a pure compound. This means, the product might be contaminated with residual TBA-OH from the neutralization step, although high caution was held to set the pH to 7.0 for every batch. An additional dialysis step would help to remove excessive TBA. However, the removal of TBA is not primarily important in this step, as excessive TBA will be removed during the following work up.

Table 2: Overview of the yields of synthesized HA-TBA batches, where the HA backbone length is depicted by the number average of the molecular weight (\overline{M}_n)

\overline{M}_n [kDa]	Yield [%] [#]
22	98 ^a
77	98 ^a
100	96 ^a
150	99 ^a
180	95 ^b
540	98 ^b

[#] still contains TBA

^a performed in a 3wt% solution regarding HA

^b performed in a 1wt% solution regarding HA

2.3 Synthesis of HA Vinyl Ester

Synthesis of HA vinyl ester (HAVE) was performed in anhydrous freshly distilled DMSO, to avoid hydrolysis of DVA and ensure solubility of DVA and HA-TBA in the reaction mixture. Moreover, all reaction steps were performed under Ar-atmosphere. Therefore HA-TBA was dissolved in DMSO to achieve a 2 wt% solution for the first batch (540 and 180 kDa) and a 4 wt% solution for the 2nd batch (77, 100, 150 kDa) regarding HA-TBA. Beads of immobilized lipase (CAL-B), hydroquinone as a radical-inhibitor and 3 eq. of DVA for the first batch (540 and 180 kDa) and 6 eq. of DVA for the 2nd batch (77, 100, 150 kDa) referring to HA-TBA were added under Ar-counter flow. The enzymatically driven transesterification reaction is shown in Figure 33 and was performed at 50 °C due to increased activity of the enzyme at mentioned temperature.¹²⁴

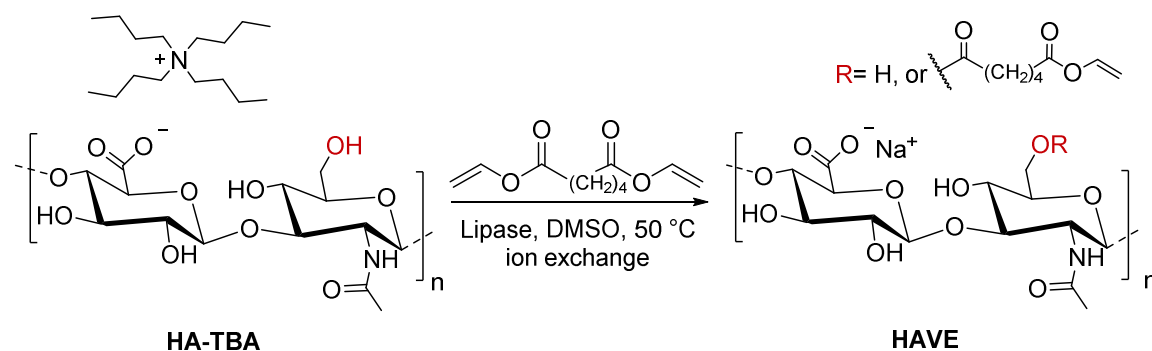


Figure 33: Enzymatically driven transesterification reaction of HA-TBA with divinyl adipate

After certain reaction times (shown in Table 3) a defined amount of reaction mixture was taken out of the vessel and CAL-B separated by suction filtration. The viscous solution was precipitated in excessive amounts of ice-cold EA. Alternatively 2-propanol can be used as a precipitating agent. By precipitation and thoroughly washing of the precipitate, residual amounts of DVA and DMSO can be separated from the reaction mixture. The cream-colored product was received and the solvent was separated by centrifugation and decantation. After the precipitate was dried in vacuo, purification and ion exchange was performed by dialysis. The dried precipitate was dissolved in demineralized water and the solution transferred to dialysis tubes with a molecular weight cutoff (MWCO) of 50 kDa (MWCO for HAVE with 22 kDa was 3.5 kDa). Ion exchange was realized by dialysis first against NaCl solution and second against demineralized water. Both solutions were changed at least 7 times, after the equilibrium was set for 3h. Finally, the solution was

transferred into a vessel, frozen with liquid nitrogen and lyophilized to receive a solid white product. An overview of the synthesized HAVEs is displayed in Table 3. Characterization of the products was performed by $^1\text{H-NMR}$ analysis in D_2O and in D_2O with the addition of NaOD . As mentioned earlier the well-separated signal at 2.0 ppm, representing the CH_3 signal of the acetyl group of the HA backbone, is used as a reference for the determination of the degree of substitution (DS). By building a relative ratio between the integrated peak area under the acetyl proton and that of the vinyl unsaturated proton at 7.1 ppm, quantification of the DS was possible. Figure 34 shows, the increase of DS when reaction time of the transesterification is increased.

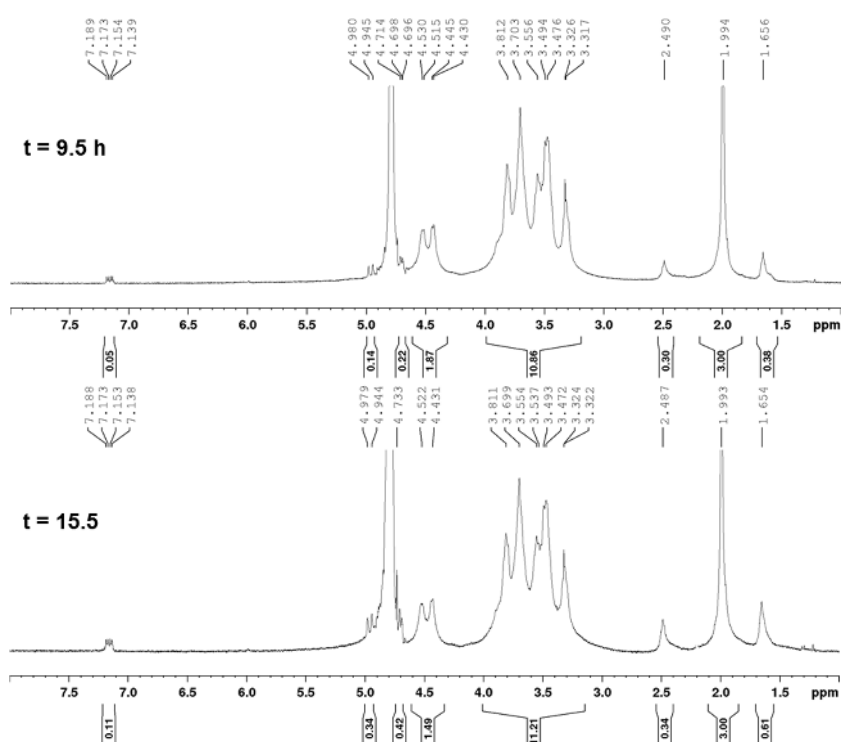


Figure 34: $^1\text{H-NMR}$ of HAVE (77 kDa) in D_2O after 9.5 h (top) and 15.5 h (bottom) lipase reaction time and the increase of vinyl signals at $\delta = 7.1$ ppm

Moreover, it can be seen that ion exchange via dialysis was complete because no residual TBA signals are present in the HAVE spectrum.

As it is known that the hydrodynamic radius (R_h) of HA in solution can be used to direct the system towards lower viscosity,¹²⁵ the effect of the addition of NaOD to HAVE solution was investigated.

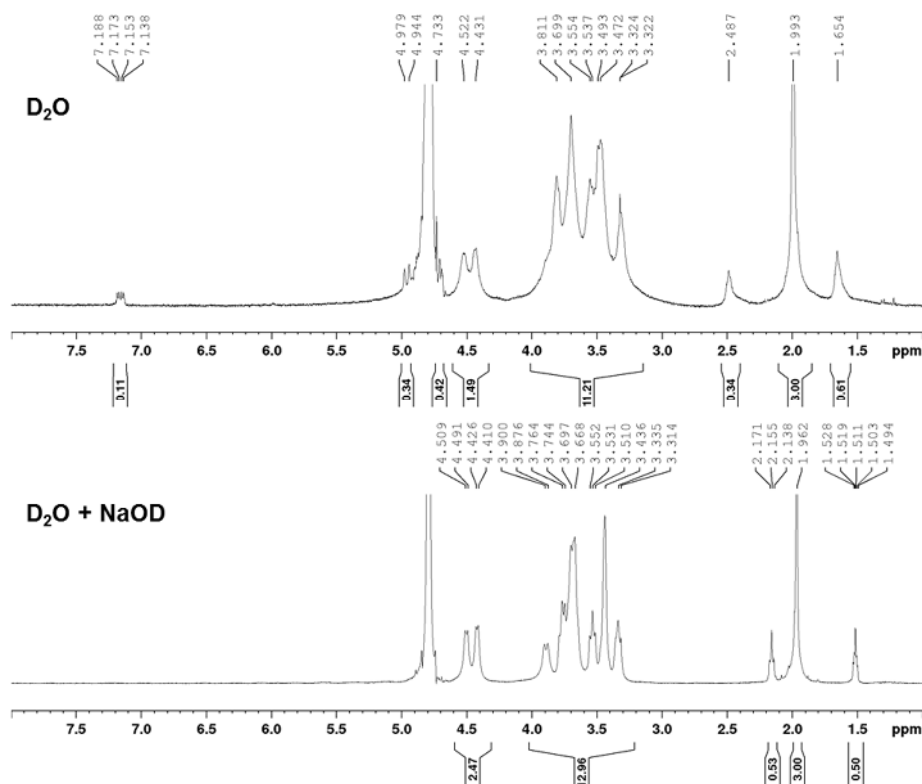


Figure 35: ¹H-NMR of HAVE (77kDa) in D₂O and the influence of NaOD addition

As can be seen in Figure 35 the addition of NaOD to HAVE in solution has a tremendous effect on the resolution of the spectrum. As the R_h of HA decreases the viscosity of the solution is lowered and the resolution of the spectrum significantly increased. Furthermore, Figure 35 shows that the vinyl signal at 7.1 ppm is missing when NaOD is added. This can be explained by the basic hydrolysis of the VE, the cleavage of the vinyl groups and the following release of acetaldehyde. The partial substitution of the primary OH of the HA backbone with vinyladipate substituents was already confirmed by the spectra of HAVE in D₂O and therefore confirmed the successful synthesis. Due to following arguments, the quantification of DS was chosen to be performed by using the ¹H-spectrum of HAVE in D₂O with the addition of NaOD. Figure 35 shows a very good consistency of the two integrals at 1.5 and 2.1 ppm representing the CH₂ signals of the vinyladipate substituents. At the bottom of Figure 35 both peaks show integral

values of 0.5 whereas for the top the signals show divergent values for the same protons also due to lower signal to noise ratio. Consequently, the bottom spectrum can be used for the quantification of the DS. In the end the well-separated signal at 1.5 ppm was referenced to the acetyl signal at 2.0 ppm. Thereafter, a value of the integral of 0.5 which represents 4 protons of the adipate, result in a value of 0.125 corresponding to a DS of 12.5%. HAVE was also synthesized alternatively by transesterification reaction without lipase. The results can be found in the Appendix. The complete list of synthesized HAVE samples with their corresponding DS are displayed in Table 3.

Table 3: Overview of the yields of synthesized HAVEs with different number average of the molecular weight (\overline{M}_n), lipase reaction time (t) and the resulting degree of substitution (DS)

\overline{M}_n * [kDa]	t [h]	DS [%]	yield [%]
22	96.0	14	97
	24.0	21	80
	96.0	40	93
	192.0	95	99
77	9.5	7	94
	15.5	13	
100	9.5	6	89
	15.5	9	
150	9.5	20	86
	15.5	27	
180	16.0	29	97
540	16.0	25	65

* of HA before modification

3 Characterization of Hydrogel formulations by Photorheology

Photoreology was used to determine the reactivity of synthesized hydrogel precursors and their mechanical properties during hydrogel formation. Rheological measurements also give an idea about the suitability of HAVE precursors for 2PP application. Although one photon absorption (1PA) is measured by this technique, it can be used to screen different parameters and investigate optimal formulations. As a photoinitiator lithium phenyl(2,4,6-trimethylbenzoyl)phosphinate (Li-TPO)⁷⁰ was used due to high water solubility and good biocompatibility, as described in

section 3.3.2.1. For the preparation of HAVE formulations, phosphate buffered saline (PBS) was used as a medium, to simulate a natural cell medium as good as possible.

Photophysical measurements were conducted for each precursor solution at least in triplicate to obtain Storage (G') and Loss Modulus (G'') as a function of irradiation time. Polychromatic UV light with a filter of 320-500 nm was used to irradiate the sample through the bottom of a glass plate. The system was subjected to different frequency (1 or 10 Hz) and strain (1% or 10%) values in oscillatory mode and measurement parameters were obtained during increasing extent of gelation. A schematic setup for the photophysical measurement is displayed in Figure 36 and further details on the setting can be found in the corresponding section of the experimental part.

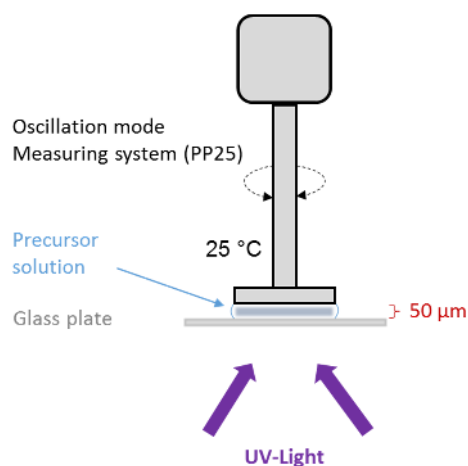


Figure 36: Schematic setup for photophysical measurements, using a disposable aluminum measuring plate with a diameter of 25 mm (PP25)

Photophysical served as a method to investigate the crosslinking density of the hydrogel based on the storage modulus derived from rheological measurements. Additionally, the reactivity of a system can be determined by the slope of the storage modulus. Generally, this photophysical rheometer is a system, where FT-IR coupling and *in situ* determination of double bond conversion is possible. This technique could not be used for highly diluted hydrogel systems which are used in this thesis. A typical photophysical measurement is shown in Figure 37.

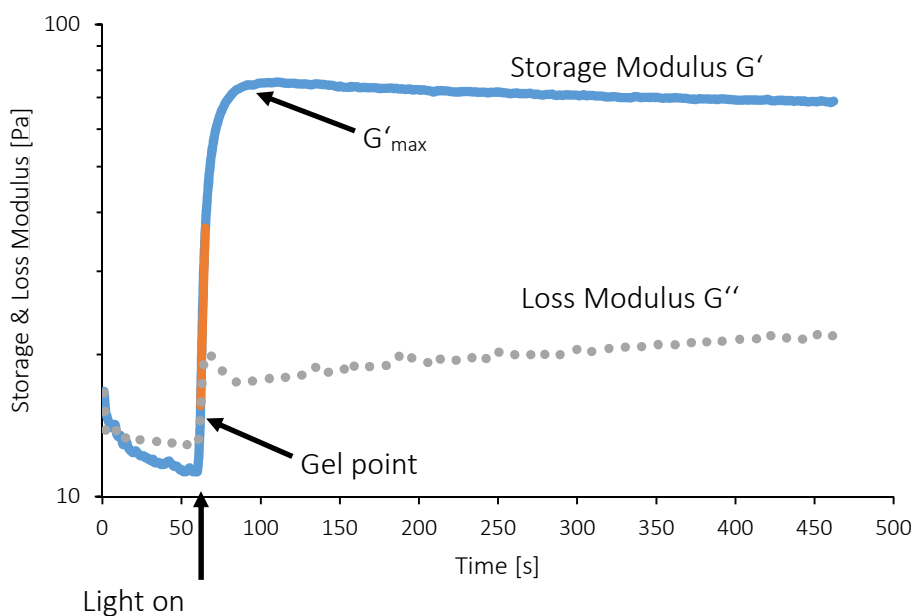


Figure 37: Exemplary photorheological measurement and the determination of the maximum storage modulus (G'_{\max}), the slope of the linear fit and the gel point

The maximum storage modulus (G'_{\max}) was determined by evaluating the maximum value of G' after irradiation with light. Additionally, each curve of G' was fitted with a line in the linear region between the start of irradiation and the convergence to G'_{\max} , so that the value of the correlation coefficient R^2 exceeded 0.98. This slope ($\Delta G' \Delta t^{-1}$) of the linear fit was taken as an indicator for the reactivity of the formulation. The gel point can also be determined as a further parameter to characterize hydrogel precursor formulations. Per definition, the gel point occurs, where the elastic- exceeds the viscous component (the intersection of G' with G'').¹²⁶ Figure 37 shows the evaluation of the delay time (t_d) which is a measure to determine the affinity for the formulation to gel.

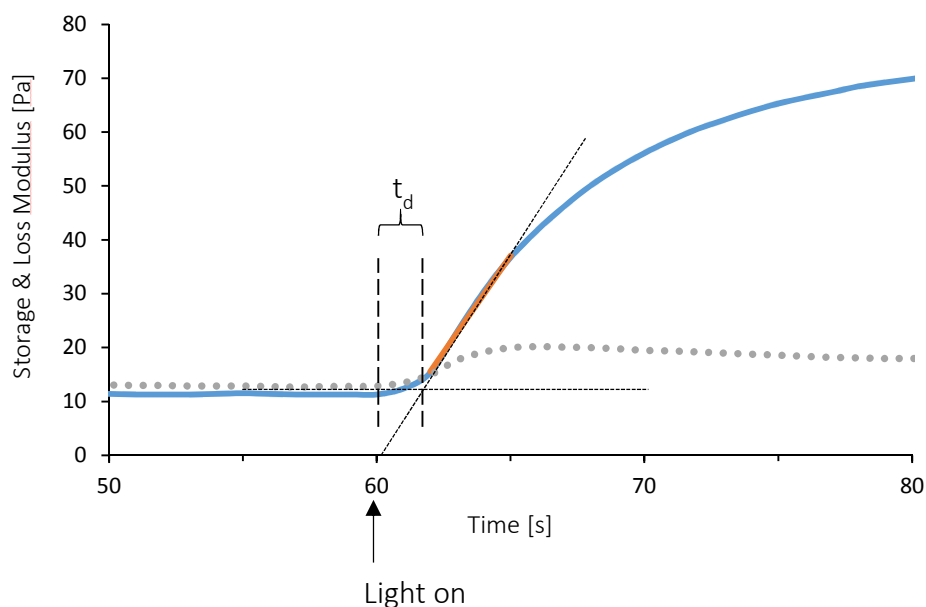


Figure 38: Determination of the delay of initiation (t_d) by using the intersection of the linear fit (orange) of the slope of the storage modulus (blue) and the linear fit of the storage modulus before irradiation (horizontal dotted line)

The intersection between the linear fit of the slope and the linear fit of the base line of G' was used to investigate the time (t_d) which the formulation needs, to react to the initiation impulse (irradiation with UV light). An ideal formulation would show all of the above mentioned determinable parameters. However, some for some of the formulations within this thesis, the gel point was not evaluable, as some formulations already showed a G' , exceeding G'' before the sample was even irradiated with UV light (Figure 39). The increased values for G' compared to G'' indicate the presence of a physical gel of the initial precursor formulation.

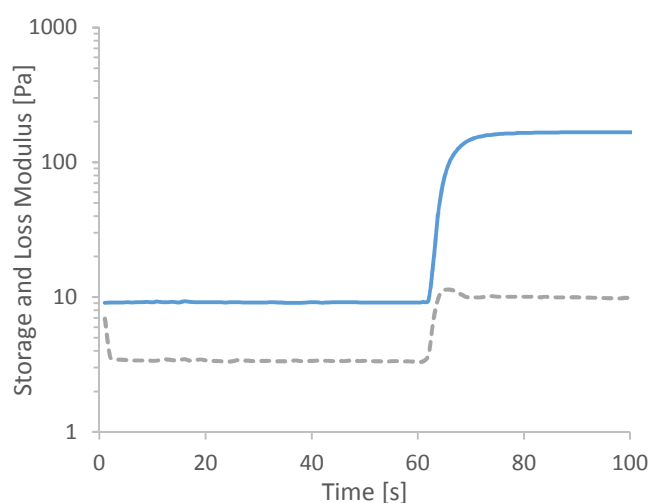


Figure 39: Precursor solution where the storage modulus (continuous line) exceeds the Loss Modulus (dotted line) in the beginning of the measurement (MW = 100 kDa, DS = 9%, 3 wt% macromer content, 80 mol% thiol-ene ratio of DTT)

Some formulations with very high MW showed the presence of these physical networks, indicated by a very high initial G' values. As stated in literature weak physical gels are shear sensitive and can therefore show a significant decrease of G' , at the critical strain close to the gel point.⁴⁰ The critical strain value is the point at which a viscoelastic material is dependent of strain. Beyond the critical strain level the materials shows non-linear behavior, which results in a decrease in G' . Those material characteristics are a reason why measurement parameters, like frequency and strain, need to be adjusted before samples are analyzed in detail. Optimal rheological conditions would lead to a significant characterization method for the gel point of a formulation. According to Shah et.al.¹²⁷ viscous properties expressed by G'' can be increased, by increasing the strain. Derived from this, the elastic properties, expressed by G' , could be lowered and the gel point eventually determined for most of the formulations. As these adjustments are beyond the scope of this thesis, the gel point could not be taken into consideration to compare systems in following section.

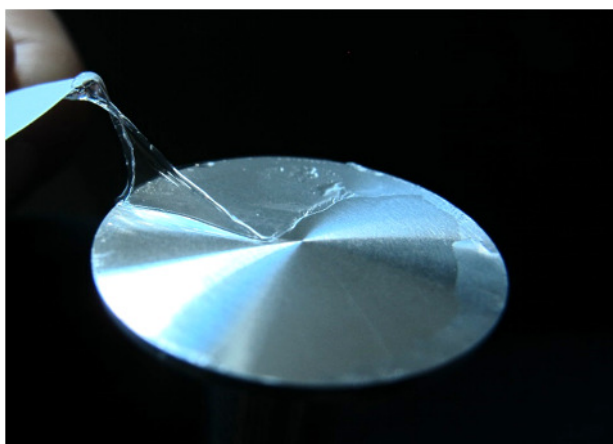


Figure 40: Exemplary formulation after photopolymerization on a measuring plate

3.1 Storage Stability

Stability tests for HAVE formulations were performed to determine the influence of storage on the mechanical properties of the hydrogel. Storage behavior can be used as an indication for the impact of different matrix components onto each other. Interactions or reactions between macromolecules or a change in reactivity of stored compounds can influence hydrogels properties. However, no studies have been made, which investigate storage stability and in consequence photoreactivity of stored HAVE formulations. The experiments were performed by combining hydrogel components, such as HAVE macromer, the crosslinking agent (thiol) and the photoinitiator (Li-TPO) in phosphate buffered saline (PBS). Hydrogel formation of these formulations was investigated (t_0) via photorheology. Afterwards, the initial formulation was stored in the fridge for 48h. Hereafter, the same precursor solution was set to room temperature, homogenized by vortex mixing and analyzed again via photorheology (t_1) (Figure 41). HAVE with a MW of 77 kDa and a DS of 13% was chosen for this experiment using 80 mol% thiol-ene ratio, with DTT as thiol component. For the calculation HAVE was considered as the ene component and represents 100 mol%.

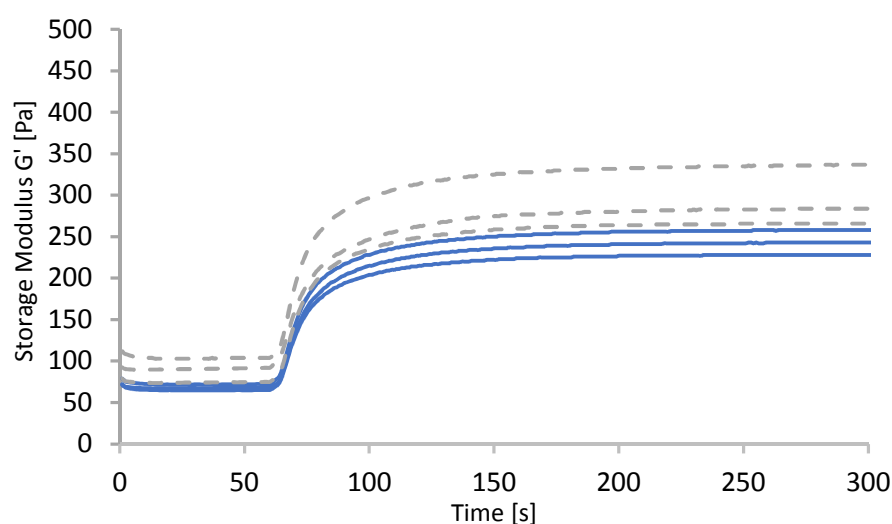


Figure 41: Storage modulus curves of HAVE formulation (77kDa, DS = 13%, 3 wt% macromer content, 80mol% thiol-ene ratio of DTT) measured directly after mixing (t_0) (—) and after storage for 48h (t_1) (---)

The initial formulation (t_0) shows quite reproducible results, whereas for the stored formulation (t_1) rather big deviations from t_0 -measurements are observed (Figure 42 a and b). In order to assure reliable results about storage behavior, G' during the first 60 s of a measurement (G'_{start}) need to be considered (Figure 42 a).

The precursor solution is therefore studied right before photopolymerization and G'_{start} values were compared with G'_{max} values.

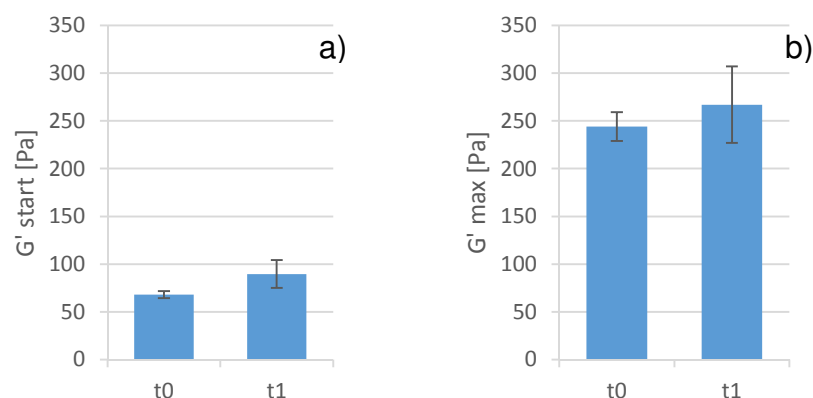


Figure 42: Storage modulus a) before UV irradiation (G'_{start}) and b) maximum storage modulus (G'_{max}) after UV irradiation of the formulation measured directly after mixing (t_0) and after storage for 48h (t_1)

Besides G'_{start} , the final storage modulus of the formulation was studied via G'_{max} (Figure 44b). In both cases, not only higher deviations, but also higher average values for G'_{start} and G'_{max} were observable for the stored formulation (t_1). Delay of initiation and the slope of G' within the linear fit were also determined within this experiment (see Appendix - Figure 70).

Measurements for t_1 show higher values for the deviation for all determined parameter (G'_{max} , G'_{start} , t_d and $\Delta G' \Delta t^{-1}$). These effects can be explained by the development of a physical gel during storage. It is unlikely that some of the PI molecules already cleaved and started the polymerization, since the solution was stored in darkness. Furthermore, the storage stability of Li-TPO was already investigated by Benedikt et.al.⁷⁰ and reported to be satisfying for neutral conditions. Therefore, radical induced thiol-ene reactions is unlikely to be a reason for the increased value of G'_{start} . Another possibility for higher G' values after storage could be already occurring reactions between reactive groups. Usually, HAVE macromers are reacting very fast with thiols under the presence of radicals. However, they could anyway undergo a slow reaction, which cannot be excluded during storage for a longer period. Besides higher G' values for the formulation stored for 48h, the deviation of the triplicate measurements shows higher values, than the measurements performed right after mixing of the solution. Any crosslinking reaction occurring during storage within the system, leads to

inhomogeneity of the precursor solution, resulting in a rise of deviation between single measurements.

To investigate the MW behavior during storage, gel permeation chromatography (GPC) measurements were performed. Therefore, a 3 wt% stock solution of HAVE (77 kDa DS = 13%) was prepared and left to dissolve overnight. The solution was divided by half on the next day and one part was measured immediately either with or without beforehand vortex mixing. The GPC samples with a concentration of 0.5 mg/ml were prepared by diluting 50 μ l of the precursor solution with 2.95 ml of GPC buffer. Cloudiness was observed for all samples, indicating limited solubility, which was confirmed by inconsistent GPC results.

To ensure best results for photorheology experiments, following mode of operation was set within this thesis. Stock solutions of HAVE macromers, photoinitiator and corresponding crosslinking agents were homogenized independently from each other in PBS stock solutions and only combined right before measurement. Accordingly, premature gelation is minimized and optimum results can be achieved. Minimizing handling errors for the sample preparation, further characterization of hydrogel properties can be ensured, as discussed in following section.

3.2 The Effect of Thiol Component

As already described in section 3.3.1.3 of the introduction, the reactivity of VE moieties can be improved by using radical induced thiol-ene Chemistry.⁶⁰ Two water soluble commercially available thiols were tested for the development of biocompatible hydrogels (Figure 43).

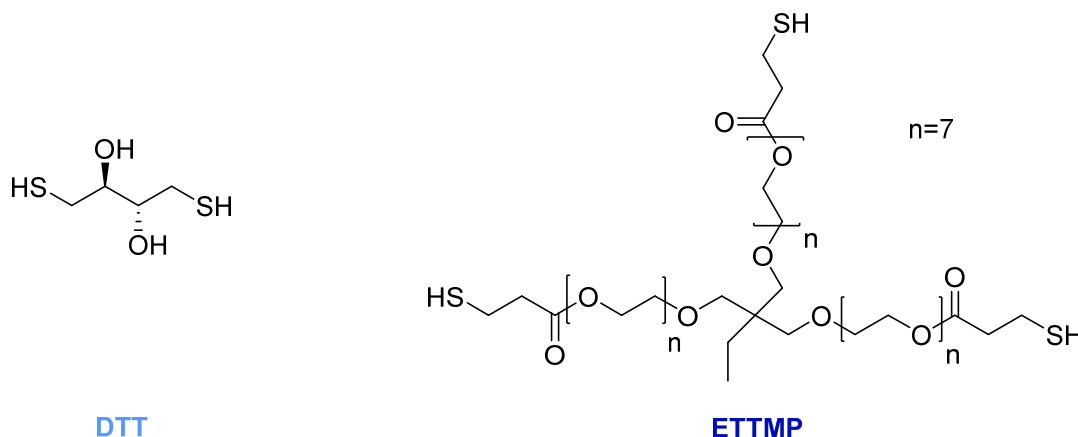


Figure 43: Thiols tested within this thesis as crosslinking agents towards their effect on hydrogel properties (DL-dithiothreitol (DTT) and ethoxylated trimethylolpropane tri(3-mercaptopropionate) (ETTMP))

The difunctional thiol, DL-dithiothreitol (DTT) was compared with a trifunctional alternative, ethoxylated trimethylolpropane tri(3-mercaptopropionate) (ETTMP). In case of the homopolymerization of HAVE macromers, the reaction mechanism follows a free radical polymerization, but by the use of thiol-ene chemistry, this reaction mechanism is shifted towards a step-growth mechanism,⁶⁰ leading to following advantages. Increased reactivity, as well as conversion and reduced sensitivity of the formulation to oxygen inhibition are beneficial for the formation of hydrogels.⁹¹ Within this chapter the variation of the thiol component on hydrogel properties should be studied. The optimal thiol-ene ratio of 80 mol% compared to ene moieties for HAVE formulations was already investigated in former studies within the research group¹⁰⁵ and was therefore used for all formulations within this thesis. For ETTMP stock solutions turbidity was observed due to limited solubility of the high-MW ETTMP. Low-MW HAVE formulations (22 kDa, DS 40%) with three different macromer contents (MC) (5, 10, 15 wt%) were tested.

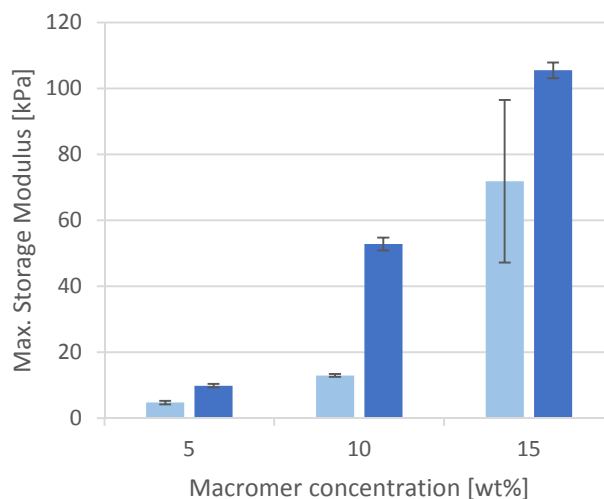


Figure 44: Maximum storage modulus of HAVE 22 kDa DS = 40% with different macromer Content (5, 10, 15 wt%) comparing DTT (light blue) and ETTMP (dark blue)

Every macromer formulation shows a higher G'_{max} , for formulations containing 80 mol% thiol-ene ratio of ETTMP instead of DTT. This leads to the assumption that the higher MW thiol (ETTMP) with its longer chain length can form a hydrogel network with higher crosslinking density. This can be first explained by the fact, that ETTMP compared to DTT is a higher functional thiol with more reactive groups per molecule. Therefore, the higher functionality of the crosslinking agent, increases the possibility, that one thiol reacts with the double bond of the vinyl ester. Not only the higher functionality, but also the increased spatial proximity is a reason for the increased crosslinking density. With increasing MW of the thiol, the distance between two complementary reactive groups is decreased and therefore the spatial proximity increased, which facilitates the reaction between two potential reactive groups (thiol and ene). The higher the MW of the thiol, the more likely the two reactive groups will undergo thiol-ene reaction. In other words, while one side of the relatively short difunctional DTT has already reacted, the second thiol of the same molecule is less likely to undergo reaction with a second VE group, due to too large distance between reactive thiol and VE groups. Furthermore the potential repulsion of HA chains can be a reason for decreasing crosslinking density. While one functionality of the DTT molecule is already attached to a HA chain, because of its reaction with VE groups, the other functional group of the same DTT molecule has a lower possibility to undergo a reaction with a second VE group of another HA chain. The repulsion of the two HA backbones might be too strong, to allow a reaction of both thiol functionalities of one DTT molecule. Although an increase in

MW of the thiol would generally lead to an increased mesh size of the hydrogel network and therefore to a decreased crosslinking density, these effects were not observed. Due to the above mentioned “blocking” of VE groups, by the reaction of one side of the DTT molecule, the crosslinking density is so much decreased, that ETTMP shows a better performance than DTT. Using ETTMP as crosslinking agent, the conversion of thiols can be increased by providing a higher possibility for thiol-ene reactions. Lower G'_{\max} values for formulations containing DTT, instead of ETTMP are obtained for all tested HAVE macromers (22, 77 and 100 kDa – see Appendix)

Besides the influence of different thiols on G'_{\max} , the slope ($\Delta G' \Delta t^{-1}$) and the delay of initiation (t_d) were also investigated regarding hydrogel properties (see Figure 45 and Figure 46).

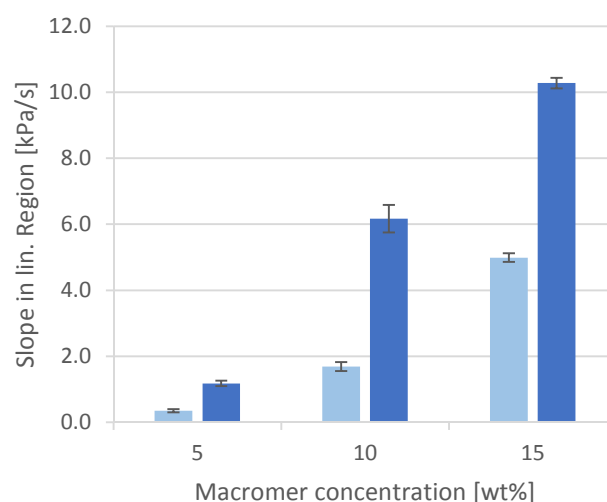


Figure 45: Slope in the linear region of the storage modulus of HAVE 22 kDa, DS 40% with different macromer content (5, 10, 15 wt%) containing 80 mol% thiol-ene ratio of DTT (light blue) or ETTMP (dark blue)

The slope of G' during photopolymerization can be seen as an indicator for the reactivity of the hydrogel system. The presence of ETTMP significantly increases reactivity for nearly all tested HAVE formulations (see also Appendix). The reason for the increased reactivity can be again explained by the increased spatial proximity and number of functional groups for systems containing ETTMP compared to DTT.

The affinity to gel, represented by the delay of initiation, is another indication for the reactivity of a system. Formulations containing ETTMP instead of DTT show significantly lower values for the delay of initiation (see Figure 46).

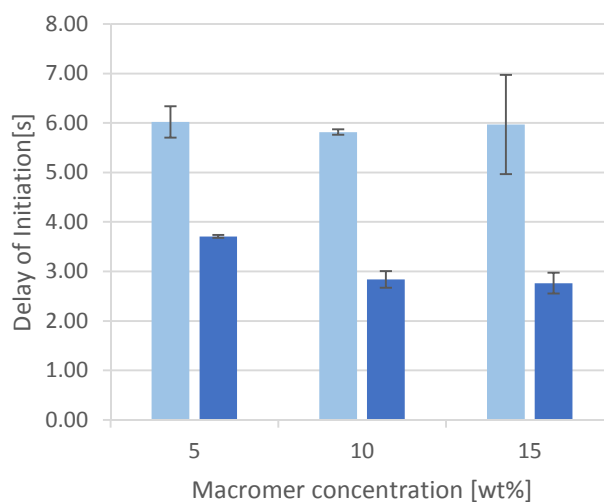


Figure 46: Delay of initiation of HAVE 22 kDa DS 40% with different macromer content (5, 10, 15 wt%) containing 80 mol% thiol-ene ratio of DTT (light blue) or ETTMP (dark blue)

The MW of the thiols is amongst the tri-functionality one major factor for the promising performance of ETTMP towards hydrogel mechanics.

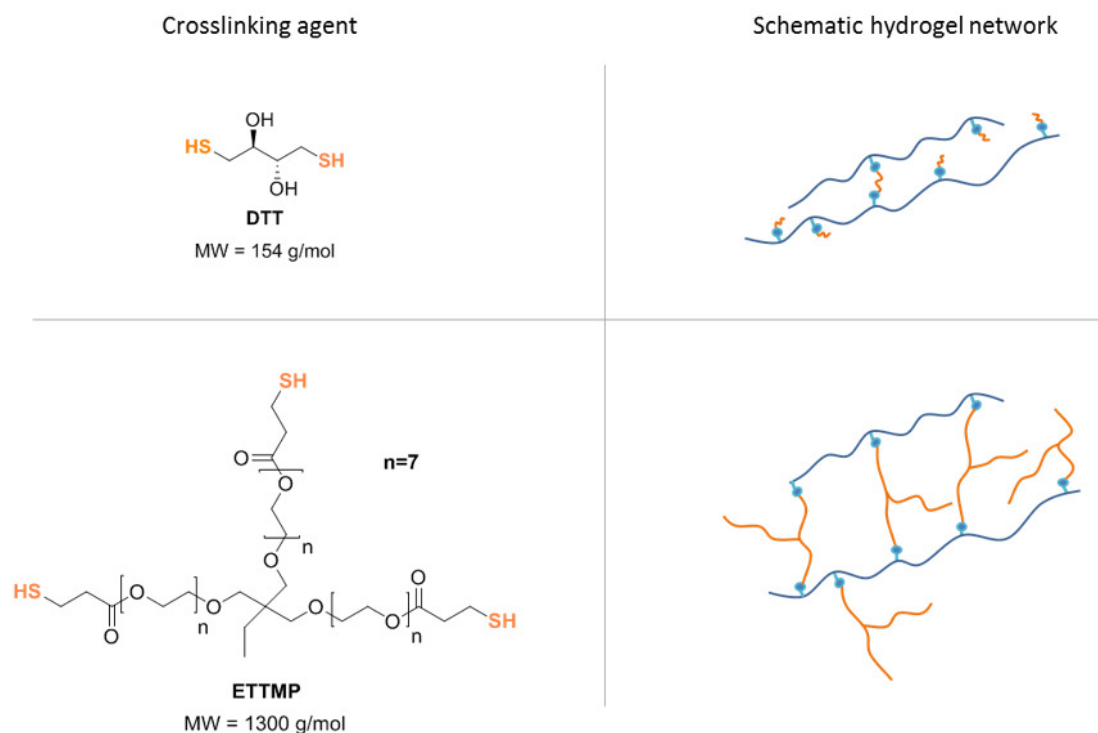


Figure 47: Schematic representation of the correlation between MW of thiols and the final hydrogel network

The crosslinking density as well as the reactivity of the hydrogel system could be increased by the use of ETTMP as crosslinking agent. One reason for the improved results is thought to be the prevention of blockage of vinyl functionalities within the system. The relatively low-MW DTT, with its short backbone, can easily diffuse within the formulation, reacting with VE groups until most of the DTT molecules are reacted. If one thiol of the difunctional molecule is already reacted, the second thiol is less likely to undergo a reaction with a second VE group, due to limited spatial proximity for those groups, especially for HAVEs with low DS, as very few VE groups are available for these macromers. For this reason, the crosslinking density of the final hydrogels is limited by lowering the possibility for further crosslinking reactions. By using relatively high-MW ETTMP within the formulation, these effects can be avoided by increasing the spatial proximity between potential reactive groups, by an increased chain size of the crosslinking agent.

Overall, photorheology measurements led to the conclusion, that the use of ETTMP as crosslinking agent shows more promising results towards tuned hydrogel properties, than the use of DTT. Consequently, the focus was laid on HAVE formulations containing 80 mol% thiol-ene ratio of ETTMP.

3.3 Variation of Parameters

After the investigation of influence of different matrix components and their impacts on the mechanical properties of the hydrogel, following chapters focus on the effects of varying different parameters onto hydrogel properties, such as the macromer content, the degree of substitution, the macromer chain length and the number of vinyl groups per chain.

3.3.1 The Effect of Macromer Content

Not only high-MW thiols, with increased functionality (as discussed in Section 3.2) can be used to tune hydrogel properties, but also the increase of the macromer content (MC). HAVE with a MW of 22 kDa and DS 40% was used to further investigate the effect of the MC of HAVE on hydrogel properties. Therefore, concentrations of 5, 10 and 15 wt% regarding HAVE were prepared, containing 80 mol% thiol-ene ratio of ETTMP for every formulation. The results of photorheology experiments are depicted in Figure 48.

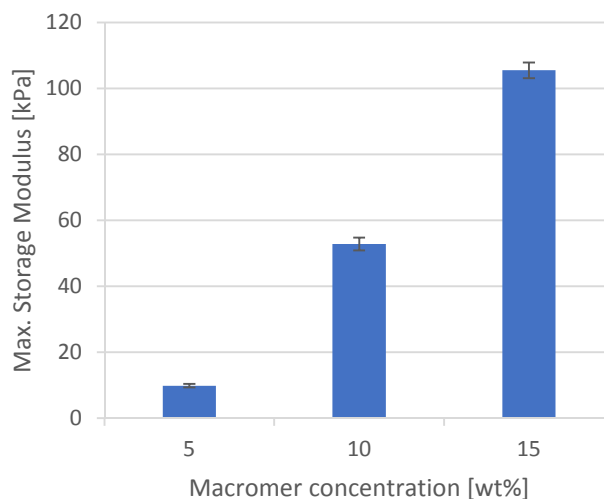


Figure 48: Maximum storage modulus of HAVE (22 kDa, DS 40%) with varying macromer content (5, 10, 15 wt%) containing 80 mol% thiol-ene ratio of ETTMP

An increasing trend of G'_{\max} values is observable, if MC is increased. Formulations containing 15 wt% HAVE show significantly higher G'_{\max} values, than formulations with 10 and 5 wt%. This can be explained by the availability of more reactive double bonds, for higher MC values. The more HAVE is present, the more functional groups are available and the higher the crosslinking density, demonstrated by increasing value for G'_{\max} . This trend is consistent for all HAVE formulations (see Appendix). Increasing MC also leads to an increase of the slope of G' within the linear region of the measurement. Higher values indicate a higher rate of polymerization, leading towards a system with higher reactivity (see Figure 49).

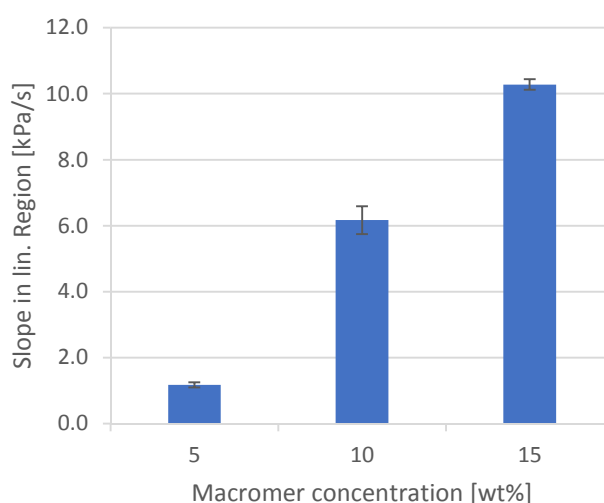


Figure 49: Slope in the linear region of the storage modulus for HAVE (22 kDa, DS 40%) with varying macromer content (5, 10, 15 wt%) containing 80 mol% thiol-ene ratio of ETTMP

The results of higher values for the slope of G' indicates a promising trend towards boosting the hydrogel kinetics, via MC. Additionally to the slope of G' , the delay of initiation has been studied via photorheology (Figure 50). An increase of MC leads to lower values for the delay. By providing a higher number of macromer chains, the crosslinking reaction is facilitated and leads to a more reactive hydrogel system.

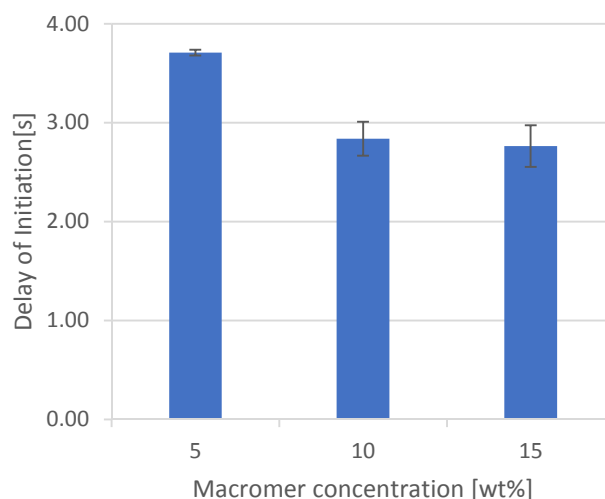


Figure 50: Delay of initiation for HAVE (22 kDa, DS 40%) with varying macromer content (5, 10, 15 wt%) containing 80 mol% thiol-ene ratio of ETTMP

In conclusion, an increase of MC, along with constant values for MW and DS, leads to a more reactive hydrogel system, represented by low values for the delay of initiation.

The increase of MC for HAVE with a DS of 95% resulted in very brittle hydrogels. Detachment of the hydrogel within the measuring system was observed (see Appendix - Figure 115 - Figure 117). These formulations reached very high G' but showed a sudden loss of G' because of delamination of the formulation from the glass plate of the rheometer. For formulations with DS of 21 and 40%, no detachment effect could be observed. In the following section 3.3.2 a macromer content of 10 wt% was chosen, to visualize the effect of the degree of substitution more clearly.

3.3.2 The Effect of Degree of Substitution

To investigate the influence of the number of functional groups per macromer on hydrogel properties, studies have been conducted to examine the effect of the DS on HAVE networks. As the DS determines the crosslinking density of the hydrogel three different DS for low-MW HAVE (22 kDa) values are presented within this section and discussed in detail concerning their effect on G'_{max} , slope of G' and the delay of initiation. Results for formulations containing 10 wt% of HAVE with a DS of 14, 21 and 40% are compared within subsequent figures. The results for formulations with 5 and 15 wt% HAVE are shown in the Appendix (Figure 74 - Figure 82)

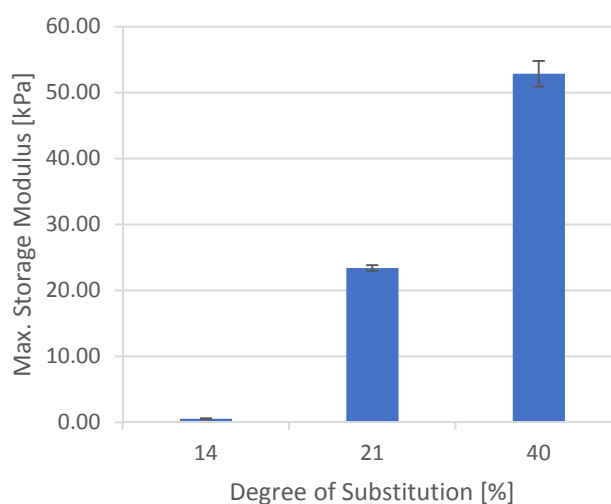


Figure 51: Maximum storage modulus of HAVE (22 kDa, macromer content = 10 wt%) with varying DS (14, 21 and 40%) containing 80 mol% thiol-ene ratio of ETTMP

Experiments showed an increase in G' with higher DS leading to values of G' above 50 kPa for HAVE with a DS of 40%. Since G' indicates the crosslinking density of the formed hydrogel and the crosslinking density correlates with the number of reactive double bonds, the effect of increasing G' by increased DS seems reasonable. In the end the higher the DS the more reactive double bonds are provided and a higher crosslinking density is observed. Very high numbers of DS and their effect on polymer networks have already been studied in literature.⁴⁴ As the number of crosslinks increases, the rigidity of the polymer network increases and the elasticity decreases. The same effect (delamination), which was observed for increasing MC in chapter above, was seen for increasing DS. HAVE with a DS of 95% resulted in very brittle hydrogels. Detachment of the hydrogel from the

measuring plate during photorheological measurements were observed (see Appendix - Figure 115 - Figure 117). These formulations reached very high G' but showed a sudden loss of G' . Nonetheless hydrogels with a DS of 14, 21 and 40% and a MC of 10 wt% did not show delamination effects.

The effect of different DS on the slope in the linear region of the storage modulus also was studied. The values for the slope increase with increasing value of DS, indicating a system with higher reactivity (Figure 52).

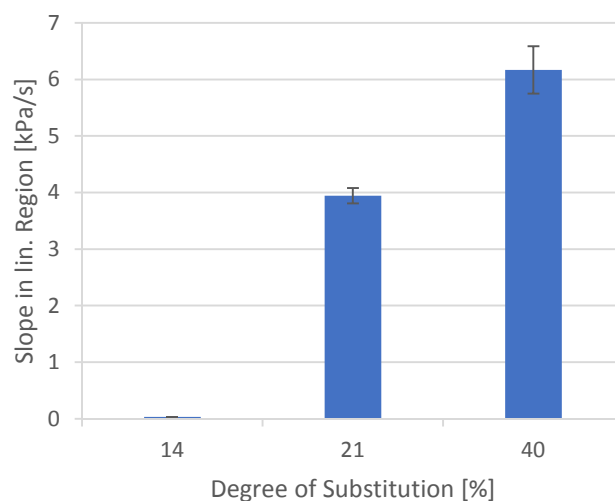


Figure 52: Slope in the linear region of the storage modulus for HAVE (22 kDa, macromer content = 10 wt%) with varying DS (14, 21 and 40%) containing 80 mol% thiol-ene ratio of ETTMP

The same increase in reactivity can be observed, when taking a closer look at the delay of initiation (Figure 53).

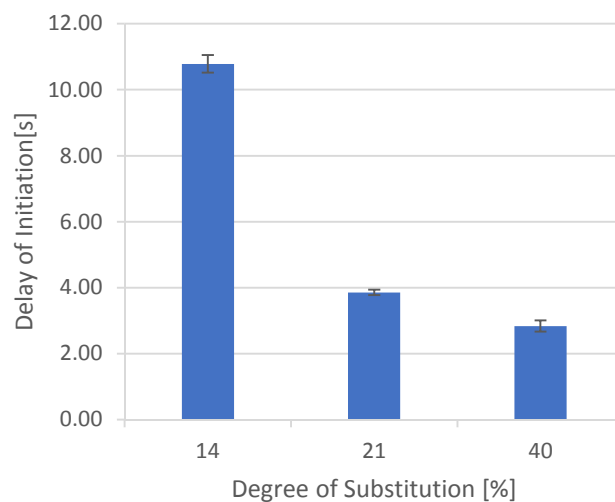


Figure 53: Delay of initiation for HAVE (22 kDa, macromer content = 10 wt%) with varying DS (14, 21 and 40%) containing 80 mol% thiol-ene ratio of ETTMP

Higher DS leads to lower values for the delay of initiation indicating a more reactive hydrogel system. HAVEs with a DS of 40% showed one third of the value of the delay of initiation than macromers with a DS of 14%. The reason for the increased reactivity is the increased number of functional groups, represented by a higher DS.

Investigation of hydrogel properties can be further discussed by examining the effect of the macromer chain length of HAVE macromers in following chapter.

3.3.3 The Effect of Macromer Chain Length

Previous chapters dealt with the investigation of macromer formulations bearing HAVEs with a MW of 22 kDa. Former studies about network properties of HAVE including small macromer chain lengths led to quite high crosslinking densities which increased brittleness of these hydrogels.¹⁰⁵ This increased the demand for more tough hydrogels. One approach for tuning flexibility is the increase of macromer chain length. Due to these longer macromer chains, the elasticity of the network is expected to be increased. High-MW HAVE macromers should lead to effective crosslinking of reactive groups. Therefore HAVE precursors with a MW exceeding 22 kDa were measured and the network density and the reactivity analyzed via photorheology. HAVE with different MW (77 and 100 kDa), but same MC (3 wt%) were compared with each other (Figure 54).

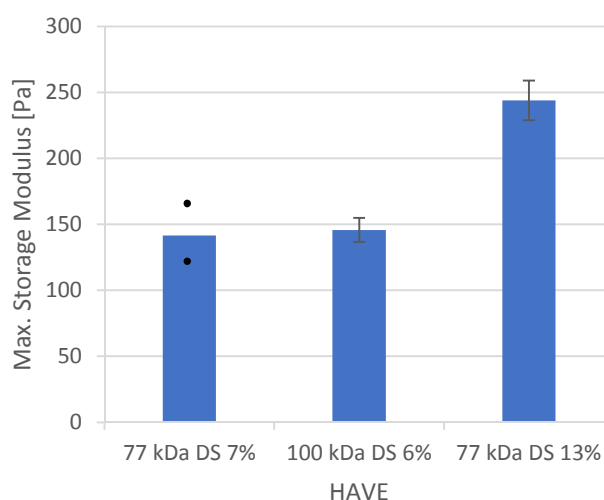


Figure 54: Maximum storage modulus of HAVEs with different MW and DS, but same macromer content (3 wt%) with 80 mol% thiol-ene ratio of ETTMP. The deviation for HAVE (77kDa, DS = 7%) is missing because only two measurements could be used for analysis.

HAVE macromers bearing similar DS (77 kDa, DS 7% and 100 kDa DS 6%) show similar G' values (~ 150 Pa). Compared to previous chapters, investigating low-MW HAVE, G' values were quite low (~ 200 Pa for 3 wt%). Formulations containing 5 wt% for HAVE (22 kDa, DS 40%) showed G' values up to 10 kPa (Figure 48), which is significantly higher than above mentioned formulations (Figure 54). However, the increase of DS for 77 kDa to a value of 13% showed consistent results, as an increasing DS generally leads to a higher crosslinking density and higher G' values. Very high viscosity of the formulation, made it difficult to pipet and resulted in loss of precursor solution. Generally, stock solutions with a MW higher than 20 kDa showed turbidity at any time during formulation preparation. This indicates limited solubility of macromers and research needs to be performed to find appropriate conditions to fully dissolve HAVE macromers.

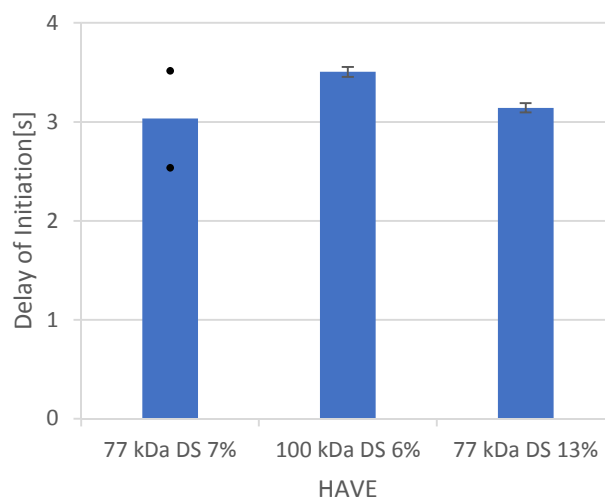


Figure 55: Delay of initiation of HAVES with different MW and DS, but same macromer content (3 wt%) with 80 mol% thiol-ene ratio of ETTMP

On the one hand, HAVE with a MW of 77 kDa and a DS of 13 % showed the highest crosslinking density, whereas on the other hand, the delay of initiation showed similar values as for the compared formulations (Figure 55) and the slope in the linear region of the storage modulus was against expectations rather low (Figure 56).

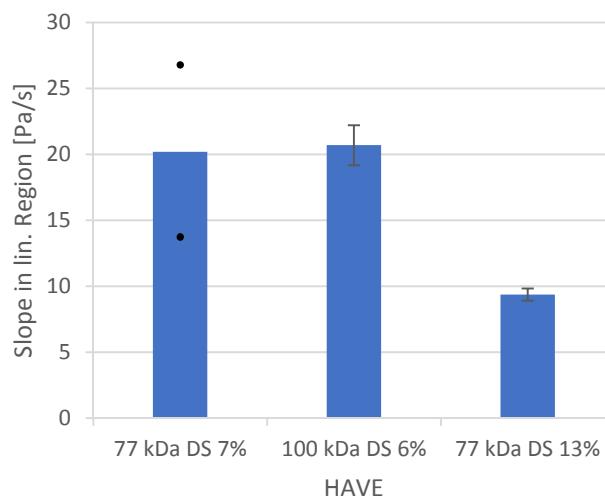


Figure 56: Slope of the storage modulus in the linear region of HAVEs with different MW and DS, but same macromer content (3 wt%) with 80 mol% thiol-ene ratio of ETTMP

Generally, an increase in MW led to solubility problems and bad reproducibility of photorheology measurements. It seems, that the increase of MW influences the system towards a development of a physical network. This is why also solubility issues have been observed for HAVE macromers with a MW of 180 and 540 kDa. Rather low values for MC (1 wt%) were obtained and cannot be compared within this section of this thesis. Furthermore these formulations were measured with DTT as crosslinking agent. They are displayed in the Appendix (Figure 101).

Although unmodified high-MW HA itself is soluble at MW around 100 kDa, the conversion of HA to HAVE increases hydrophobicity, due to the presence of higher amount of hydrophobic functional groups and therefore decreases solubility. It is well known, that the hydrodynamic radius (R_h) of HA plays an important role in the solubility of HA polymers. At semi-diluted or concentrated solutions, the molecular chains overlap, since the hydrodynamic domains of HA are quite large, even at low concentrations.^{128,129} It is possible, that VE modification of HA increases R_h of HA. Due to this, it can be very difficult, to handle HA at rather high concentrations. When hydrophobic interactions between macromolecules increase, the mobility of the chains is drastically decreased and they are not able to flow individually. The formation of a physical gel is therefore hindering the handling of HAVE solutions. Anyhow, high-MW HAVE formulations were further studied, taking the number of functional groups per polymer chains into consideration.

3.4 Hydrogel Network considering Vinyl-Groups per Macromer Chain

An additional determining factor for the characterization of hydrogel networks and their crosslinking density is the number of vinyl functionalities per macromer chain ($n_{\text{vinyl}} [\text{ }^{-1}]$). By this, the hydrogel network can be evaluated in a way, so that the effect of the macromer chain length and DS is eliminated and only the crosslinking of each backbone repeating unit is considered. This method enables the study of G' and consecutively the crosslinking density of hydrogel networks. A higher value for n_{vinyl} means, that more vinyl groups are available per macromer chain, which would theoretically lead to a denser network. The value for n_{vinyl} can be easily calculated for all available HAVEs by consideration of DS and MW of the macromolecules, like it is displayed in Table 4. MW unit indicates the MW of one disaccharide unit of the HA polymer.

Table 4: Overview of number of repeating units $[\text{ }_n]$ and number of vinyl functionalities per repeating unit $n_{\text{vinyl}} [\text{ }^{-1}]$ of HAVE with different molecular weight and degree of substitution

MW unit [Da]	401.36											
MW chain [kDa]	22		77		100		150		180		540	
$[\text{ }_n]$	55		192		249		374		448		1345	
DS [%]	14	21	40	7	13	6	9	20	27	29	25	
$n_{\text{vinyl}} [\text{ }^{-1}]$	8	12	22	13	25	15	22	75	101	130	336	

HAVE formulations with 77 kDa and 100 kDa were measured with a MC of 3 wt%. Each of them are displayed with two different DS and most of them were measured with both thiol components (DTT and ETTMP), except formulation 100 kDa DS 9%, where only DTT is available (Appendix: Figure 104 - Figure 106).

Photorheological measurements are displayed hereafter, whereupon the average values for G'_{max} are displayed in an increasing order for n_{vinyl} for every formulation (Figure 57). Previous work within the research group showed that increasing macromer chain length, led to an increase of G' .¹⁰⁵ This trend can only be studied when macromers with same DS but different chain length are available. For high-MW HAVE macromers synthesized within this thesis (180 kDa, 540 kDa) the solubility was limited to 1 wt%. This is why they cannot be compared with other formulations in this chapter. The results of these measurements are depicted in

Figure 101 to Figure 103 (Appendix). Figure 57 shows G'_{\max} observed from measurements of HAVE macromers with a MW of 77 kDa and 100 kDa.

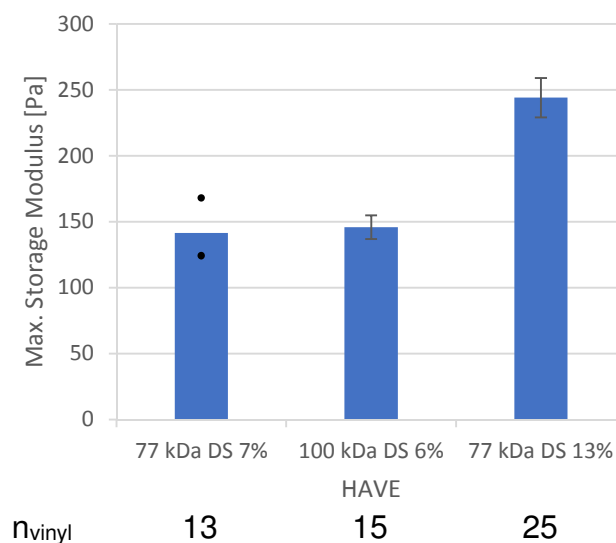


Figure 57: Maximum storage modulus of different high-MW HAVES with a macromer content of 3 wt% containing 80 mol% thiol-ene ratio of ETTMP ordered according to increasing value for n_{vinyl}

Formulation with a MW of 77 kDa and a DS of 13% shows the highest crosslinking density. The rather high value for $n_{\text{vinyl}} = 25$ can be used as a possible explanation for the increased crosslinking density. Furthermore, this HAVE bears a shorter macromer chain length, than HAVE with a MW of 100 kDa. The influence of DTT compared to ETTMP has also been studied and is depicted in Figure 89-Figure 91 (Appendix). The slope in the linear region of G' (Figure 58) and the delay of initiation (Figure 59) have also been investigated within the experiments.

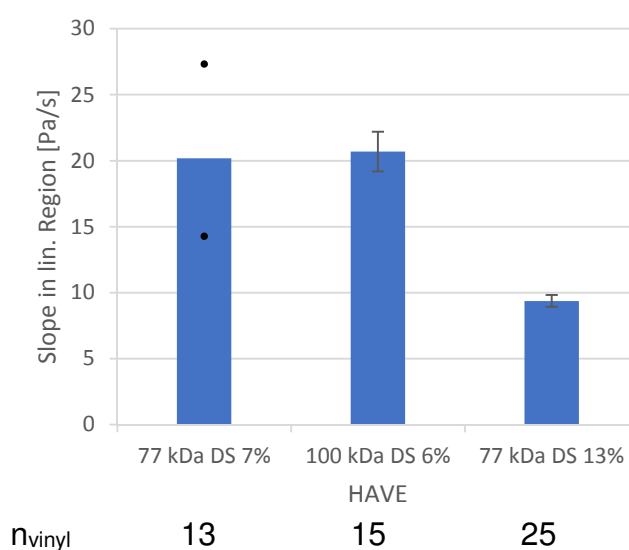


Figure 58: Slope of the storage modulus in the linear region of different high-MW HAVES containing 80 mol% thiol-ene ratio of ETTMP ordered according to increasing value for n_{vinyl}

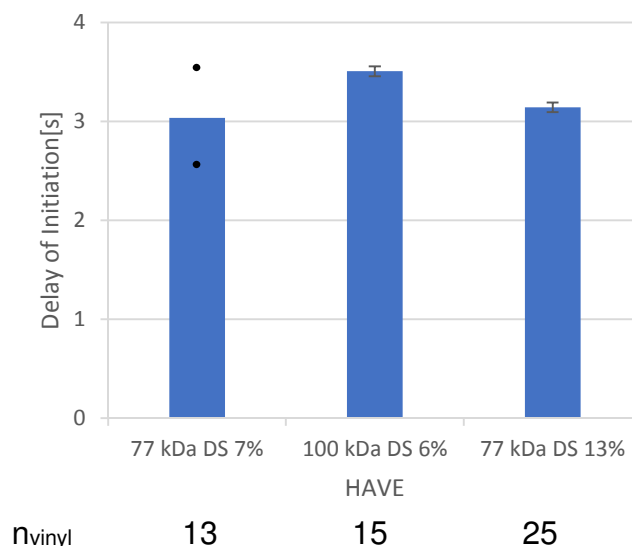


Figure 59: Delay of initiation of different high-MW HAVEs containing 80 mol% thiol-ene ratio of ETTMP ordered according to increasing value for n_{vinyl}

Solubility issues of high-MW HAVE macromers (> 50 kDa) along with very low MC and in consequence very low G' values show some major drawbacks concerning applicability of synthesized hydrogel precursors. The high viscosity made HAVE samples hard to pipette quantitatively within small sample volumes. Not only solubility problems but also the limited reactivity for diluted systems narrowed the range of comparable macromers within this thesis. Optimum parameters towards handling of HAVE macromers seem to be precursors with a MW below 50 kDa, but higher than 22 kDa. Within this thesis, an increase of crosslinking density could be observed until a MW of 80 kDa. Above this value the further increase of macromer chain length resulted in problems, such as solubility issues. These caused difficulties for the preparation of formulations exceeding 3 wt%. Additionally, literature research was performed and did not result in findings towards HA hydrogels bearing a MW higher than 100 kDa. Most of the studies were performed with values < 50 kDa.¹³⁰

Recent research focuses on low-MW HAVE (22 kDa) with a DS of 20% to further tune hydrogel properties by the addition of native ECM compounds. Exploiting the beneficial effects of the well soluble low-MW HAVE, interpenetrating matrices will be studied within the next chapter.

3.5 Collagen as additional Matrix Compound

To investigate the effect of collagen on hydrogel properties, as already mentioned in literature,¹³¹⁻¹³⁶ rheological studies were performed in combination with HAVE macromers. Collagen in general is already well known for applications in TE and is often used as a substrate for cell cultures.²⁰ It is besides elastin, fibronectin, laminins, glycoproteins, proteoglycans and GAGs, one of the many proteins within the ECM.⁶ Lyophilized rat tail collagen (mainly type 1) is used within this study.

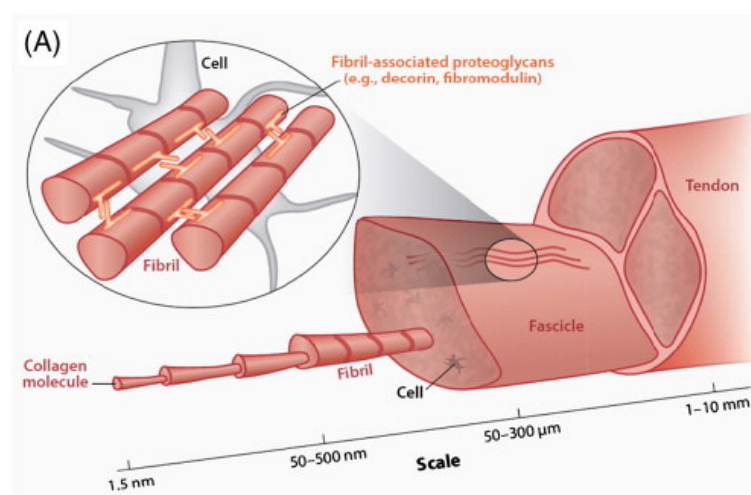


Figure 60: Hierarchical structure of tendon based on single collagen molecules spanning up to fibrils and fascicles within the ECM¹³⁷

Similar to interpenetrating networks (IPNs), collagen can be used as a mechanical support to reinforce hydrogel networks and produce IPNs under physiological conditions. These matrices consist of two different types of networks. One, based on chemically crosslinked HAVE, and the other based on collagen, where triple helices build a network held together by physical interactions. Generally, collagen is an amphipathic natural polymer and transforms into a hydrogel itself by self-assembly of its triple helix at optimum pH and temperature.¹³⁸ Many hydrogels do not promote cellular adhesion and -function because most cells do not have receptors to hydrogel forming polymers and therefore cannot adhere. These receptors usually bind onto amino acid motifs, such as the sequence arginine-glycine-aspartate (RGD). If materials bear RGD sequences, they stimulate cell growth and minimize the risk of immune reactivity or pathogen transfer.¹³⁹ Collagen is one of the proteins, naturally present within the ECM, carrying this RGD sequence.¹⁴⁰ Due to this reason, collagen is an optimal candidate for the fabrication of cytocompatible hydrogels for TE. The advantages which arise from systems

which incorporate physical self-assembly of macromolecules in combination with gelation by covalent crosslinking were already described beforehand (Section 3.2 – Introduction). These benefits from physical self-assembly will be studied within this chapter by photorheological measurements of HAVE in combination with collagen. The thermo-responsivity of collagen fibers will be studied within a HAVE matrix to investigate the influence of collagen to a HA-matrix, concerning mechanical support.

Low-MW HAVE (22 kDa) with a DS of 21% was used to visualize collagen network formation in the presence of HAVE as best as possible. Measurements of HAVE (22 kDa, DS = 95%) can be found within the Appendix. The beneficial effects of ETTMP (increased G' - showed in Section 3.2) were further employed within this chapter for the preparation of hydrogel formulations. The precursor solution was therefore combined, consisting of collagen stock solution (0.8 wt%), HAVE stock solution (4 wt%), ETTMP stock solution (20 wt%) and Li-TPO stock solution (2 wt%). Since collagen is only soluble for a longer period of time in acidic conditions, it was dissolved in 0.2% acetic acid (pH = 3.8) to prepare the stock solution of collagen. PBS buffer (pH = 7.4) was used for the preparation of stock solutions of HAVE, ETTMP and Li-TPO. Equivalentents of each stock solution were pipetted into vials to achieve final concentrations listed in Table 5.

Table 5: Concentrations of stock and final solutions for measurements combining HAVE (22 kDa, DS = 21%) with collagen

	C_{stock} [wt%]	C_{final}
HAVE	4	1.02 wt%
Collagen	0.8	0.32 wt%
ETTMP	20	80 mol%
Li-TPO	2	0.05 wt%

All reagents were cooled before combining the stock solutions to avoid premature gelation of collagen. Photorheological measurements were performed by pipetting the precursor solution onto the glass plate of the photorheometer and adding paraffin oil after the measuring plate was lowered to measuring position, to avoid H₂O evaporation.

3.5.1 Preliminary Tests

(Photo)rheology measurements of three different formulations were performed (see Table 6). Formulation **A** consisted of 0.3 wt% collagen, which was combined with NaOH to neutralize the solution before measurement. Formulation **B** consisted of 1 wt% HAVE macromer, ETTMP with thiol-ene ratio of 80 mol% and 0.05 wt% photoinitiator (Li-TPO). Formulation **C** represents a combination of both aforementioned formulations and is discussed in detail in Section 3.5.2.

Table 6: Different compositions of HAVE/collagen formulations for photorheology measurements

Formulation	A	B	C
Components	Collagen	HAVE	Collagen
	NaOH	ETTMP	NaOH
	PBS	Li-TPO	HAVE
		PBS	ETTMP
			Li-TPO
			PBS

For formulation **A**, the beforehand cooled collagen stock solution was neutralized with a micro pH electrode to a pH of 7.1, using 0.1 M NaOH. By addition of cooled PBS, the final collagen concentration was obtained (0.32 wt%). As the pH determines collagen fibrillogenesis and formulations **A** and **C** had to be neutralized right before measurement, the volume for one single measurement at a time was prepared. Each following mixture was prepared right before measurement, to avoid premature gelation of collagen.

For detailed investigation of the thermoresponsive collagen fibrillogenesis, rheology measurements were performed. During the first 2 min of the measurement, the temperature was maintained at 5°C to examine the Moduli of the initial solution. After heating with a gradient of 6.4 °C/min, the temperature was maintained constant (37 °C) for the rest of the measurement. The gelation of collagen is initiated within the period, where temperature is increased. After 60 min, the association of collagen fibers is mostly finished, represented by nearly constant Storage Moduli values (Figure 61).

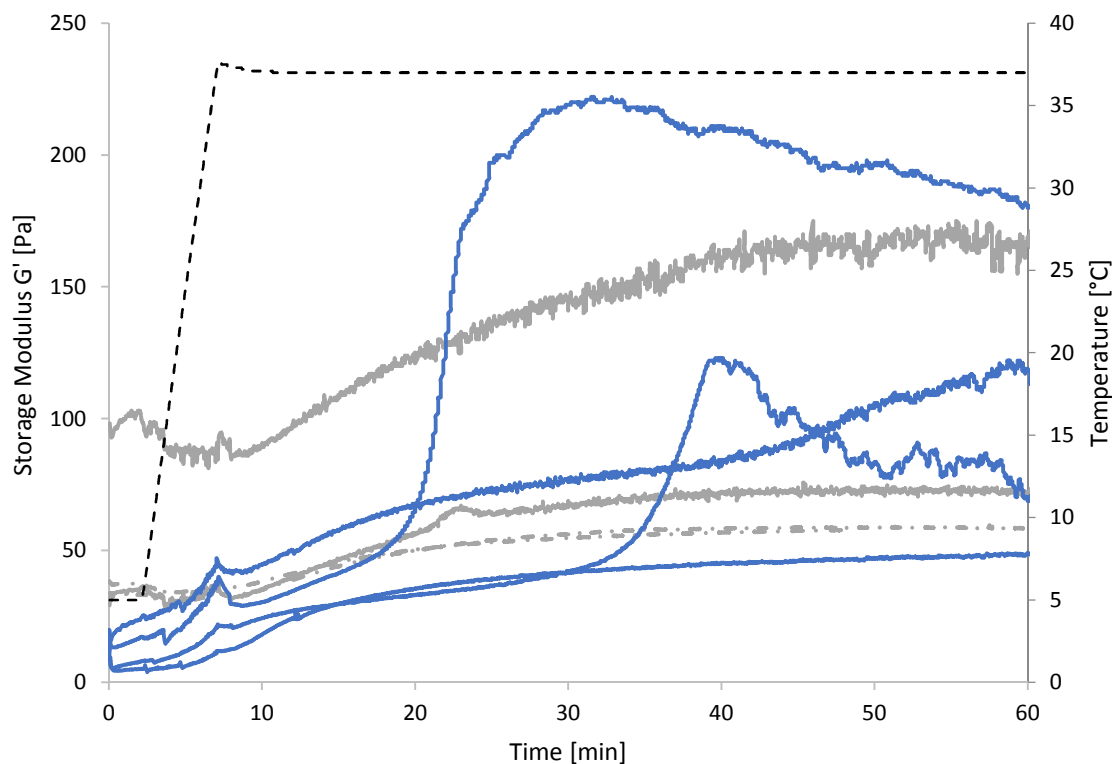


Figure 61: Temperature-responsive collagen gelation of formulation A (first tests with 1 Hz frequency and 1% strain (—) and 10 Hz frequency 10% strain (- · -), 1 Hz frequency, 1% strain and measurement right after collagen neutralization (—))

Continuous and dotted grey lines in Figure 61 represent first measurements, where the reagent solutions were not cooled initially and the time between preparation of the formulation and measurement was relatively long. These measurements show quite high Storage Moduli already at the start of the analysis, which is an indication that collagen fibers already associated before the measurement. Because the amount of formulation for one measurement is also quite low, it must be taken care to intensively cool the formulation at every moment during preparation of the precursor solution. Furthermore, it is shown, that measurements with a frequency of 1 Hz and 1% strain reached higher G' values at the end of the measurement. Therefore, subsequent measurements of all formulations were performed with a frequency of 1 Hz and a strain of 1%. The spike in the curve at 7 min is the transition of the temperature gradient to a constant temperature and occurs for every measurement.

Not only formulation **A** (collagen alone) was measured during preliminary testing, but also formulation **B** (containing HAVE without collagen) was analyzed as a reference. Accordingly, HAVE (22 kDa, DS = 21%), ETTMP and Li-TPO stock

solutions were pipetted into an Eppendorf vial, adding PBS to lead to a final concentration of 1.02 wt% HAVE. To investigate the effect of temperature on the network formation, formulation **B** was measured at 5 °C and at 37 °C (Figure 62).

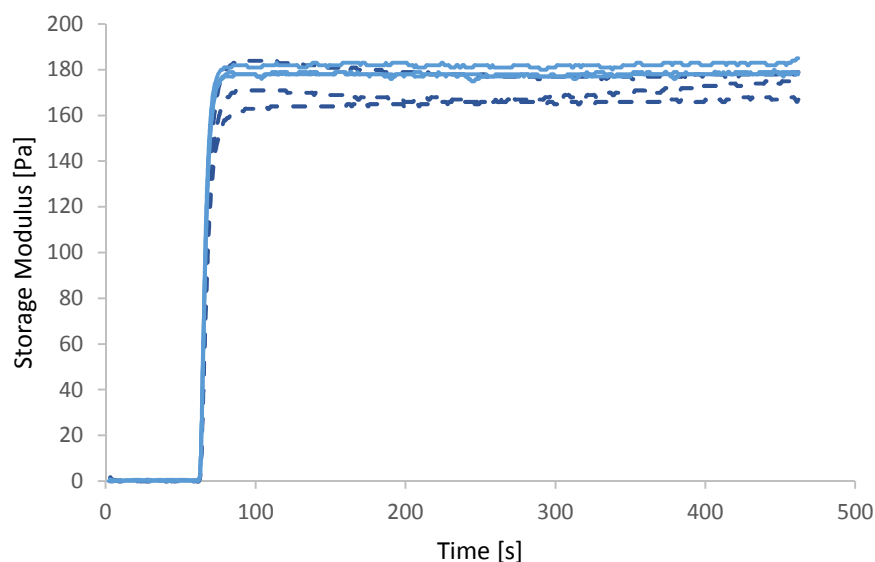


Figure 62: Photopolymerization of formulation B (HAVE, MW = 22 kDa, DS = 21%, 80 mol% thiol-ene ratio ETTMP) at 5 °C (—) and 37 °C (---)

After 60 s of measurement, the formulation was irradiated with UV light, whereupon the polymerization process was initiated. The hydrogel network formation can be examined by detecting the increase of G' during UV irradiation. Reproducible measurements could be obtained, showing an achievement of the maximum G' within seconds and constant G' values until the end of the measurement. Measurements at 5 °C show a slight better reproducibility than measurements at 37 °C, but still similar maximum G' values could be obtained. Since the reference formulations **A** and **B** have been examined extensively and the system parameters have been set, HAVE in the presence of collagen (formulation **C**) will be studied within the next chapter.

3.5.2 The Influence of Collagen on HAVE hydrogels

Followed by the reference measurements, where collagen and HAVE were investigated on their own, formulation **C** will be studied within this chapter. Two different experiments are going to be studied. First, the photopolymerization of HAVE in the presence of already associated collagen fibrils and secondly the crosslinking of HAVE before fibrillogenesis of collagen. For this purpose, one experiment is performed, where HAVE is photopolymerized at 5 °C followed by an increase in temperature, initiating the collagen association. The other experiment is realized by collagen network formation at 37 °C and the photopolymerization of HAVE at the same temperature. Preliminary tests (Figure 62) showed, that UV irradiation of HAVE at 5°C as well as at 37 °C results in similar final Storage Moduli. Therefore, the influence of one crosslinked network onto the network formation of the second matrix compound can be studied directly.

Formulation C_a: Photopolymerization at 5°C

Measurements were performed where HAVE was polymerized before collagen could gel via an increase in temperature. For these experiments the first 60 s of measurement were performed at a set temperature of 5 °C. Photopolymerization was initiated at 5 °C and a constant storage modulus was achieved after 9.77 min. Hereinafter the temperature was increased with a heating rate of: 6.4 °C/min. Due to the increasing temperature, collagen gelation was initiated. After 37 °C were reached, the temperature remained constant for the rest of the measurement. Rheological data was collected until collagen fibrillogenesis was mostly completed (after 60 min), indicated by no further increase of the storage modulus.

Formulation C_b: Photopolymerization at 37 °C

Regarding measurements, where collagen gelation precedes HAVE crosslinking the heating rate (6.4 °C/min) started after 2 min of measurement. Collagen gelation was allowed for 67 min until photopolymerization was initiated at 37 °C. The measurement was continued for another 10 min.

Formulation **C** itself was prepared by neutralizing (pH = 7.1) collagen stock solution in an Eppendorf vial via the addition of 0.1 M NaOH. Exact indications of quantity can be found within the Experimental Section of this thesis. All reagents were cooled with an ice bath before combination of the stock solutions and one

measurement at a time was prepared to avoid premature collagen gelation. Aliquots of HAVE, ETTMP and Li-TPO stock solutions were combined with PBS to achieve final concentrations as depicted in Table 5. In the case of formulation **C_a**, where HAVE was photopolymerized at 5 °C, Storage Moduli of around 40 Pa were achieved (Figure 63). Following increase of temperature, led to a further increase of G' of about 100 Pa.

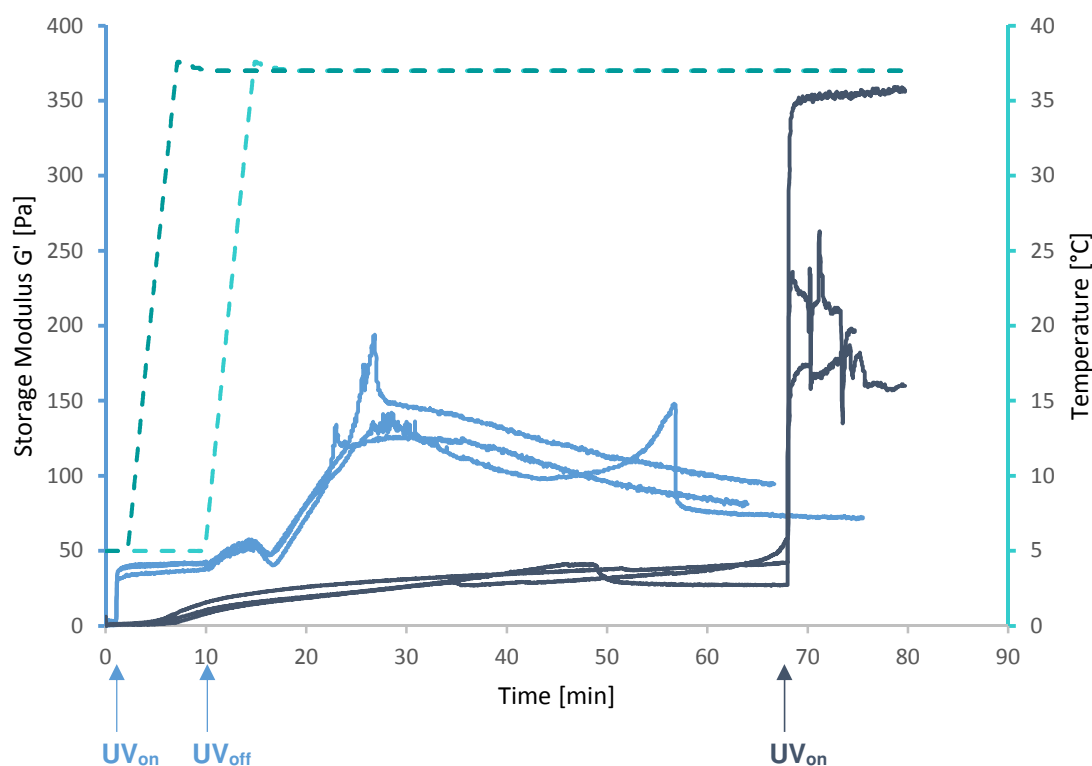


Figure 63: Trends of Storage Moduli of formulation C. Collagen gelation after photopolymerization of HAVE (22 kDa, DS = 21%) - Formulation **C_a** - (light blue) and before photopolymerization of HAVE - Formulation **C_b** - (dark blue) containing 80 mol% thiol-ene ratio of ETTMP and 0.05 wt% Li-TPO

In the case of formulation **C_b**, where collagen fibrillogenesis was performed before HAVE crosslinking, G' slowly increases, until G' values of 40 Pa. Following UV irradiation after 67 min leads to a sudden and drastic increase of G' . Typical delamination effects were observed for two out of three measurements for formulation **C_a**, indicated by the sudden decrease of G' . These delamination effects were not observed for formulation **A** - only containing collagen (Figure 61). Collagen formulations in combination with HAVE (22 kDa, DS = 95% - see Appendix) also showed delamination, due to higher DS values resulting in an even more crosslinked hydrogel network, increasing the possibility of delamination. One reason may be the driving force of collagen to form an extensively dense

network, but due to the presence of already present HAVE crosslinks, the collagen network formation is hindered at a certain threshold.

Over all, quite reproducible results were achieved for all cases. Consequently, one exemplary curve per formulation (**A**, **B**, **C_a**, **C_b**) is depicted and described hereinafter (Figure 64).

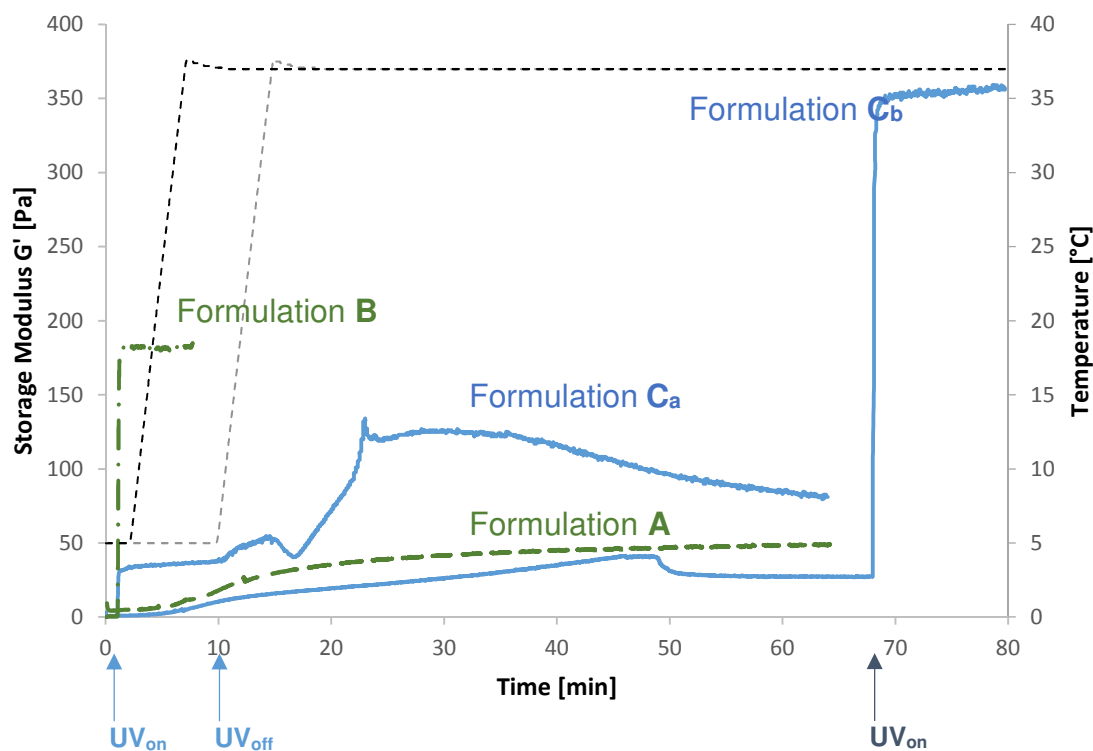


Figure 64: Comparison of exemplary G' curves, including Formulation A - collagen without HAVE (— · —), Formulation B - HAVE alone (— · · —), Formulation C_a and C_b - HAVE in combination with collagen (—) within a defined temperature program (-----),

In the case, where HAVE was photopolymerized at 5 °C (formulation **C_a**), maximum Storage Moduli of around 40 Pa were achieved during the first 10 min of measurement. Following increase of temperature, led to a further increase of G' to about 130 Pa. Whereas, HAVE alone (formulation **B**) showed much higher values for G' (170 Pa) compared to formulation **C_a**. Consequently, the presence of collagen within the formulation has a significant impact on HAVE crosslinking, namely leading to lower G' than for the system consisting of HAVE alone. Contrary to this, HAVE has a positive effect on hydrogel formation, if formulation **C_a** is compared with formulation **A**. Collagen alone has a Maximum storage modulus of 40 Pa, whereas collagen fibrillogenesis in the presence of a beforehand crosslinked HAVE network, reaches G' values of 130 Pa. Considering also the

trend of the curves, formulation **C_a** forms fibrils more faster than formulation **A**. Hence, HAVE seems to support triple helix association of collagen.

Taking a closer look to formulation **C_b**, where collagen fibrillogenesis was performed before HAVE crosslinking, G' slowly increases, until similar G' values as for formulation **A** were achieved (40 Pa). Consequently, HAVE does not seem to drastically influence collagen association. Following UV irradiation of formulation **C_b** after 67 min leads to a sudden and drastic increase of G' to 350 Pa. In conclusion, maximum G' values compared to all other measurements were observed for formulation **C_b**.

It is noticeable, that delamination is only occurring for the formulation containing HAVE and collagen [formulation **C_a** (22 min) and **C_b** (49 min)]. Formulation **A** and **B** do not show these effects at all. This is an indication, that delamination is only occurring, when another crosslinked network, either HAVE or collagen, is already present within the formulation. Further crosslinking of collagen is hindered to a certain extent and interference of the two different networks leads to delamination. It is assumed, that during delamination, oil from outside of the measuring volume creeps inside the crosslinked hydrogel and induces detachment of the gel.

Collagen fibrillogenesis before photopolymerization seems to have a positive impact on HAVE crosslinking (formulation **C_b**), forming a stiffer hydrogel than the system without collagen (formulation **B**). By increasing the amount of collagen and HAVE, hydrogel properties could be further tuned towards higher Storage Moduli. While triple helix association is occurring, collagen does not seem to be greatly affected by non-crosslinked HAVE macromers. One reason might be the very small macromer size of HAVE (22 kDa). The small molecules are able to diffuse between collagen helices and only crosslink after collagen network is already associated. Still, HAVE is keeping its high reactivity, indicated by the drastic increase of G' after UV irradiation is started. Contrary to this observation, HAVE seems to be affected by the presence of non-associated collagen helices. Photopolymerization of HAVE at 5 °C (formulation **C_a**) in the presence of uncrosslinked collagen led to a loss of almost a fifth of the value of G' . Subsequent collagen association does not even reach G' values of formulation **B**.

In conclusion HAVE networks were thoroughly studied either with or without beforehand collagen triple helix association. A significant increase of G'_{\max} was observed for HAVE-collagen formulation **C_b**, compared to HAVE (**A**) or collagen measurements (**B**) alone, especially in the case where HAVE was photopolymerized at 37°C within the presence of an already existing collagen network. The physical associated network of the collagen helices seem to build a mechanical support for the HAVE matrix, facilitating the interpenetration of HAVE into collagen fibrils. The possibility to photopolymerize HAVE on demand, without significant decrease of crosslinking density, within different temperature ranges (as depicted in Figure 62), enables precise hydrogel design, especially suited for IPNs. Concluding, HAVE-collagen IPNs are promising candidates for cytocompatible hydrogels with tailorable mechanical properties for tissue engineering.

4 Proof of Concept

Two Photon Polymerization

One of the most promising techniques for the fabrication of hydrogels with high resolution, is the technology of two photon polymerization (2PP), using a pulsed near-infrared (NIR) laser.⁹⁸ Photopolymerization and solidification of hydrogel precursors is thereby only induced in the focal point of the laser and does not occur along the path of the beam through the precursor solution.⁹² High penetration depth are still kept, as the applied NIR laser offers high transparency towards biological tissues and minimizes photo-damage of native matrices. First structuring on the basis of biocompatible macromers was already performed at the Institute of Materials Science and Technology of TU Wien.^{141,142} VE functionalities were also used and showed promising performance regarding structuring of complex structures.¹⁴³ Due to these results, further studies were elaborated, where HAVE precursors were used to encapsulate murine fibroblasts (L929) via 2PP. Out of the different available precursors, 2PP printing was carried out with HAVE, known from photorheology to show relatively high crosslinking density (MW of 22 kDa, DS of 95%) in order to achieve most promising results.

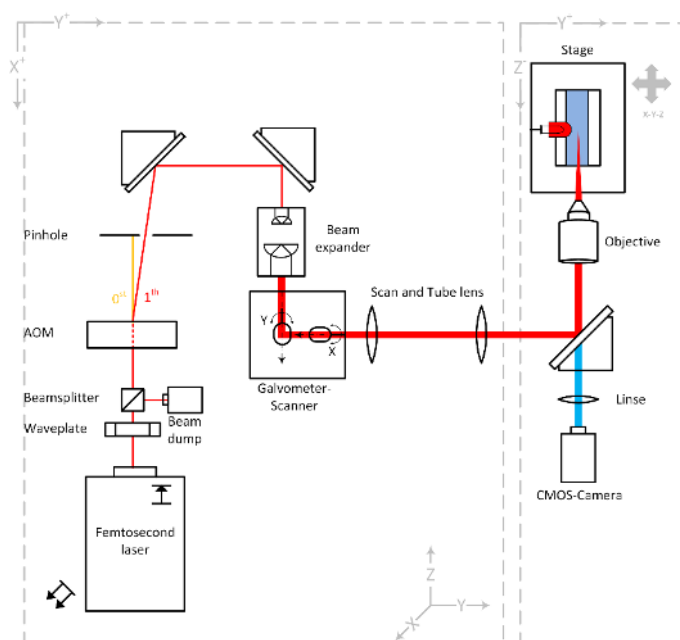


Figure 65: Experimental setup for the 2PP structuring process¹⁴⁴

A formulation based of HAVE with 80 mol% thiol-ene ratio using DTT was prepared by mixing stock solutions of HAVE (20 wt%) and 2 mM of the two photon initiator

P2CK ((3,3'-(((1E,1'E)-(2-oxocyclopentane-1,3-diyldene) bis(methanylylidene)) bis(4,1-phenylene)) bis(methylazanediy))dipropanoate, Figure 66).⁹⁵

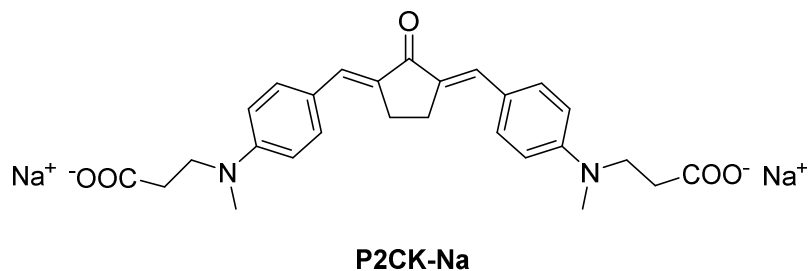


Figure 66: Two-photon active photoinitiator used within HAVE structuring

Final formulations were prepared by mixing stock solutions 1:1 with cells in medium or PBS solution (cell-free control). HAVE microfabrication was performed by scanning the focus of the laser beam of the 2PP device through the prepared formulation with a speed of 100 mm s⁻¹ and varied laser powers. Development of samples in medium or PBS solution and subsequent washing ensured the removal of remaining precursor as well as non-encapsulated cells. Images of the printed constructs and calcein stained cells were taken with a laser scanning microscope after 24 h (Figure 67). The cell-free control formulation was successfully printed within all laser powers. Although, laser power < 30 mW seem to result in very fragile hydrogel constructs, indicated by low crosslinking densities due to underexposure. Consequently, cell encapsulation for laser powers of 10 and 20 mW was impossible. Possibly, these structures were destroyed, detached, and washed away during the rinsing procedures. Cell encapsulation experiments with all other parameters were successful. These experiments were performed by Peter Gruber and Marica Markovic at the Institute of Materials Science and Technology of TU Wien.

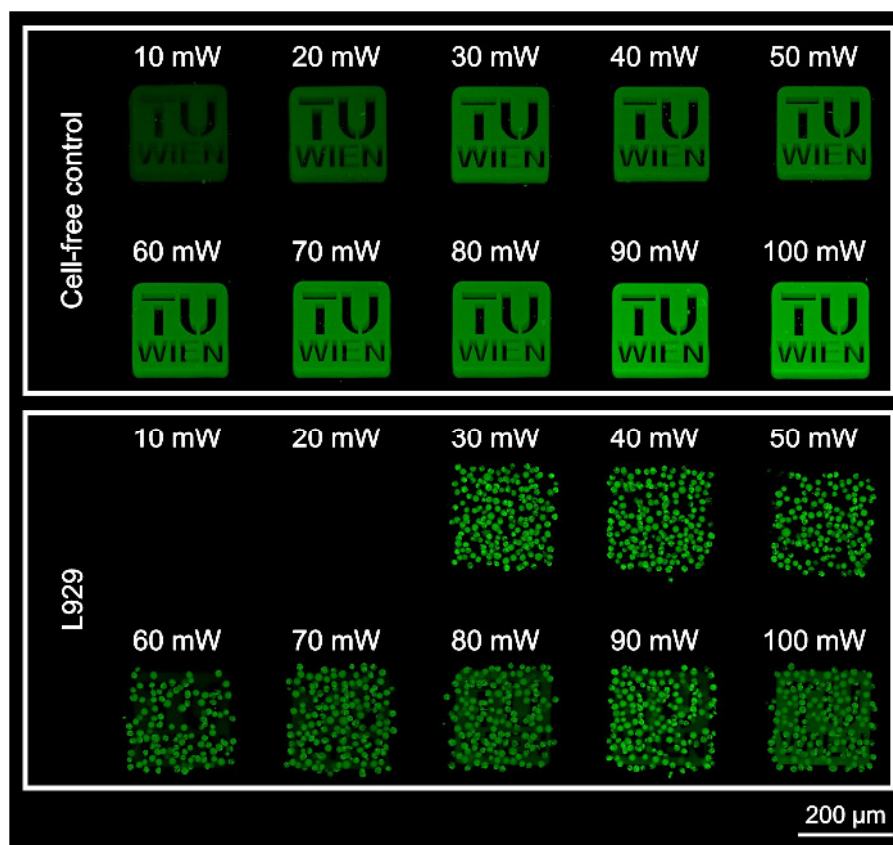


Figure 67: Laser scanning microscope images of printed HAVE hydrogels (22 kDa, DS = 95%, macromer content = 10 wt%, 80 mol% thiol-ene ratio DTT, printed with varied laser powers (10 - 100 mW), writing speed of 100 mm s⁻¹ and corresponding hydrogel constructs including encapsulated calceine stained L929 cells after 24 h (bottom - L929).

Concluding, encapsulation of murine fibroblasts in an optimized formulation by two-photon polymerization was successful. By the tailoring of HAVE precursors towards defined macromer sizes and DS, it was possible to find hydrogel precursors for the successful encapsulation of living cells, using 2PP for the first time.

Experimental Part

2 Synthesis

Acidic and Enzymatic Degradation Studies

A 0.5 wt% solution was prepared by dissolving 100 mg of HA-Na in 20 mL H₂O dest. overnight. The initial pH of the solution was determined as 7.9. After the first GPC sample was drawn (1 mL), the pH was adjusted to 1.05 with ~0.5 mL 2 N HCl. The drawn sample was diluted with 4 mL PBS to a concentration of 1 mg/mL and the pH adjusted to a value of 7.0 with 0.15 mL of 3 N NaOH. For the degradation study at 60 °C the solution was heated to mentioned temperature and samples drawn every 2 hours and GPC samples prepared as above mentioned.

Table 7: Number Average Molecular Weight and corresponding PDI values for the acidic degradation

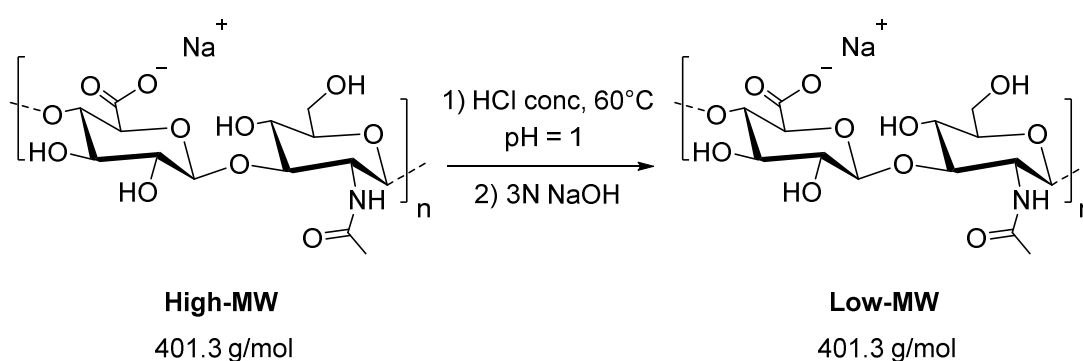
t [h]	23 °C				60 °C			
	1 st run		2 nd run		1 st run		2 nd run	
	Mn [MDa]	PDI []	Mn [MDa]	PDI []	Mn [MDa]	PDI []	Mn [MDa]	PDI []
0	1.84	1.56	1.72	1.61	1.62	1.58	1.69	1.54
2	1.69	1.73	1.93	1.56	0.27	1.56	0.38	1.44
4	1.56	1.73	1.79	1.62	0.16	1.60	0.24	1.44
6	1.57	1.74	1.72	1.63	0.10	1.63	0.15	1.55
8	1.40	1.67	1.32	1.70	0.07	2.02	0.11	1.61
10	1.40	1.67	1.31	1.70	0.07	1.77	0.07	1.78
12	1.39	1.67	1.03	1.94	0.06	2.05	0.06	1.82
24	1.25	1.74	1.14	1.79	0.04	1.82	0.04	1.74

For the enzymatic degradation, 10 mg HA was dissolved in 5 mL PBS to receive a 2 mg/mL solution. After stirring for 1 h at room temperature the first GPC measurement (t = 0) was performed by diluting 1.5 mL of HA solution with 1.5 mL PBS, to achieve a 1 mg/mL solution. Meanwhile 1.43 mg hyaluronidase (HASE) was dissolved in 1 mL acetate buffer, and an aliquot added to the HA solution to achieve an activity of HASE of 5 U/mg regarding HA. The flask was placed in a tempered water bath of 37.5 °C and GPC samples (1.5 mL) were drawn every 5 min and diluted 1:1 with PBS buffer to achieve a concentration of 1 mg/mL. For the inactivation of the enzyme the samples were heated to 98 °C for 10 min. The suspension was centrifuged, to remove denatured Bovine Serum Albumin (BSA) and remaining solution analyzed by GPC. Resulting MW of HA are depicted in Table 8.

Table 8: Enzymatic degradation

t [min]	Mn [MDa]	PDI
0	1.16	2.1
5	0.08	2.3
10	0.08	2.4
15	0.08	2.3
20	0.07	2.4
25	0.07	2.4

2.1 Preparation of Low-Molecular Weight HA



	M [g/mol]	m [g]	n [mmol]	V _{H₂O} [mL]	V _{HCl} [mL]	V _{NaOH} [mL]
HA-Na	401.3*	0.5007	1.25	250	1.7	
		0.5004	1.25	250	1.8	#
		3.0017	7.48	500	7.3	

* M refers to repeating unit

detected by pH Meter

For each batch, HA sodium salt was dissolved overnight in H₂O dest. to obtain a 0.2 wt% solution (0.6 wt% for 150, 100, 77 kDa). The solution was stirred moderately at room temperature with a mechanical stirrer. The homogenized solution showed a pH of 8.03. The degradation was started by addition of ~2 mL conc. HCl until a pH of 1.02 was reached at 32 °C. Thereafter the flask was immersed in an oil bath and the reaction mixture heated to 60 °C. After respective times of degradation (see Table 9) the flask was placed in an ice bath and the pH adjusted to 7.1 with ~ 6 mL 3 N NaOH. The solution was concentrated to half the initial volume and transferred to dialysis tubes with a MW cut-off of 50 kDa. The HA solution was dialyzed against H₂O dest. with at least 6 changes of H₂O dest. The solution of the dialysis tubes was transferred

into a flask, the volume reduced by half and frozen with liquid N₂. The product was lyophilized (0.05 mbar, -81 °C) for at least 3 days.

Table 9: Degradation times and yields of different batches, resulting in several different MW of HA

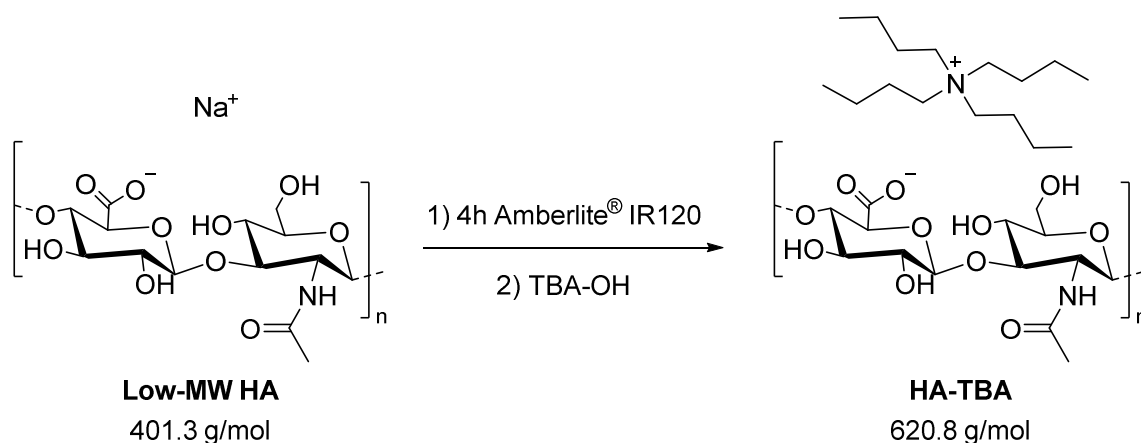
<u>t [h]</u>	<u>\overline{M}_n [kDa]</u>	<u>PDI []</u>	<u>Yield [g]</u>	<u>Yield [%]</u>	<u>Yield [%]</u>
3	540	1.8	0.3504	70.0	
6	180	1.9	0.4017	80.3	
5.5	150	2.5	0.8289	27.6	
7.5	100	2.1	0.5061	16.9	68.5*
9.5	77	2.4	0.7217	24.0	

**calculated by combination of yields of every batch*

¹H-NMR: (400 MHz, 512 scans, D₂O), δ (ppm):

4.6 - 4.4 (m, 2 H, anomeric carbons C₁,C₁' , Int = 2), 3.9 - 3.2 (m, 10 H, [ring]CH and CH₂-OH, Int = 12 H), 2.0 (s, 3 H, CH₃-(C=O)-NH, Int = 3)

2.2 Synthesis of Tetrabutylammonium Salt of HA



	1 st batch		2 nd batch		
	540 kDa	180 kDa	150 kDa	100 kDa	77 kDa
HA-Na [g]	0.282	0.290	0.828	0.506	0.722
HA-Na [mmol]	0.70	0.72	2.06	1.26	1.80
H ₂ O dest. [mL]	28.2	29.0	27.6	16.9	24.1
Amberlite [g]	0.846	0.87	3.92	2.39	3.42

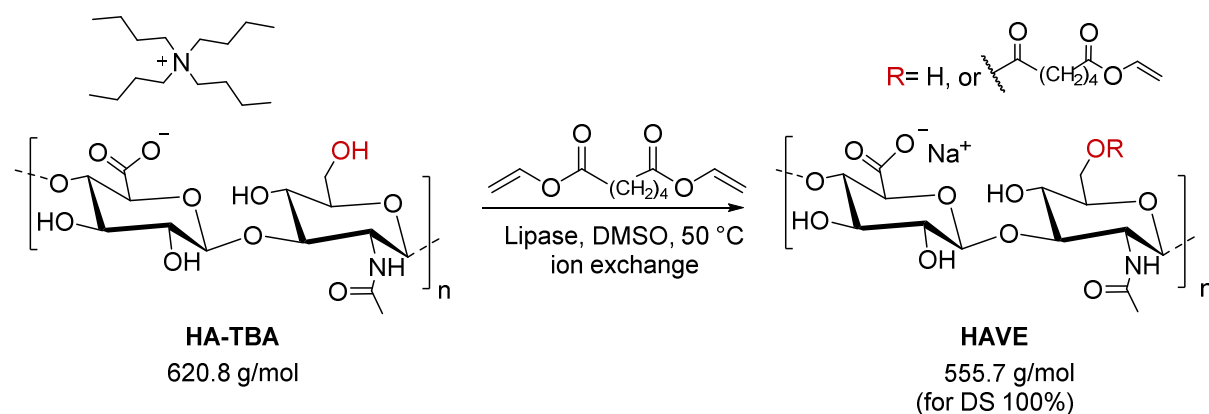
Low-MW HA was dissolved in a 100 mL round bottom flask in H₂O dest. in order to obtain 1 wt% solution for 1st batch (3 wt% solution for 2nd batch). The solution was stirred with a magnetic stirrer for 2 h at room temperature. After complete dissolution, 3 mass equivalent (5 eq. for 2nd batch) of highly acidic ion exchange resin Amberlite® IR120 (hydrogen form) was added. The slurry was stirred for 4h at room temperature, whereas at the end the pH was measured to be 2.3 at 25 °C. The ion exchange resin was separated from the very viscous solution via suction filtration and washed with demineralized water. The pink filtrate was neutralized to a pH of 7.01 by the addition of a 40% aqueous solution of TBA-OH. The volume of the HA-TBA solution was reduced by evaporation in vacuo, to approximately 100 mL. The solution was frozen with liquid N₂ and lyophilized for at least 24h (0.05 mbar, -81 °C).

	1 st batch		2 nd batch		
	540	180	150	100	77
\overline{M}_n [kDa]	540	180	150	100	77
Yield [g]	0.428	0.428	1.268	0.750	1.091
Yield [%]	98	95	99	96	98

¹H-NMR: (400 MHz, 512 scans, D₂O), δ (ppm):

4.6 - 4.4 (m, 2 H, anomeric carbons C₁,C₁', Int = 2), 3.9 - 3.3 (m, 10 H, [ring]CH and CH₂-OH, Int = 12), 3.2 - 3.1 (m, 8 H, 4x -CH₂-N⁺, Int = 14), 2.0 (s, 3 H, CH₃-(C=O)-NH, Int = 3), 1.7 - 1.6 (m, 8 H, 4x -CH₂-CH₂-N⁺, Int = 14), 1.4 - 1.3 (sext, 8 H, 4x CH₃-CH₂, Int = 14), 1.0 - 0.9 (t, 12 H, 4x CH₃-CH₂-, Int = 20)

2.3 Synthesis of HA Vinyl Ester



	M [g/mol]	eq.	ρ [g/mL]	1 st batch					
				540 kDa			180 kDa		
				n [mmol]	m [g]	V [mL]	n [mmol]	m [g]	V [mL]
HA-TBA	620.8	1		0.58	0.363		0.56	0.350	
CAL-B		8*			0.029			0.028	
HQ	110.1	0.05		0.03	0.003		0.03	0.003	
DMSO abs.	78.1		1.1			23.3			15.2
DVA	198.2	3	1.05	1.75	0.347	0.3	1.69	0.336	0.3

* [wt%]

		2 nd batch				
		HA-TBA	CAL-B	HQ	DMSO abs	DVA
M [g/mol]		620.78		110.11	78.13	198.22
eq.		1	8 wt%	0.05		6
ρ [g/mL]					1.1	1.05
150 kDa	n [mmol]	1.94		0.10		11.66
	m [g]	1.206	0.096	0.011		2.311
	V [mL]				30	2.2
100 kDa	n [mmol]	1.17		0.06		6.99
	m [g]	0.724	0.058	0.006		1.386
	V [mL]				20	1.3
77 kDa	n [mmol]	1.71		0.09		10.25
	m [g]	1.060	0.085	0.009		2.031
	V [mL]				26	1.9

The first batch (540 and 180 kDa) was prepared by dissolving the corresponding amount of HA-TBA (as listed in table above) in dry DMSO overnight where the solution changed color from intense rose to pale orange. The corresponding amount of hydroquinone (HQ), lipase (CAL-B) was added in Ar counterflow via a funnel and divinyl adipate (DVA) (3 eq. for the first and 6 eq. for the second batch) was added via

a septum. After all reagents were added the final concentration regarding HA was 2 wt% for the first batch and 4 wt% for the second batch. The reaction mixture was heated to a temperature of 50 °C and stirred for various reaction times which are listed in Table 10. Via a pipette half of the reaction mixture was drawn at defined times out of the reaction flask. Due to high viscosity of the reaction mixture no exact mL values can be displayed. Lipase beads were filtered off by suction filtration and washed with ~5 mL of DMSO. The solution was precipitated in ice-cold ethyl acetate (EA) and the beige precipitate isolated via centrifugation for 5 min at 10 °C at 5000 rpm. EA was removed via decantation and the precipitate washed 2x with cold EA. The dried precipitate was dissolved in a small amount of H₂O dest. and transferred into dialysis tubes with a MWCO of 50 kDa. The dialysis was performed against sodium chloride (7 changes) and afterwards against deionized water (7 changes). The volume of the dialyzed solution was reduced to ~50 mL and frozen by liquid N₂ and lyophilized at -81 °C and 0.01 mbar. The successful synthesis of HAVE was confirmed by ¹H-NMR. The Degree of Substitution (DS) of the white product was determined via referring the CH₃ signal at 2.0 ppm to the CH₂ signals at 1.5 ppm of the adipate group for the hydrolyzed HAVE NMR spectra (with the addition of 3 μl NaOD).

¹H-NMR: (400 MHz, 512 scans, D₂O), δ (ppm):

7.2-7.1 (q, x H, -CH=CH₂), 4.9 (d, x H, -CH=C(H)H), 4.7 (m, x H, CH=C(H)H), 4.6 – 4.4 (m, 2 H, anomeric carbons C₁,C₁'), 3.9 – 3.2 (m, 10 H, [ring]CH and CH₂-OH), 2.5 (bs, 4 H, -CH₂-C(=O)-O-), 2.0 (s, 3 H, CH₃-(C=O)-NH), 1.7 (bs, 4 H, -CH₂-CH₂-C(=O));

¹H-NMR: (400 MHz, 512 scans, D₂O + 3 μl NaOD), δ (ppm):

4.5 – 4.4 (m, 2 H, anomeric carbons C₁,C₁'), 3.9 – 3.3 (m, 12 H, [ring]CH and CH₂-OH), 2.2 (m, x H, -CH₂-C(=O)-O-), 2.0 (s, 3 H, CH₃-(C=O)-NH), 1.5 (s, x H, -CH₂-CH₂-C(=O));

x represents the degree of substitution

Table 10: Yields after the synthesis of HAVEs directed by different reaction times resulting in products with different Molecular Weight and degree of substitution

t [h]	Yield* [g]	Yield [%]	DS [%]	MW [kDa]
9.5	0.1634		7	
15.5	0.5141	94	13	77
9.5	0.1719		6	
15.5	0.2589	89	9	100
9.5	0.1951	86	20	150

15.5	0.5438		27	
16	0.243	97	29	180
16	0.168	65	25	540

* The yield is calculated with considering the respective DS

Alternative synthesis of HA Vinyl Ester

	HA-TBA	CAL-B	Hydrochinone	DMSO abs	DVA
M [g/mol]	620.78		110.11	78.13	198.22
eq.	1	8 wt%	0.05		6
ρ [g/mL]				1.1	1.05
n [mmol]	0.15		0.01		0.89
150 kDa m [g]	0.092	-	0.001		0.177
V [mL]				2.31	0.17

The synthesis of HAVE without lipase was performed as close as to the procedure as for the synthesis of HAVE with lipase. This alternative synthesis was performed solely for HA with a MW of 150 kDa. Therefore 92.4 mg HA-TBA were dissolved overnight in 2.31 ml DMSO abs. to receive a 4 wt% solution. On the next day 1 mg of HQ was added in Ar counterflow and 0.17 mL of DVA were added via a septum. The reaction mixture was heated to 50 °C and stirred for 9.5h. Thereafter the lipase was filtered off by suction filtration and washed with ~0.5 mL of DMSO. The solution was precipitated in ice-cold ethyl acetate (EA) and the beige precipitate isolated via centrifugation for 5 min at 10 °C at 5000 rpm. EA was removed via decantation and the precipitate washed 2x with cold EA. The dried precipitate was dissolved in a small amount of H₂O dest. and transferred into dialysis tubes with a MWCO of 50 kDa. The dialysis was performed against sodium chloride (7 changes) and afterwards against deionized water (7 changes). The dialyzed solution was frozen by liquid N₂ and lyophilized at -81 °C and 0.01 mbar. The final DS was determined via ¹H-NMR referring the CH₃ signal at 2.0 ppm to the CH₂ signals at 1.5 ppm of the adipate group for the hydrolyzed HAVE NMR spectra (with the addition of 3 μ l NaOD).

¹H-NMR: (400 MHz, 512 scans, D₂O), δ (ppm):

7.2-7.1 (q, x H, -CH=CH₂), 4.9 (d, x H, -CH=C(H)H), 4.7 (m, x H, CH=C(H)H), 4.5 – 4.4 (m, 2 H, anomeric carbons C₁,C₁'), 3.9 – 3.2 (m, 10 H, [ring]CH and CH₂-OH), 2.5 (bs, 4 H, -CH₂-C(=O)-O-), 2.0 (s, 3 H, CH₃-(C=O)-NH), 1.7 (bs, 4 H, -CH₂-CH₂-C(=O));

¹H-NMR: (400 MHz, 512 scans, D₂O + 3 μl NaOD), δ (ppm):

4.5 – 4.4 (m, 2 H, anomeric carbons C₁, C₁'), 3.9 – 3.3 (m, 12 H, [ring]CH and CH₂-OH),

2.2 (m, x H, -CH₂-C(=O)-O-), 2.0 (s, 3 H, CH₃-(C=O)-NH), 1.5 (s, x H, -CH₂-CH₂-C(=O));

x represents the degree of substitution

Table 11: Yield of alternatively synthesized HAVE (150 kDa), via a transesterification reaction without the addition of lipase

t [h]	Yield [mg]	Yield [%]	DS [%]	MW [kDa]
9.5	54.8	85	21	150

3 Characterization of Hydrogel formulations by Photorheology

Photoreology measurements were performed with a modular compact rheometer (Anton-Paar MCR 302 WESP). Filtered UV light (320-500 nm) from a light source (Omniscure S2000 EXFO) with a high-pressure mercury lamp was used to irradiate the sample. A two-headed light guide formed the connection between the Omnicure and the photoreometer whereas the lamp was directly triggered by the rheometer. The light source was calibrated with a R2000 radiometer from EXFO and the light intensity directly measured on the surface of the glass plate with an Ocean Optics USB 2000+ radiometer. All measurements were carried out with a shaft for disposable measuring systems D-CP/PP 7 (Cat. No.: 10636) with a 25 mm diameter disposable aluminum measuring plate. Oscillation mode measurements were performed at different set temperatures (5, 25, 37 °C) with either 1% or 10% strain and a frequency of 1 Hz or 10 Hz. Planarity of the glass plate was checked before every start of measurement and did not exceed a deviation of $\pm 10\mu\text{m}$. The gap size between the two plates of the measuring system was 50 μm . The light intensity at the tip of the light guide was determined by the R2000 radiometer to a value of 3.16 W cm^{-2} , which referred to a light intensity of 30 mW cm^{-2} directly above the glass plate. Storage and Loss Modulus were measured every second for all formulations and the light source was automatically switched on by the rheometer after 60 s of the measurement for HAVE measurements. The starting point for the UV irradiation for formulations containing collagen and HAVE were varied and are listed in Section 3.5.2. The ratio of thiol to ene was 80 mol% thiol component in every case whereupon the functionality of the thiol was also considered. In order to calculate the mol for HAVES with different DS, the MW was calculated by adding up the HA backbone unit with a MW of 400.3 g/mol and the corresponding percentage of vinyladipate functionality with a MW of 155.18 g/mol per unit. Therefore, different MW for HAVE repeating units were calculated accounting different DS for every batch.

Table 12: Calculated Molecular Weight for HAVE repeating units accounting different Degrees of Substitution

HAVE [kDa]	DS [%]	M [g/mol]
	100	555.48
22	14	422.03
77	7	411.16
	13	420.47
100	6	409.61
	9	414.27
150	20	431.34
	27	442.20
180	29	445.30
540	25	439.10

All formulations were prepared in the yellow light laboratory to prevent premature gelation. Stock solutions of HAVE, DTT, ETTMP and Li-TPO were prepared separately in each case with PBS (pH = 7.04) as solvent. Photorheological measurements were conducted for each precursor formulation at least in triplicate to obtain curves for storage modulus (G') and their corresponding standard deviation. In order to obtain homogeneous and bubble-free formulations a vortex mixer and a mini centrifuge was used. For collagen/HAVE measurements all reaction solutions were stored on ice to prevent premature collagen gelation. If not stated otherwise wt% refer to wt/vol%.

3.1 Storage Stability

To investigate the storage stability of HAVE precursors, formulations were measured by photorheology directly after preparation of the formulation and after 48h of storage at 7 °C. HAVE with a MW of 77 kDa and a DS of 13% and a thiol-ene ratio of 80 mol% of DTT, was chosen for this experiment. Stock solutions of HAVE, DTT and Li-TPO were prepared and concentrations are listed in Table 13.

Table 13: Concentrations of stock solutions in PBS for storage stability tests

	C_{stock} [wt%]
HAVE	4
DTT	0.5
Li-TPO	0.5

To receive a final formulation volume of 375 μl , HAVE stock solution (280 μl) was first pipetted into an Eppendorf vial and subsequently 37.5 μl Li-TPO stock solution and 42.7 μl DTT stock solution were added. At the end, 14.8 μl PBS was added to achieve

a final HAVE concentration of 3 wt%. For each measurement 60 μl of formulation were pipetted onto the glass plate of the photorheometer and Storage and Loss Moduli were measured. After the initial formulation was studied, the same formulation was stored in the fridge for 48h. Hereafter, the precursor solution was set to room temperature, homogenized by vortex mixing and analyzed again via photorheology (t_1).

Table 14: Average values and the corresponding Standard Deviation for the storage modulus before Initiation (G'_{start}), maximum storage modulus (G'_{max}), slope of the storage modulus ($\Delta G' \Delta t^{-1}$) and the delay on initiation (t_d) for HAVE 77 kDa, DS = 13%, macromer content = containing 80 mol% thiol-ene ratio of DTT

	G'_{start} [Pa]		G'_{max} [Pa]		$\Delta G' \Delta t^{-1}$ [Pa/s]		t_d [s]	
	Avg.	SD	Avg.	SD	Avg.	SD	Avg.	SD
t_0	68.09	3.57	244.00	15.0	9.21	0.53	3.17	0.07
t_1	89.67	14.60	267.21	39.95	9.88	1.58	2.98	0.21

3.2 The Effect of Thiol Component

To investigate the effect of thiol compound on hydrogel network density, following stock solutions of HAVE, DTT, ETTMP and Li-TPO were prepared, using PBS (pH = 7.04) as solvent. Low-MW HAVE (22 kDa, DS 40%) was used either with 80 mol% thiol-ene ratio of DTT or ETTMP. Furthermore three different macromer contents (5, 10, 15 wt%) were tested. Because very small sample volumes are prepared for each formulation, centrifugation was used to collect the formulation on the bottom of the vial and facilitate pipetting. To receive a final volume of 200 μl for each macromer content, stock solutions were combined according to

Table 16. Results of the measurement are depicted in Table 17.

Table 15: Concentrations of stock solutions in PBS for HAVE (22 kDa, DS 40%)

	c_{stock} [wt%]
HAVE	20
DTT	20
ETTMP	10
Li-TPO	5

Table 16: Volumes of stock solutions for the preparation of precursor solutions either containing 80 mol% thiol-ene ratio DTT or ETTMP

	15 wt%	10 wt%	5 wt%	15 wt%	10 wt%	5 wt%
V_{HAVE} [μ l]	150	100	50	150	100	50
V_{DTT} [μ l]	-	-	-	8	5	3
V_{ETTMP} [μ l]	45	30	15	-	-	-
V_{Li-TPO} [μ l]	2	2	2	2	2	2
V_{PBS} [μ l]	3	68	133	40	93	145

Table 17: Average values and the corresponding standard deviation for the storage modulus (G'_{max}), slope of the storage modulus ($\Delta G' \Delta t^{-1}$) and the delay on initiation (t_d) for HAVE 22 kDa, DS = 40%, containing 80 mol% thiol-ene ratio of DTT or ETTMP with a macromer content of either 5, 10 or 15 wt%

	[wt%]	G'_{max} [kPa]		$\Delta G' \Delta t^{-1}$ [kPa/s]		t_d [s]	
		Avg.	SD	Avg.	SD	Avg.	SD
DTT	5	4.75	0.54	0.35	0.05	6.02	0.32
	10	12.97	0.42	1.69	0.14	5.82	0.05
	15	71.84	24.66	4.99	0.13	5.97	1.01
ETTMP	5	9.86	0.56	1.17	0.08	3.71	0.03
	10	52.83	1.94	6.17	0.42	2.84	0.17
	15	105.50	2.38	10.28	0.16	2.76	0.21

3.3 Variation of Parameters

3.3.1 The Effect of Macromer Content

To investigate the effect of macromer size on the storage modulus and reactivity of the formulation, HAVE with a MW of 22 kDa and a DS of 40% was tested. Formulations of 15, 10 and 5 wt% macromer content were prepared according to the procedure described in chapter 3.2.

Table 18: Average values and the corresponding standard deviation for the maximum storage modulus (G'_{max}), slope of the storage modulus ($\Delta G' \Delta t^{-1}$) and the delay on initiation (t_d) for HAVE 22 kDa, DS = 40%, containing 80 mol% thiol-ene ratio of DTT or ETTMP with a macromer content of either 5, 10 or 15 wt%

	[wt%]	G'_{max} [kPa]		$\Delta G' \Delta t^{-1}$ [kPa/s]		t_d [s]	
		Avg.	SD	Avg.	SD	Avg.	SD
ETTMP	5	9.86	0.56	1.17	0.08	3.71	0.03
	10	52.83	1.94	6.17	0.42	2.84	0.17
	15	105.50	2.38	10.28	0.16	2.76	0.21

3.3.2 The Effect of Degree of Substitution

The effect of the substitution degree was investigated by comparing HAVE with a macromer content of 10 wt% with different DS (14, 21 and 40%). HAVE with a MW of 22 kDa and 80 mol% thiol-ene ratio of ETTMP was used. Different concentrations of stock solutions (Table 19) were used, as the measurements were not performed on the same day.

Table 19: Concentrations of stock solutions in PBS for HAVE 22 kDa, 10 wt% macromer content and either degree of substitution of 14, 21 or 40 % containing 80 mol% thiol-ene ratio ETTMP

	HAVE (DS 14%)	HAVE (DS 21%)	HAVE (DS 40%)
	C_{stock} [wt%]	C_{stock} [wt%]	C_{stock} [wt%]
HAVE	20	20	20
ETTMP	10	30	10
Li-TPO	1	1	5

Table 20: Volumes of stock solutions used to prepare precursor solutions of HAVE 22 kDa, 10 wt% macromer content and either degree of substitution of 14, 21 or 40 % containing 80 mol% thiol-ene ratio ETTMP

	DS [%]		
	14	21	40
V_{HAVE} [μl]	200	100	100
V_{ETTMP} [μl]	8	21	30
$V_{\text{Li-TPO}}$ [μl]	20	10	2
V_{PBS} [μl]	172	69	68

Formulations were prepared by diluting corresponding stock solutions as listed in Table 20. The results of the measurements including standard deviation for the maximum storage modulus, slope of the storage modulus the delay of initiation are listed in Table 21.

Table 21: Average values and the corresponding standard deviation for the maximum storage modulus (G'_{max}), slope of the storage modulus ($\Delta G' \Delta t^{-1}$) and the delay on initiation (t_d) for HAVE 22 kDa, macromer content of 10 wt%, containing 80 mol% thiol-ene ratio of ETTMP with a degree of substitution of either 14, 21 or 40 wt%

	DS [%]	G'_{max} [kPa]		$\Delta G' \Delta t^{-1}$ [kPa/s]		t_d [s]	
		Avg.	SD	Avg.	SD	Avg.	SD
ETTMP	14	0.56	0.02	0.03	0.002	10.78	0.27
	21	23.40	0.43	3.94	0.14	3.85	0.08
	40	52.83	1.94	6.17	0.42	2.84	0.17

3.3.3 The Effect of Macromer Chain Length

The effect of the macromer chain length was investigated by comparing HAVE with a macromer content of 3 wt% but different MW and DS (77 kDa DS = 7%, 100 kDa, DS = 6% and 77 kDa, DS = 13%,). Formulations contained 80 mol% thiol-ene ratio ETTMP. Different concentrations of stock solutions (Table 22) were used.

Table 22: Concentrations of stock solutions in PBS for HAVE 77 kDa DS = 7%, 100 kDa, DS = 6% and 77 kDa, DS = 13%, macromer content of 3 wt%, containing 80 mol% thiol-ene ratio of ETTMP

	77 kDa (DS 7%)	100 kDa (DS 6%)	77 kDa (DS 13%)
	c_{stock} [wt%]	c_{stock} [wt%]	c_{stock} [wt%]
HAVE	5.3	8	5
ETTMP	5	20	5
Li-TPO	1	1	1

Formulations were prepared by diluting corresponding stock solutions as listed in Table 23. The results of the measurements including standard deviation for the maximum storage modulus, slope of the storage modulus the delay of initiation are listed in Table 24.

Table 23: Volumes of stock solutions used to prepare precursor solutions for HAVE 77 kDa DS = 7%, 100 kDa, DS = 6% and 77 kDa, DS = 13%, macromer content of 3 wt%, containing 80 mol% thiol-ene ratio of ETTMP

	HAVE		
	77 kDa (DS 7%)	100 kDa (DS 6%)	77 kDa (DS 13%)
V_{HAVE} [μl]	115	150	120
V_{ETTMP} [μl]	4	3	13
$V_{\text{Li-TPO}}$ [μl]	10	20	10
V_{PBS} [μl]	71	227	57

Table 24: Average values and the corresponding standard deviation for the maximum storage modulus (G'_{max}), slope of the storage modulus ($\Delta G' \Delta t^{-1}$) and the delay on initiation (t_d) for HAVE 77 kDa DS = 7%, 100 kDa, DS = 6% and 77 kDa, DS = 13%, macromer content of 3 wt%, containing 80 mol% thiol-ene ratio of ETTMP

	HAVE	G'_{max} [kPa]		$\Delta G' \Delta t^{-1}$ [kPa/s]		t_d [s]	
		Avg.	SD	Avg.	SD	Avg.	SD
	77kDa DS 7% *	(116.00; 167.00)	-	(13.00; 27.39)	-	(3.47; 2.60)	-
ETTMP	100 kDa DS 6%	145.80	9.01	20.69	1.51	3.51	0.05
	77 kDa DS 13%	244.00	15.00	9.37	0.45	3.14	0.05

* Only 2 values available

3.4 Hydrogel Network considering Vinyl-Groups per Macromer Chain

Formulations were prepared as described in Section 3.3.3 and results of the measurements are depicted in Table 24.

3.5 Collagen as additional Matrix Compound

Collagen/HAVE formulations were prepared using HAVE with a MW of 22 kDa with a DS of 21% and lyophilized rat tail collagen (mainly type 1). Collagen stock solution was prepared in 0.2% acetic acid and all other stock solutions were prepared, using PBS buffer (pH = 7.4). Formulations containing HAVE were prepared with a thiol to ene ratio of 80 mol% thiol-ene ratio of ETTMP.

Table 25: Concentration of stock and final solutions for measurements containing HAVE, collagen, Li-TPO and 80 mol% thiol-ene ratio of ETTMP

	c_{stock} [wt%]	c_{final} [wt%]	c_{final} [mol%]
HAVE	4	1.02	-
Collagen	0.8	0.32	-
ETTMP	20	-	80
Li-TPO	2	0.05	-

Collagen Stock solution was prepared by dissolving 12 mg of the lyophilized protein in 1.5 mL acetic acid (0.2%, pH = 3.8) over night in the fridge. HAVE stock solution was prepared by dissolving 11.6 mg of HAVE in 290 μ L of PBS to receive a 4 wt% solution. For each measurement equivalents (described in section 3.5.1 and 3.5.2) of each stock solution were pipetted into Eppendorf vials to achieve final concentrations listed in Table 25.

3.5.1 Preliminary Tests

Table 26: Different compositions of HAVE/collagen formulations for photorheology measurements

Formulation	A	B	C
Components	Collagen	HAVE	Collagen
	NaOH	ETTMP	NaOH
	PBS	Li-TPO	HAVE
		PBS	ETTMP
			Li-TPO
			PBS

For formulation **A** 60 μ L of cooled collagen stock solution were neutralized (pH = 7.1) in an Eppendorf vial using 4 μ L of cooled 0.1 M NaOH. The pH was monitored with a micro pH electrode. Addition of 72 μ L cooled PBS led to a final collagen concentration of 0.32 wt%.

Formulations for the photopolymerization of HAVE without collagen were prepared by pipetting 140 μl of HAVE stock solution into an Eppendorf vial, adding 19 μl of ETTMP stock solution, 11 μl Li-TPO stock solution and 210 μl PBS reaching a final HAVE concentration of 1.02 wt%.

3.5.2 The Influence of Collagen on HAVE hydrogels

All reagents were first cooled with an ice bath and added subsequently from beforehand prepared stock solutions to achieve homogeneous formulations. 37 μl collagen stock solution were pipetted into an Eppendorf vial and neutralized to $\text{pH} = 7.1$ via addition of 6 μl of 0.1 M NaOH. Addition of 23 μl HAVE, 3 μl ETTMP, 2.5 μl Li-TPO stock solution and 18.4 μl PBS led to final concentrations as depicted in Table 25. The formulation was homogenized by vortex mixing and pipetted onto the glass plate of the photorheometer. Paraffin oil was added on the edge of the measuring plate after the measuring position was reached.

Measurements were performed where HAVE was polymerized before collagen gelation was initiated by the increase of temperature. For these experiments the measurement was started with a set temperature of 5 $^{\circ}\text{C}$ during the first 60 s. Photopolymerization was initiated at 5 $^{\circ}\text{C}$ and after a constant storage modulus was achieved (after 9.77 min), the temperature was increased with a heating rate of: 6.4 $^{\circ}\text{C}/\text{min}$. From this time on collagen gelation was initiated. After 37 $^{\circ}\text{C}$ were reached the temperature remained constant for the rest of the measurement. Rheological data was collected until collagen fibrillogenesis was mostly completed, which was indicated by the stop of increase of the storage modulus.

For the measurements where HAVE was polymerized after collagen gelation, rheological data was collected at the beginning at 5 $^{\circ}\text{C}$ and the heating rate (6.4 $^{\circ}\text{C}/\text{min}$) initiated after 2 min of measurement. Collagen could gel for 67 min until photopolymerization was initiated. By this method HAVE was polymerized at 37 $^{\circ}\text{C}$ in contrast to before mentioned 5 $^{\circ}\text{C}$. The measurement was performed until constant Storage Moduli were observed.

4 Proof of Concept

First of all HAVE stock solution was prepared by dissolving the macromer in PBS and storing the solution in the fridge overnight. Shortly before structuring, the second stock solution was prepared, by weighing the corresponding amount of P2CK and DTT in an Eppendorf vial and filling up with PBS until concentrations of stock solutions are achieved, as depicted in Table 27. All formulations containing P2CK were prepared in the orange lab and stored in the dark during transportation to avoid premature photoinitiation.

Table 27: Stock solutions in PBS for the preparation of the final formulation for 2PP structuring

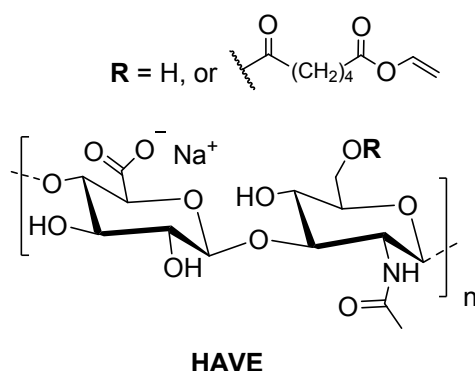
	C_{stock}	
	[wt%]	[mmol]
HAVE	20	-
P2CK	-	2
DTT	1.92	-

Stock solutions were mixed in a 1:1 (v/v) ratio, to achieve following final concentrations for 2PP structuring: 10 wt% macromer content HAVE, 1 mmol P2CK and 80 mol% thiol-ene ratio DTT. Therefore, 50 μL of HAVE stock solution was combined with the suspension containing L929 murine fibroblast (concentration 10^7 cells mL^{-1}) in medium and pipetted into a surface-treated Ibidi μ -dish (35 mm with glass bottom). L929 murine fibroblasts were beforehand cultured in Dulbecco's modified Eagle's medium with 4.5 g L^{-1} glucose in an incubator at $37 \text{ }^\circ\text{C}$. In order to perform the cell-free control experiment, the HAVE precursor formulation was mixed with the same amount of PBS solution. Two-photon microfabrication was performed, using a Ti:sapphire laser system ($\lambda = 800 \text{ nm}$, pulse width: 70 fs, scanning speed: 100 mm s^{-1}). A detailed description of the system parameters can be found within the Section Materials and Methods. Hydrogel structures were printed by scanning the focused laser beam with varied laser power (10 – 100 mW) through the precursor formulation, according to the information from the sliced CAD file. Cells were stained by calcein after 24 h and printed hydrogel constructs including encapsulated cells were visualized by laser scanning microscopy

Summary

The fast-evolving field of tissue engineering (TE) has particularly focused on hydrogels, since these biomaterials provide structural properties, similar to extracellular matrix (ECM). The scope of this thesis was to synthesize and characterize newly developed biomaterials and investigate their performance. For this approach hyaluronic acid (HA) was used as a backbone material, because of its natural abundance in the human body. Modification of this polymer leads to macromers with polymerizable functional groups. Vinyl ester (VE) functionalities were chosen, as they have already been employed as possible biomaterials for TE.^{105,106} They are potent alternatives for state of the art monomers, such as (meth)acrylates, which under certain conditions show the disadvantage of cytotoxicity.

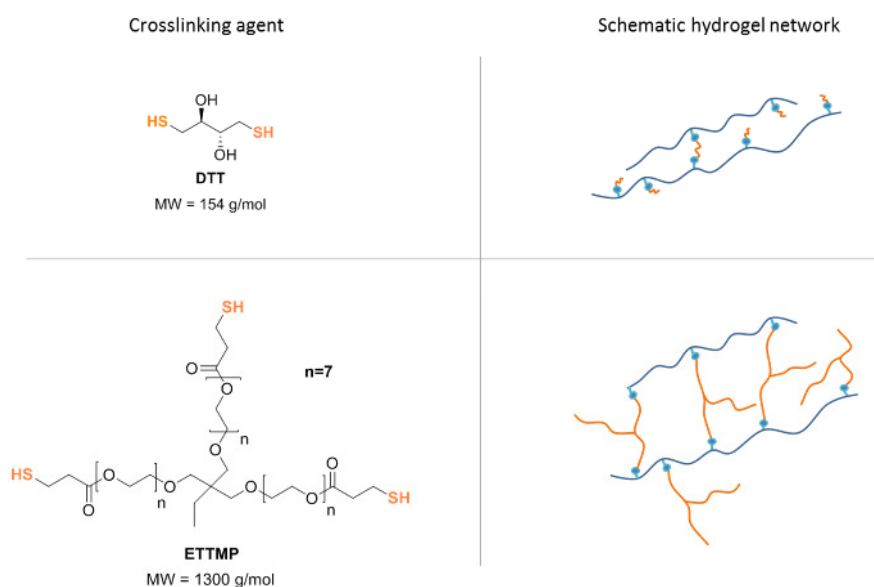
The synthesis of hyaluronic acid vinyl esters (HAVEs) was performed by the acidic degradation of HA, followed by the enzymatic transesterification reaction of the tetrabutylammonium salt of HA with commercially available DVA.



The degree of substitution (DS) of vinyl functionalities on the polysaccharide backbone was thereby adjusted by the lipase reaction time. Characterization of HAVE precursors and the determination of corresponding DS was examined via ¹H-NMR analysis. A new concept was employed to determine the DS of HAVE via the selective hydrolysis of VE functionalities, by the addition of NaOD to the NMR solvent (D₂O). A convenient determination of the DS via the well-separated methylene signal of the adipate functionality was possible via the increased resolution of the NMR spectra. Still, the presence of VE moieties on the HA backbone was confirmed via NMR spectra in D₂O solely.

Via the selective degradation of the polymer backbone, a variety of molecular weight (MW) was accessible. Different approaches were investigated (acidic- and enzymatic

degradation) and compared within this thesis. The acidic degradation was chosen for the synthesis of all precursors, as the enzymatic degradation yielded in uncontrollable fragmentation of HA, indicated by very high PDI values. Different macromers were compared, focusing on the effect of chain length on hydrogel properties. Besides different MW ranges, also a variety of DS was accessible. Former studies within this research group investigated the effect of thiol-ene chemistry on HAVE hydrogels. By the introduction of thiols, it was possible to boost reactivity of HAVE and increase the reaction rate of the usually relatively slow homopolymerization of VEs. Previous studies showed, that 80 mol% thiol-ene ratio was most appropriate for HAVE precursors and was therefore used for all formulations, taking account of the functionality of the thiol. Increased conversion and crosslinking density compared to homopolymerization of HAVE was observed. HAVE macromers, in combination with different thiols were tested and their impact on viscoelastic properties was investigated. The use of a high-MW crosslinking agent (ETTMP) showed a drastic increase in crosslinking density compared to low-MW DTT. It is assumed, that the difunctional crosslinking agent shows the tendency to occupy most VE functionalities only with one side of the multifunctional molecule. This leads to the formation of “loose ends” and a low crosslinking density of the HAVE hydrogel.

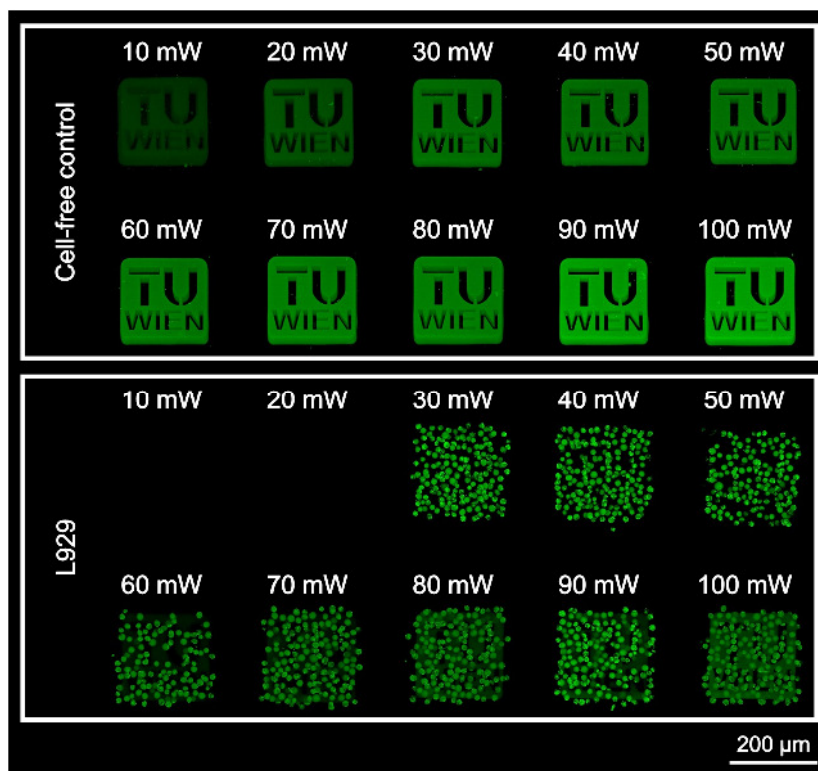


The high MW and therefore long macromer chains of the trifunctional ETTMP increased the spatial proximity between thiols and VE and increased the conversion of complementary reactive groups. Photorheology was used to investigate the trends of storage- and loss modulus during hydrogel formation. These moduli indicate

crosslinking density and reactivity of HAVE precursors, which are determined by system parameters, such as MW, DS, macromer content (MC) and crosslinking agent (thiol). Photorheology studies showed the effect of MC on mechanical properties of HAVE hydrogels, whereas an increase in MC led to higher crosslinking densities, indicated by higher storage modulus. With increasing MC, the number of reactive chains increased, resulting in a denser hydrogel network. Furthermore, an increase of MC guided the system towards higher reactivity, indicated by shorter delays of initiation and higher slope in the linear region of the storage modulus. The same effect could be observed if DS was increased. HAVE macromers with higher DS showed higher crosslinking density, as well as reactivity than precursors with low DS.

As the crosslinking density can also be guided by the MW, the effect of increasing MW was studied within this thesis. Usually HAVE macromers with very low MW (~20 kDa) and high DS (95%) showed the tendency to form rather brittle hydrogels. Therefore, the MW of macromers was successively increased. Unfortunately, an increase of polymer chain lengths brought along undesired effects. Rather low solubility for high MW macromers (≥ 77 kDa) was observed. Handling of solutions with a MC above 3 wt% was very difficult, due to very high viscosity.

To solve these issues, low-MW HAVE in combination with collagen was used to design new hydrogel matrices based on interpenetrating networks. These networks consist of two or more crosslinked polymers. Chemically crosslinked HAVE represents the first network, whereas the second matrix consists of collagen, which is physically crosslinked, by temperature-responsive fibrillogenesis. Collagen (type 1) was used, especially because, much like HA, this protein is naturally present in the ECM. Collagen in general is able to transform into a self-assembled hydrogel at optimum pH (7) and temperature (37 °C). This fibrillogenesis should be used to investigate the effect on HAVE networks and especially the order of fibrillogenesis compared to photopolymerization of HAVE is studied. Precursors with low DS (21%) and low MW (22 kDa) were used to produce these new type of interpenetrating networks. Usually HAVE with a DS of 21% shows rather low crosslinking density on its own, but photorheological measurements confirmed the idea, that collagen builds a mechanical support for HAVE hydrogels, particularly if HAVE is photopolymerized after collagen triple helix association.



Finally HAVE precursors were tested towards printability via two-photon polymerization. Cell encapsulation experiments were performed and showed promising results regarding cell viability.

By the synthesis, characterization and comparison of a variety of different HAVE precursors, it was possible to gain a broad overview on the most promising and potent types of macromers. Due to their versatility and especially possibility, to use them within interpenetrating networks, HAVE precursors show great potential towards applications in TE.

Materials and Methods

Chemicals:

ETTMP: THIOCURE® from Bruno Bock (MW = 1300 g/mol)

PBS buffer: 136.9 mM NaCl, 2.7 mM KCl, 5.1 mM Na₂HPO₄, 0.9 mM KH₂PO₄, 0.02% NaN₃, pH = 7.37

Acetate buffer: 1.1 M NaAc, 0.15 M NaCl, 0.01% BSA, pH = 5.23

Sigma-Aldrich

Collagen: rat tail collagen (mainly type 1 collagen) from Roche Cat.no.: 11179179001; 3x10mg lyophilized cell culture grade;

Hyaluronic acid sodium salt from streptococcus equi: Prod. No. 53747, CAS Nr.: 9067-32-7

Hyaluronidase from bovine testes, Type I - S (400 - 1000 U/mg), Prod.No. H3506, CAS Nr.: 37326-33-3

Amberlite® IR120 hydrogen form: Prod.No. 216534, CAS Nr.: 39389-20-3

L929 murine fibroblasts were obtained from Sigma and cultured in Dulbecco's modified Eagle's medium with 4.5 g L⁻¹ glucose in an incubator at 37 °C, 95% rel. humidity, and 5% CO₂. Dulbecco's modified Eagle's medium was supplemented with 10 vol.% fetal bovine serum and 1 vol.% of 10 000 U mL⁻¹ Penicillin/Streptomycin.

pH-Meters

The pH measurements for the monomer synthesis were performed with a WTW pH meter 330i. Collagen measurements were via a Mettler Toledo InLab Micro pH electrode with an S7 screw head equipped with a F2 FiveGo™ pH Meter

Dialysis

The purification and also the cation exchange of the synthesized polymers was performed with Pre-wetted RC Tubing dialysis membranes Spectra/Por®6 from Spectrum®Labs.com with a molecular weight cutoff (MWCO) of 50 kDa. The dialysis tubes, which were delivered in a wet state were thoroughly washed with distilled water to remove the sterile storage solution. To seal one side of the dialysis tube, it was clamped with a clip and the polymer solution transferred into the tube via a funnel. The volume of the solution inside the dialysis tube did not exceed 2/3 of the maximum

volume of the tube. Air bubbles were removed by pressing the dialysis walls onto each other before sealing the second end of the tube with another clip. Up to 3 clamped dialysis tubes, which corresponds to approximately 30 mL of polymer solution were immersed into a 5 L beaker, which was filled with a 0.3 M NaCl solution and stirred with a magnetic stirrer. After 3h the diffusion was accelerated by exchanging the used NaCl solution to a new one. The solvent change of NaCl solution was performed at least 7 times and afterwards the dialysis was performed with demineralized water with also 7 changes of solvent. After complete dialysis, the clamps were opened and the purified polymer solution transferred into a flask and lyophilized.

Lyophilization

Aqueous HA solutions were freeze-dried by immersing the flask containing the sample in liquid nitrogen until all water was frozen. The solvent was then removed by sublimation on a Christ freeze-drying system Gamma 2-20 at a pressure of 0.01 mbar and a temperature of the cooling coils of -85 °C.

NMR

¹H-NMR spectra (25 °C) were measured with a *Bruker DPX-200* (200MHz) or an *Avance DRX-400* (400 MHz) fourier transform spectrometer. The chemical shift is displayed in parts per million (ppm) referenced to the according solvent (D₂O δ = 4.79 ppm, DMSO-d₆ δ = 2.50 ppm) with tetramethylsilane (TMS) at δ = 0 ppm. Multiplicities are given as: s = singlet, bs = broad singlet, d = doublet, q = quartet, sext = sextet, m = multiplet). Deutero-chloroform (CDCl₃) and Deutero-water (D₂O) from the company Eurisotop were used as solvents. The grade of deuteration was at least 99.5%.

GPC

GPC analysis was performed with a Viscotek GPC system, including a Viscotek GPCmax VE2001 GPC solvent/sample module (100 µl loop), a solvent degasser, a Viscotek VE3580 refractive index concentration detector, a Waters pre-column, a Waters ultrahydrogel linear 7.8x30mm column, and a Waters ultrahydrogel 250 7.8x30 mm column with 10 µm particle size. The eluent was PBS buffer (NaH₂PO₄ 0.05 M, NaCl 0.1 M, NaN₃ 0.05%) at a temperature of 30 °C and a flow rate of 0.5 mL min⁻¹. Pullulan calibration standards (Shodex Standard P-82) were used for

standard calibration to determine the number average of molecular weight (\overline{M}_n) and the Polydispersity Index (PDI).

Photorheology

Photorheological measurements were performed with a modular compact rheometer (Anton-Paar MCR 302 WESP). Filtered UV light (320-500 nm) from a light source (Omniscure S2000 EXFO) with a high-pressure mercury lamp was used to irradiate the sample. A two-headed light guide formed the connection between the Omnicure and the photorheometer whereas the lamp was directly triggered by the rheometer. The light source was calibrated with a R2000 radiometer from EXFO and the light intensity directly measured on the surface of the glass plate with an Ocean Optics USB 2000+ radiometer. All measurements were carried out with a shaft for disposable measuring systems D-CP/PP 7 (Cat. No.: 10636) with a 25 mm diameter disposable aluminum measuring plate. Oscillation mode measurements were performed at a set temperature of 25 °C with either 1 or 10% strain and a frequency of 1 or 10 Hz. Planarity of the glass plate was checked before every start of the measurement and did not exceed a deviation of $\pm 10\mu\text{m}$. The gap size of the plate to plate measuring system was 50 μm .

Two-Photon Polymerization

Cell encapsulation experiments were performed by using a 2PP system. The used 2PP process is based on a Ti:sapphire laser system (wavelength 800nm, pulse width 70 fs, objective Zeiss C-Achroplan 32x/0.85, scanning speed 100 mm s⁻¹, hatch 0.3 μm , layer spacing 0.5 μm) and was already described in previous studies.¹⁴¹ A description of the process can be found in literature.¹⁴⁵ Based on a sliced CAD file structures were printed by scanning the focused laser beam with varied laser powers (10 – 100 mW, 10 mW steps) through the hydrogel formulation.

Confocal Microscopy

Confocal 3D image stacks of the fabricated 2PP-scaffolds were taken with a Zeiss Axio Observer Z1 and a LSM 700 unit. Data processing was performed using ZEN11 software from Zeiss. As an objective 20 x EC Plan Neofluar 20 x/05 was used.

Abbreviations

AMT	Additive Manufacturing Techniques
BSA	Bovine Serum Albumine
CAD	Computer-Aided Design
CAL-B	Lipase <i>Candida Antarctica</i> (acrylic resin)
Da	Dalton
DLP-SLA	Digital Light Processing- based Stereolithography
DS	Degree of Substitution
DTT	DL-Dithiothreitol
DVA	Divinyl Adipate
EA	Ethyl acetate
ECM	Extracellular Matrix
EDC	1-Ethyl-3-(3-dimethylaminopropyl)carbodiimides
Ene	Macromer, containing a polymerizable double bond
ETTMP	Ethoxylated Trimethylolpropane Tri(3-Mercaptopropionate)
FDM	Fused Deposition Modeling
GAG	Glycosaminoglycane
GM-HA	Glycidyl Methacrylate modified Hyaluronic Acid
GPC	Gel Permeation Chromatography
G'_{max}	Maximum Storage Modulus
G''	Loss Modulus
HA	Hyaluronic Acid
HASE	Hyaluronidase
HAVE	Hyaluronic Acid Vinyl Ester
HOBt	1-Hydroxybenzotriazole
HQ	Hydroquinone
IJP	Inkjet Printing
IPN	Interpenetrating Network
LCST	Lower Critical Solution Temperature
MC	Macromer Content
MW	Molecular Weight
MWCO	Molecular Weight Cutoff
NHS	N-hydroxysuccinimide
n_{vinyl}	Number of vinyl functionalities per polymer chain

P2CK	3,3'-((((1E,1'E)-(2-oxocyclopentane-1,3-diylidene) bis(methanylylidene)) bis(4,1-phenylene)) bis(methylazanediy)) dipropanoate
PAA	Polyacrylic acid
PBS	Phosphate Buffered Saline
PEG	Polyethylene glycole
PHEMA	Polyhydroxy ethyl methacrylate
PIM	Polyimides
PNIPAAm	Poly(N-isopropylacrylamide)
PU	Polyurethane
PVA	Polyvinylalcohol
PVP	Polyvinylpyrrolidone
RGD	Tripeptide Sequence (Arginine-Glycine-Aspartate)
R_h	Hydrodynamic Radius
SLA	Stereolithography
SLS	Selective Laser Sintering
TBA	Tetrabutylammonium
TBA-OH	Tetrabutylammonium hydroxide
t_d	Delay of Initiation
TE	Tissue Engineering
VE	Vinyl Ester
2PP	Two Photon Polymerization
3D	Three-Dimensional
$\Delta G' \Delta t^{-1}$	Slope in the linear region of the Storage Modulus

Appendix

2.3 Alternative Synthesis of HAVE

Additionally, an alternative synthesis of HAVE was investigated. Transesterification reactions of monosaccharides was already performed in literature.¹⁰³ Due to the reason, that literature states these transesterification reactions with relatively low-MW saccharides, the hypothesis was proposed to investigate the activity of the enzyme towards the primary hydroxyl group of the relatively high-MW HA polymer. In other words, the transesterification of HA was implemented via enzyme, but also during another batch with same starting material under identical reaction conditions without the addition of lipase.

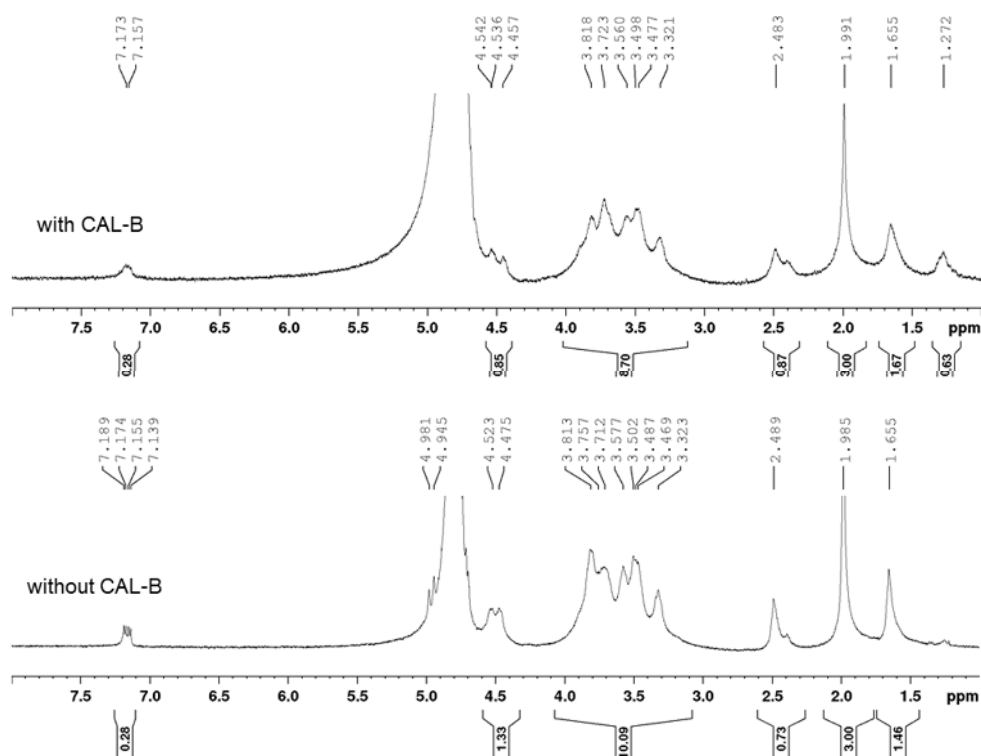


Figure 68: Comparison of ¹H-spectra of HAVE (D₂O) after transesterification performed for same reaction times, once with and once without lipase (CAL-B)

Figure 68 shows that the vinyl signals at 7.1 ppm show the same integral values for the reaction with and without lipase. In the top spectrum an additional signal at 1.272 ppm indicates a partial hydrolysis of the vinyl ester.

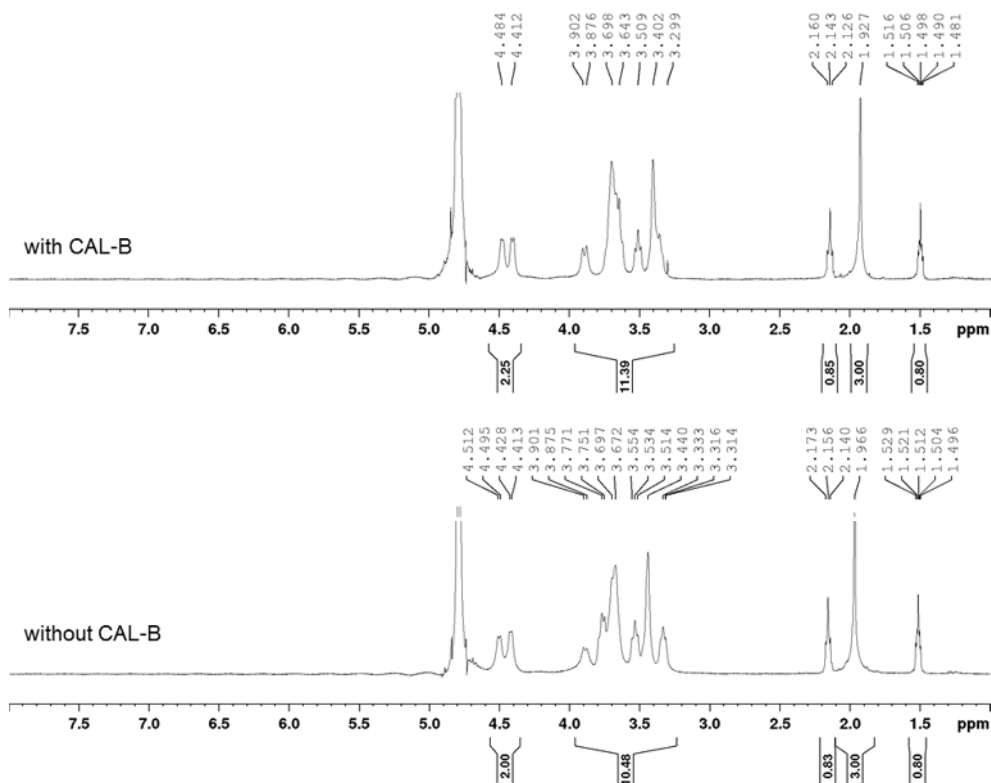


Figure 69: Comparison of ^1H -spectra of HAVE ($\text{D}_2\text{O} + 3 \mu\text{l NaOD}$) after transesterification performed with and without lipase (CAL-B)

Comparing the integrals of the CH_2 signals of vinyl adipate at 1.5 ppm, the same effect can be observed for Figure 69 as for Figure 68. The DS for Figure 68 is determined in the top and bottom spectrum to be 28% and for Figure 69 in both cases 20%. All samples were characterized by referring to the CH_2 signal at 1.5 ppm.

3.1 Storage Stability

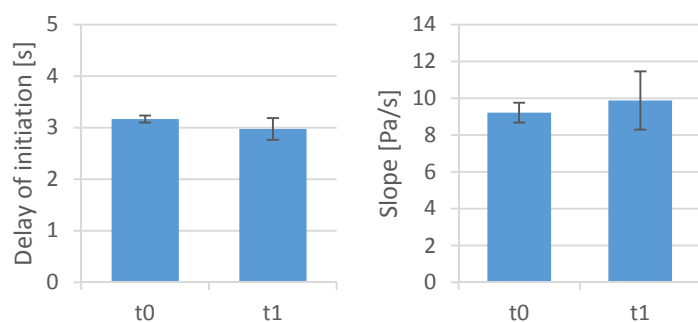


Figure 70: Delay of initiation and Slope in the linear region of the storage modulus from stored HAVE formulation (MW = 77kD, DS = 13 %, macromer content = 3 wt%, 80 mol% thiol-ene ratio of DTT)

3.2 The Effect of Thiol Component (HAVE 22 kDa, DS = 21%)

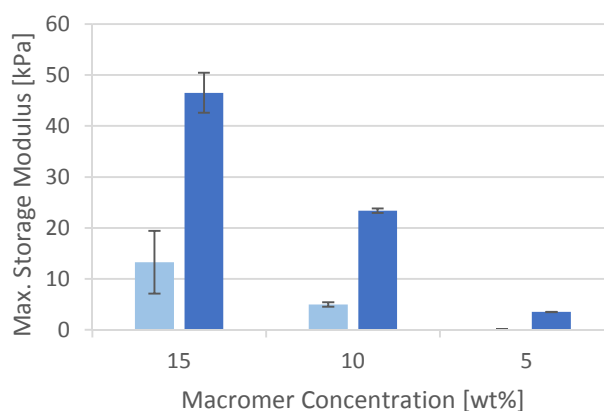


Figure 71: Maximum storage modulus for HAVE (22 kDa, DS 21%) with 80 mol% thiol-ene ratio of DTT (light blue) and ETTMP (dark blue) with varying macromer content (5, 10, 15 wt%)

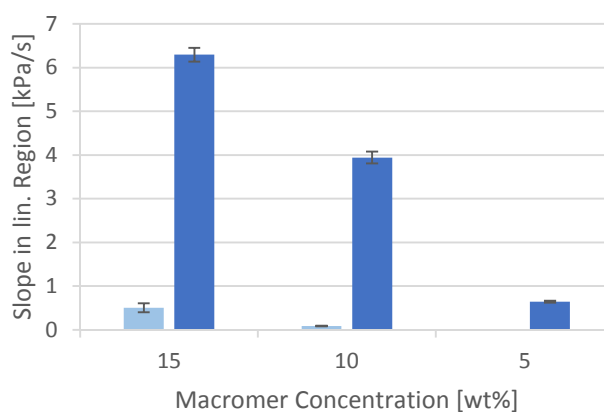


Figure 72: Slope in linear region of the storage modulus for HAVE (22 kDa, DS 21%) with 80 mol% thiol-ene ratio of DTT (light blue) and ETTMP (dark blue) with varying macromer content (5, 10, 15 wt%)

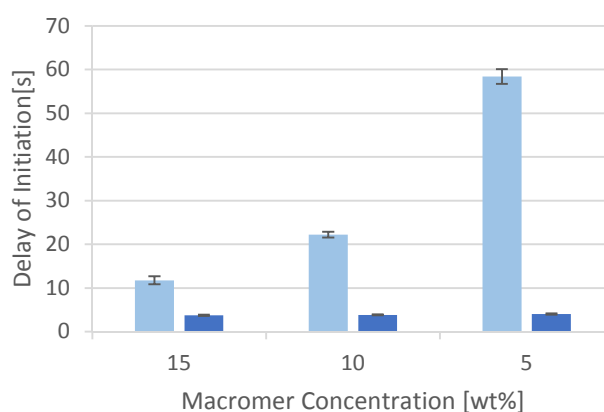


Figure 73: Delay of initiation for HAVE (22 kDa, DS 21%) with 80 mol% thiol-ene ratio of DTT (light blue) and ETTMP (dark blue) with varying macromer content (5, 10, 15 wt%)

Table 28: Values for the maximum storage modulus, the slope in linear region of the storage modulus and the delay of initiation for HAVE (22 kDa, DS 21%) with 80 mol% thiol-ene ratio of DTT and ETTMP with varying macromer concentration (5, 10 ,15 wt%)

	[wt%]	G'_{\max} [kPa]		$\Delta G' \Delta t^{-1}$ [kPa/s]		t_d [s]	
		Avg.	SD	Avg.	SD	Avg.	SD
DTT	5	0.10	0.01	0.841	0.15	58.43	1.68
	10	4.96	0.44	84.16	7.413	22.21	0.69
	15	13.26	6.15	503.99	104.94	11.77	0.89
ETTMP	5	3.53	0.04	645.88	22.21	4.02	0.16
	10	23.4	0.43	3941.96	135.74	3.85	0.08
	15	46.5	3.93	6295.84	159.46	3.74	0.12

HAVE: 22 kDa, DS = 21, 40, 95%, 5 wt% macromer content

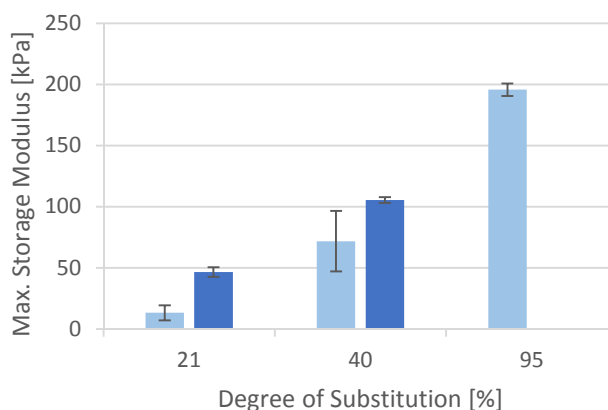


Figure 74: Maximum storage modulus for HAVE (22 kDa, macromer content = 5 wt%) with 80 mol% thiol-ene ratio of DTT (light blue) and ETTMP (dark blue) with varying DS (21 ,40 ,95%)

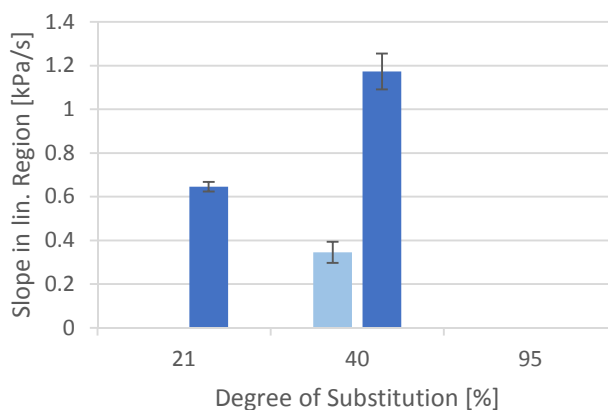


Figure 75: Slope in linear region of the storage modulus for HAVE (22 kDa, macromer content = 5 wt%) with 80 mol% thiol-ene ratio of DTT (light blue) and ETTMP (dark blue) with varying DS (21 ,40 ,95%)

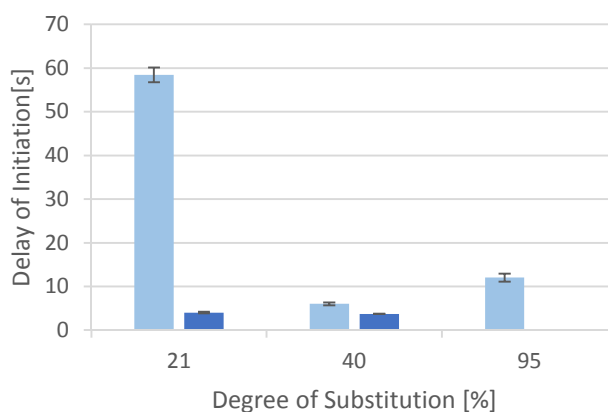


Figure 76: Delay of initiation for HAVE (22 kDa, macromer content = 5 wt%) with 80 mol% thiol-ene ratio of DTT (light blue) and ETTMP (dark blue) with varying DS (21, 40 ,95%)

Table 29: Values for the maximum storage modulus, the slope in linear region of the storage modulus and the delay of initiation for HAVE (22 kDa, macromer content = 5 wt%) with 80 mol% thiol-ene ratio of DTT and ETTMP with varying DS (21, 40 ,95%)

	DS [%]	G'_{max} [kPa]		$\Delta G' \Delta t^{-1}$ [kPa/s]		t_d [s]	
		Avg.	SD	Avg.	SD	Avg.	SD
DTT	21	0.10	0.01	0.0008	0.0002	58.43	1.68
	40	4.75	0.54	0.3454	0.0489	6.02	0.32
	95	0.05	0.02	0.0016	0.0002	12.03	0.92
ETTMP	21	3.53	0.04	0.6459	0.0222	4.02	0.16
	40	9.86	0.56	1.1733	0.0816	3.71	0.03
	95	-	-	-	-	-	-

HAVE: 22 kDa, DS = 14, 21, 40, 95%, 10 wt% macromer content

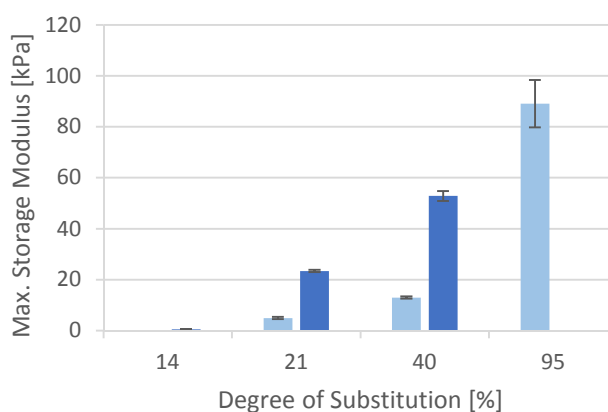


Figure 77: Maximum storage modulus for HAVE (22 kDa, macromer content = 10 wt%) with 80 mol% thiol-ene ratio of DTT (light blue) and ETTMP (dark blue) with varying DS (14, 21, 40 ,95%)

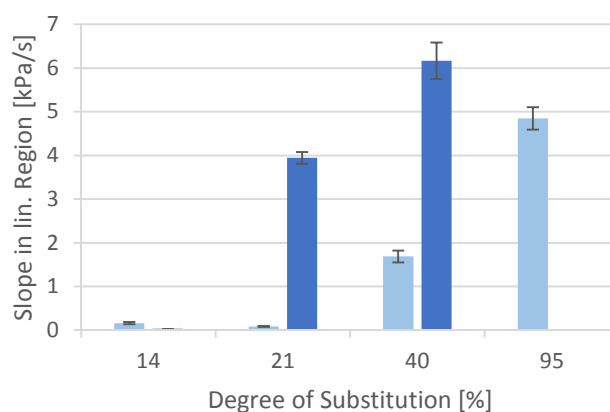


Figure 78: Slope in linear region of the storage modulus for HAVE (22 kDa, macromer content = 10 wt%) with 80 mol% thiol-ene ratio of DTT (light blue) and ETTMP (dark blue) with varying DS (14, 21, 40 ,95%)

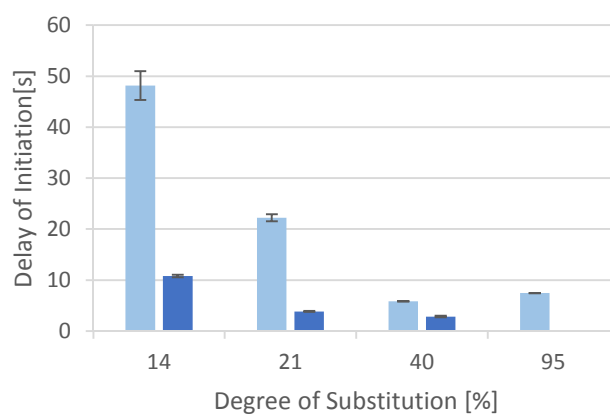


Figure 79: Delay of initiation for HAVE (22 kDa, macromer content = 10 wt%) with 80 mol% thiol-ene ratio of DTT (light blue) and ETTMP (dark blue) with varying DS (14, 21, 40 ,95%)

Table 30: Values for the maximum storage modulus, the slope in linear region of the storage modulus and the delay of initiation for HAVE (22 kDa, macromer content = 10 wt%) with 80 mol% thiol-ene ratio of DTT and ETTMP with varying DS (14, 21, 40, 95%)

DS [%]	G'_{\max} [kPa]		$\Delta G' \Delta t^{-1}$ [kPa/s]		t_d [s]		
	Avg.	SD	Avg.	SD	Avg.	SD	
DTT	14	0.029	0.004	0.161	0.026	48.16	2.82
	21	4.963	0.437	0.084	0.007	22.21	0.69
	40	12.970	0.416	1.687	0.135	5.82	0.05
	95	89.067	9.265	6.167	0.419	7.45	0.03
ETTMP	14	0.561	0.022	0.032	0.002	10.78	0.27
	21	23.401	0.432	3.942	0.136	3.85	0.08
	40	52.825	1.936	4.845	0.254	2.84	0.17
	95	-	-	-	-	-	-

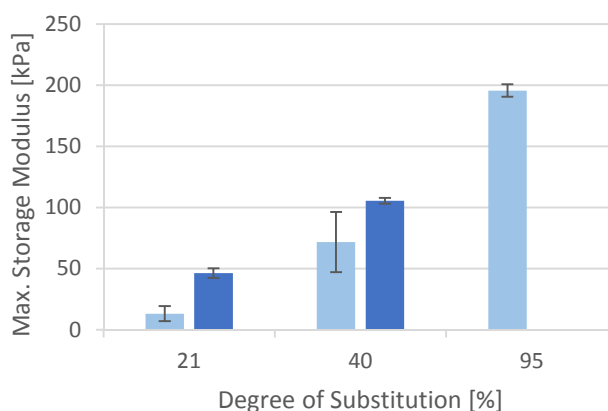
HAVE: 22 kDa, DS = 21, 40, 95%, 15 wt% macromer content

Figure 80: Maximum storage modulus for HAVE (22 kDa, macromer content = 15 wt%) with 80 mol% thiol-ene ratio of DTT (light blue) and ETMP (dark blue) with varying DS (21, 40, 95%)

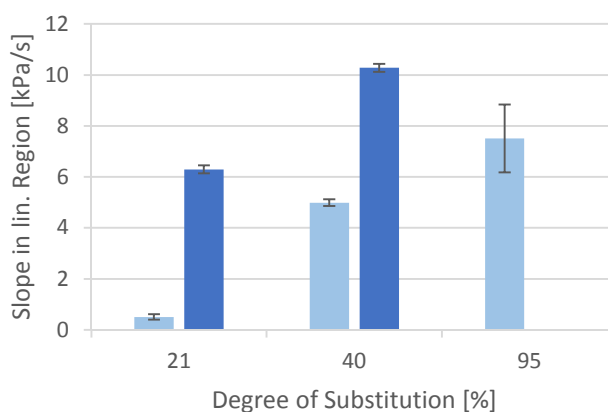


Figure 81: Slope in linear region of the storage modulus for HAVE (22 kDa, macromer content = 15 wt%) with 80 mol% thiol-ene ratio of DTT (light blue) and ETMP (dark blue) with varying DS (21, 40, 95%)

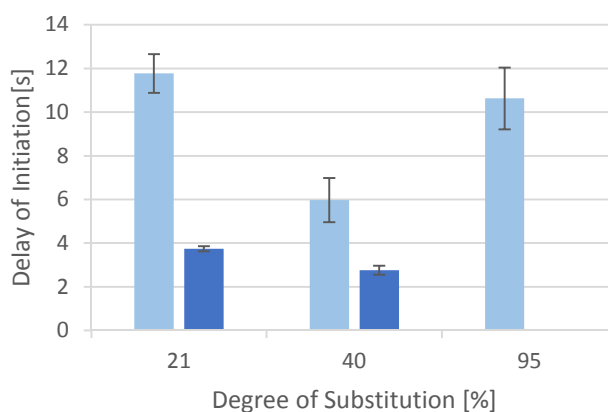


Figure 82: Delay of initiation for HAVE (22 kDa, macromer content = 10 wt%) with 80 mol% thiol-ene ratio of DTT (light blue) and ETMP (dark blue) with varying DS (21, 40, 95%)

Table 31: Values for the maximum storage modulus, the slope in linear region of the storage modulus and the delay of initiation for HAVE (22 kDa, macromer content = 15 wt%) with 80 mol% thiol-ene ratio of DTT and ETTMP with varying DS (21, 40 ,95 %)

	DS [%]	G'_{\max} [kPa]		$\Delta G' \Delta t^{-1}$ [kPa/s]		t_d [s]	
		Avg.	SD	Avg.	SD	Avg.	SD
DTT	21	13.26	6.15	0.50	0.10	11.77	0.89
	40	71.84	24.66	4.99	0.13	5.97	1.01
	95	195.67	5.03	7.51	1.33	10.63	1.42
ETTMP	21	46.51	3.93	6.30	0.16	3.74	0.12
	40	105.50	2.38	10.28	0.17	2.76	0.21
	95	-	-	-	-	-	-

HAVE: 77 kDa, DS = 13%

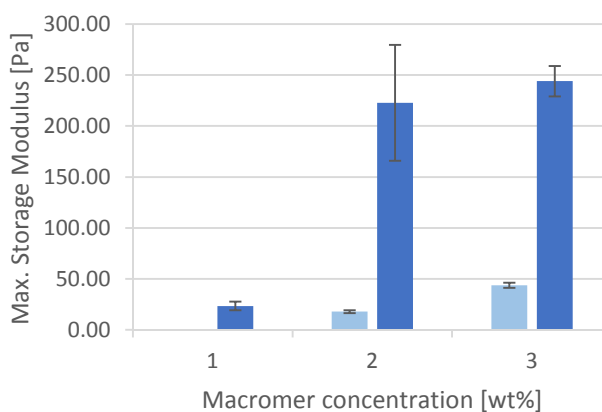


Figure 83: Maximum storage modulus for HAVE (77 kDa, DS = 13%) with 80 mol% thiol-ene ratio of DTT (light blue) and ETTMP (dark blue) with varying macromer concentration (1, 2, 3 wt%)

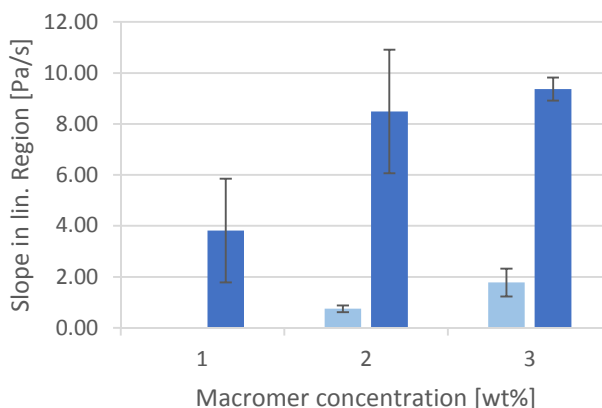


Figure 84 Slope in linear region of the storage modulus for HAVE (77 kDa, DS = 13%) with 80 mol% thiol-ene ratio of DTT (light blue) and ETTMP (dark blue) with varying macromer concentration (1, 2, 3 wt%)

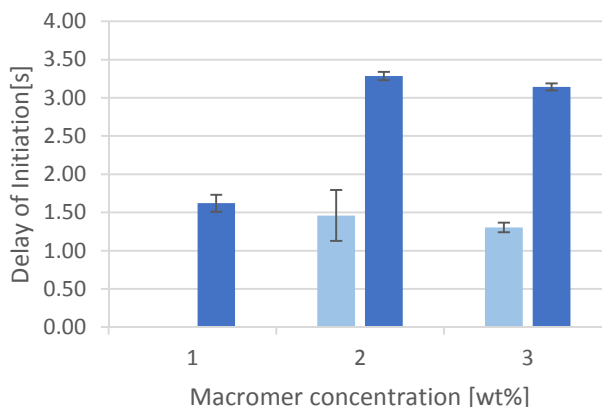


Figure 85: Delay of initiation for HAVE (77 kDa, DS = 13%) with 80 mol% thiol-ene ratio of DTT (light blue) and ETTMP (dark blue) with varying macromer concentration (1, 2, 3 wt%)

Table 32: Values for the maximum storage modulus, the slope in linear region of the storage modulus and the delay of initiation for HAVE (77 kDa, DS = 13%) with 80 mol% thiol-ene ratio of DTT and ETTMP with varying macromer concentration (1, 2, 3 wt%)

	MC [wt%]	G'_{max} [Pa]		$\Delta G' \Delta t^{-1}$ [Pa/s]		t_d [s]	
		Avg.	SD	Avg.	SD	Avg.	SD
DTT	1	-	-	-	-	-	-
	2	18.16	1.42	0.75	0.13	1.46	0.33
	3	43.73	2.63	1.78	0.54	1.31	0.06
ETTMP	1	23.50	4.32	3.82	2.03	1.62	0.11
	2	222.67	56.85	8.49	2.43	3.29	0.05
	3	244.16	15.34	9.37	0.45	3.14	0.05

HAVE: 77 kDa, DS = 7 and 13%, macromer content = 3 wt%

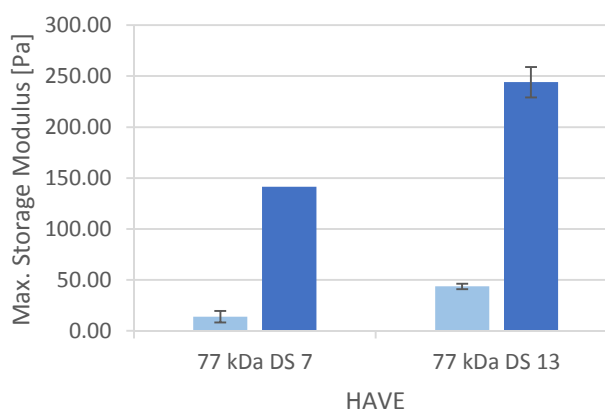


Figure 86: Maximum storage modulus for HAVE (77 kDa, macromer content = 3 wt%) with 80 mol% thiol-ene ratio of DTT (light blue) and ETTMP (dark blue) with varying degree of substitution (7, 13%)

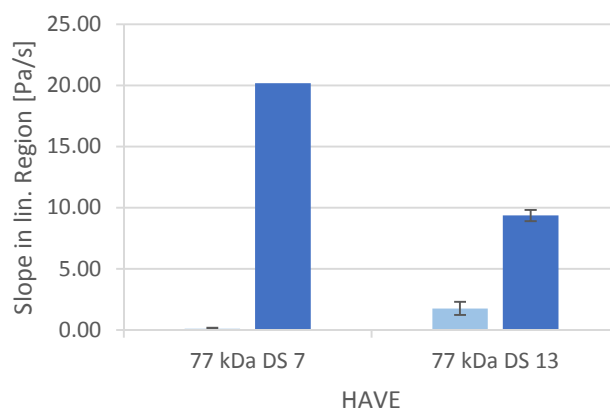


Figure 87: Slope in linear region of the storage modulus for HAVE (77 kDa, macromer content = 3 wt%) with 80 mol% thiol-ene ratio of DTT (light blue) and ETTMP (dark blue) with varying degree of substitution (7, 13%)

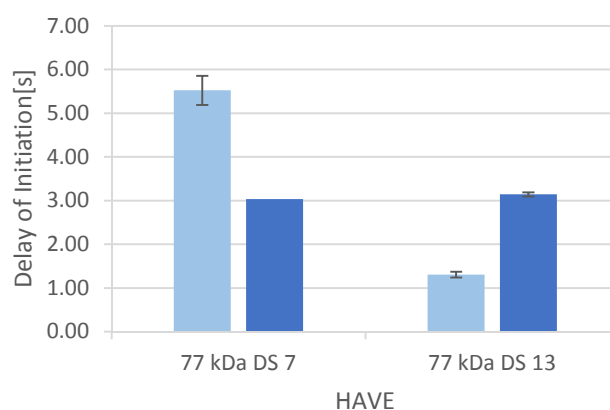


Figure 88: Delay of initiation for HAVE (77 kDa, macromer content = 3 wt%) with 80 mol% thiol-ene ratio of DTT (light blue) and ETTMP (dark blue) with varying degree of substitution (7, 13%)

Table 33: Values for the maximum storage modulus, the slope in linear region of the storage modulus and the delay of initiation for HAVE (77 kDa, macromer content = 3 wt%) with 80 mol% thiol-ene ratio of DTT and ETTMP with varying degree of substitution (7, 13%)

	DS [%]	G'_{max} [Pa]		$\Delta G' \Delta t^{-1}$ [Pa/s]		t_d [s]	
		Avg.	SD	Avg.	SD	Avg.	SD
DTT	7	13.96	5.66	0.13	0.08	5.52	0.34
	13	43.73	2.63	1.78	0.54	1.31	0.06
ETTMP	7*	(116.13; 167.05)	-	(13.24; 27.39)	-	(3.47; 2.60)	-
	13	244.12	15.43	9.37	0.45	3.14	0.05

* only 2 values available

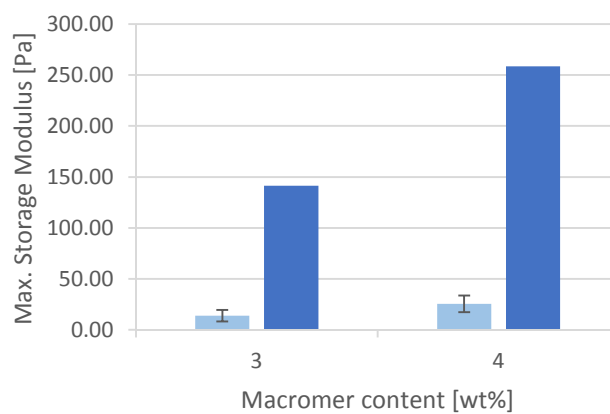
HAVE: 77 kDa, DS = 7%

Figure 89: Maximum storage modulus for HAVE (77 kDa, DS = 7%) with 80 mol% thiol-ene ratio of DTT (light blue) and ETMP (dark blue) with varying macromer content (3, 4 wt%)

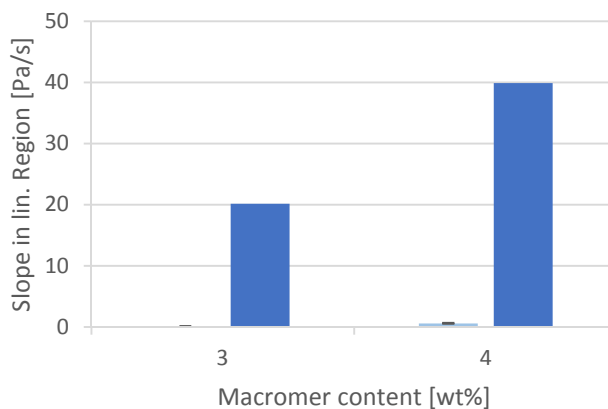


Figure 90: Slope in linear region of the storage modulus for HAVE (77 kDa, DS = 7%) with 80 mol% thiol-ene ratio of DTT (light blue) and ETTMP (dark blue) with varying macromer content (3, 4 wt%)

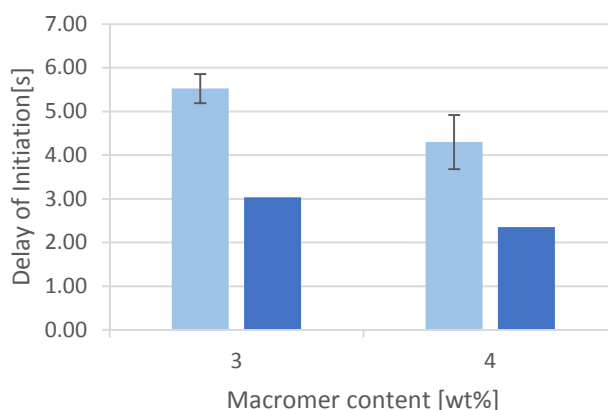


Figure 91: Delay of initiation HAVE (77 kDa, DS = 7%) with 80 mol% thiol-ene ratio of DTT (light blue) and ETTMP (dark blue) with varying macromer content (3, 4 wt%)

Table 34: Values for the maximum storage modulus, the slope in linear region of the storage modulus and the delay of initiation for HAVE (77 kDa, DS = 7%) with 80 mol% thiol-ene ratio of DTT and ETTMP with varying macromer content (3, 4 wt%)

	MC [wt%]	G'_{max} [Pa]		$\Delta G' \Delta t^{-1}$ [Pa/s]		t_d [s]	
		Avg.	SD	Avg.	SD	Avg.	SD
DTT	3	13.96	5.66	0.13	0.08	5.52	0.34
	4	25.57	8.15	0.62	0.06	4.30	0.62
ETTMP	3	(116; 167)	-	(13.03; 27.39)	-	(3.47; 2.60)	-
	4	(391; 126)	-	(50.49; 29.28)	-	(2.76; 1.94)	-

*only 2 measurements available (high viscosity)

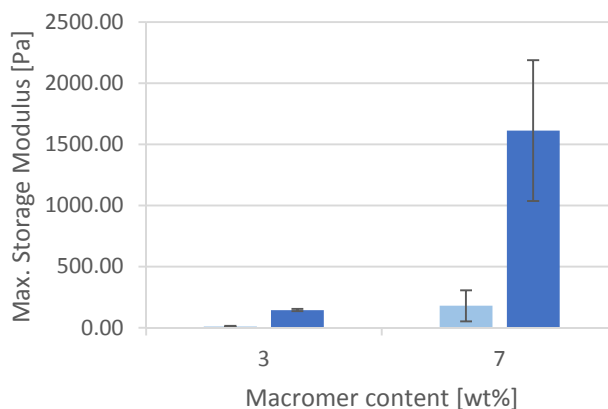
HAVE: 100 kDa, DS = 6%

Figure 92: Maximum storage modulus for HAVE (100 kDa, DS = 6%) with 80 mol% thiol-ene ratio of DTT (light blue) and ETTMP (dark blue) with varying macromer content (3, 7 wt%)

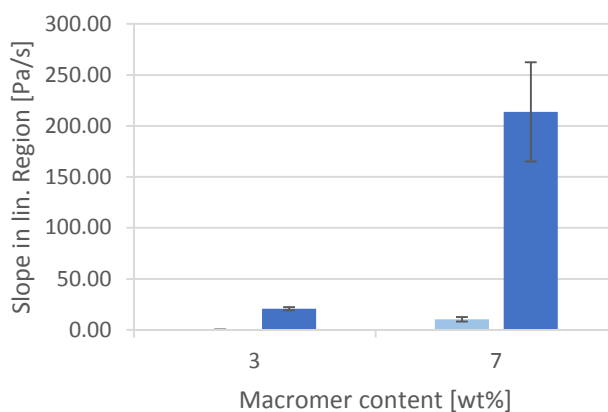


Figure 93: Slope in linear region of the storage modulus for HAVE (100 kDa, DS = 6%) with 80 mol% thiol-ene ratio of DTT (light blue) and ETTMP (dark blue) with varying macromer content (3, 7 wt%)

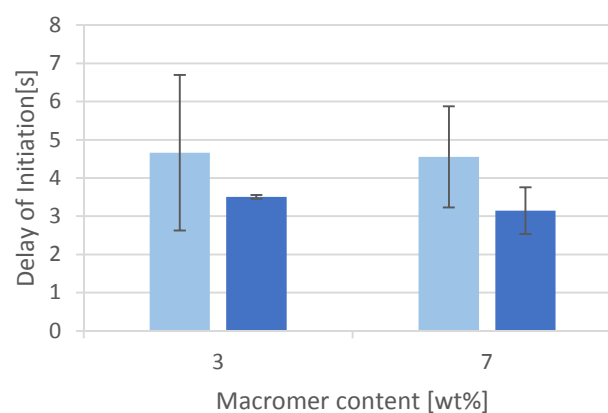


Figure 94: Delay of initiation for HAVE (100 kDa, DS = 6%) with 80 mol% thiol-ene ratio of DTT (light blue) and ETTMP (dark blue) with varying macromer content (3, 7 wt%)

Table 35: Values for the maximum storage modulus, the slope in linear region of the storage modulus and the delay of initiation for HAVE (100 kDa, DS = 6%) with 80 mol% thiol-ene ratio of DTT and ETTMP with varying macromer content (3, 7 wt%)

	MC [wt%]	G'_{max} [Pa]		$\Delta G' \Delta t^{-1}$ [Pa/s]		t_d [s]	
		Avg.	SD	Avg.	SD	Avg.	SD
DTT	3	11.66	6.08	0.17	0.14	4.66	2.04
	7	180.44	128.24	10.26	2.25	4.55	1.33
ETTMP	3	145.80	9.01	20.69	1.51	3.51	3.14
	7	1613.01	575.31	213.82	48.57	0.05	0.61

HAVE: 100 kDa, DS = 9%

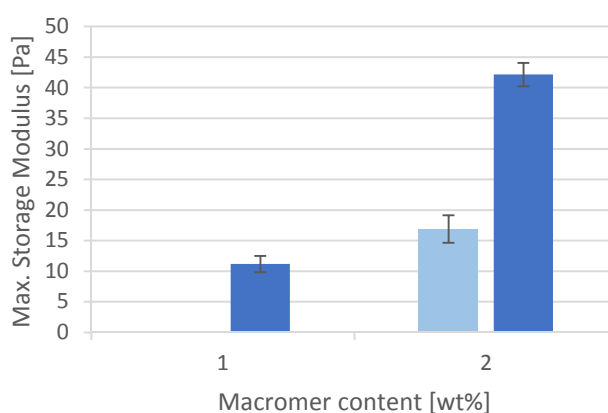


Figure 95: Maximum storage modulus for HAVE (100 kDa, DS = 9%) with 80 mol% thiol-ene ratio of DTT and ETTMP with varying macromer content (1, 2 wt%)

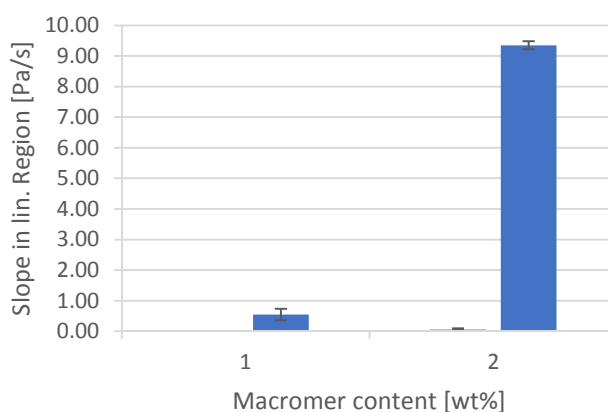


Figure 96: Slope in linear region of the storage modulus for HAVE (100 kDa, DS = 9%) with 80 mol% thiol-ene ratio of DTT and ETTMP with varying macromer content (1, 2 wt%)

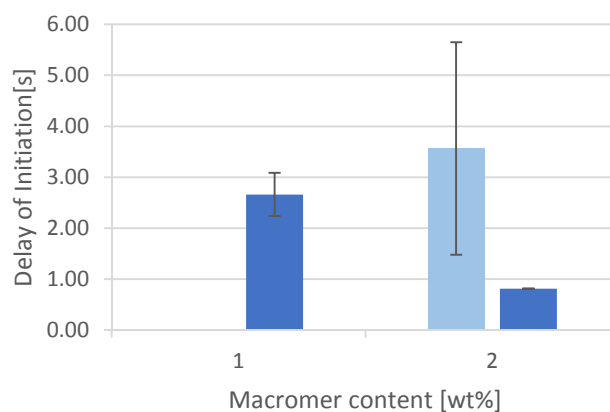


Figure 97: Delay of initiation for HAVE (100 kDa, DS = 9%) with 80 mol% thiol-ene ratio of DTT and ETTMP with varying macromer content (1, 2 wt%)

Table 36: Values for the maximum storage modulus, the slope in linear region of the storage modulus and the delay of initiation for HAVE (100 kDa, DS = 9%) with 80 mol% thiol-ene ratio of DTT and ETTMP with varying macromer content (1, 2 wt%)

	MC [wt%]	G'_{\max} [Pa]		$\Delta G' \Delta t^{-1}$ [Pa/s]		t_d [s]	
		Avg.	SD	Avg.	SD	Avg.	SD
DTT	1*	-	-				
	2	16.90	2.26	0.07	0.03	3.57	2.09
ETTMP	1	11.17	1.34	0.55	0.19	2.66	0.42
	2	42.15	1.92	9.35	0.13	0.81	0.01

* no reaction

3.3.1 The Effect of Macromer Content

(HAVE: 22 kDa, DS = 95%)

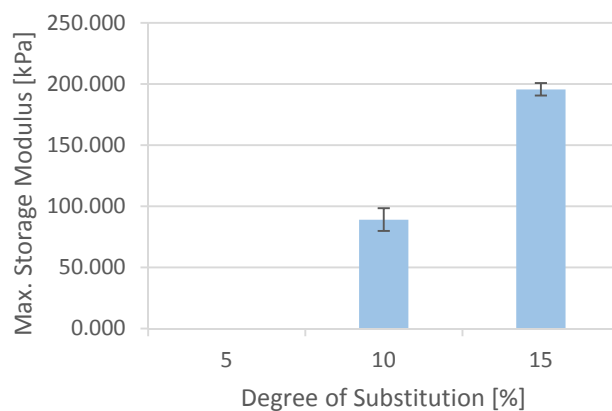


Figure 98: Maximum storage modulus for HAVE (22 kDa, DS 95%) with 80 mol% thiol-ene ratio of DTT with varying macromer content (5, 10, 15 wt%)

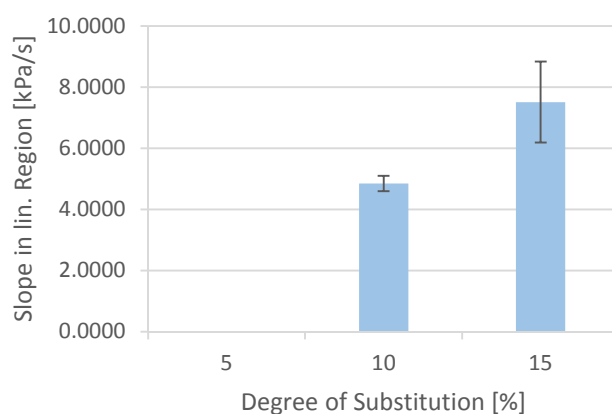


Figure 99: Slope in linear region of the storage modulus for HAVE (22 kDa, DS 95%) with 80 mol% thiol-ene ratio of DTT with varying macromer content (5, 10, 15 wt%)

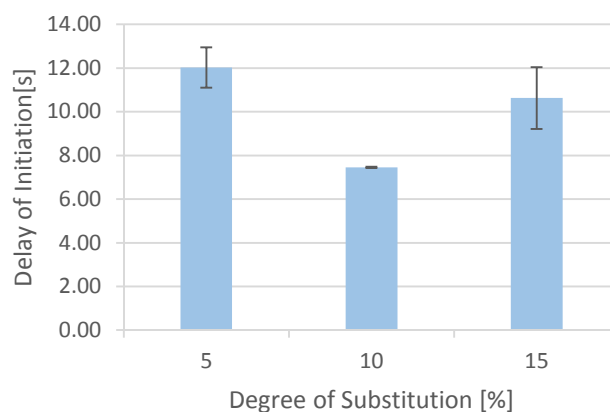


Figure 100: Delay of initiation for HAVE (22 kDa, DS 95%) with 80 mol% thiol-ene ratio of DTT with varying macromer content (5, 10, 15 wt%)

Table 37: Values for the Maximum storage modulus, the slope in linear region of the storage modulus and the delay of initiation for HAVE (22 kDa, DS 95%) with 80 mol% thiol-ene ratio of DTT with varying macromer content (5, 10, 15 wt%)

MC [wt%]	G'_{\max} [kPa]		$\Delta G' \Delta t^{-1}$ [kPa/s]		t_d [s]	
	Avg.	SD	Avg.	SD	Avg.	SD
5	0.047	0.002	0.0016	0.0002	12.03	0.92
10	89.07	9.27	4.85	0.25	7.45	0.03
15	195.67	5.03	7.51	1.33	10.62	1.42

3.3.3 Effect of Macromer Chain length

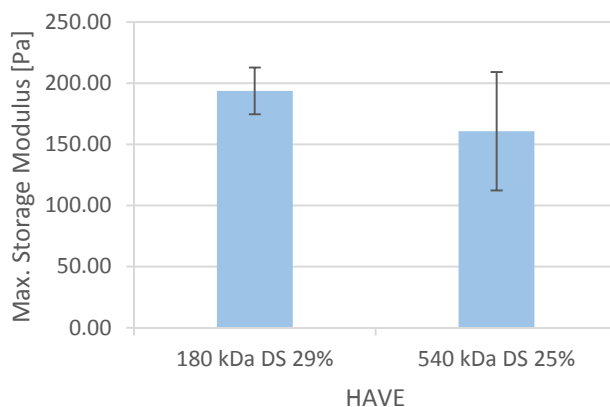


Figure 101: Maximum storage modulus for HAVE 180 kDa, DS = 29% and HAVE 540 kDa, DS = 25% with 80 mol% thiol-ene ratio of DTT with a macromer content of 1 wt%

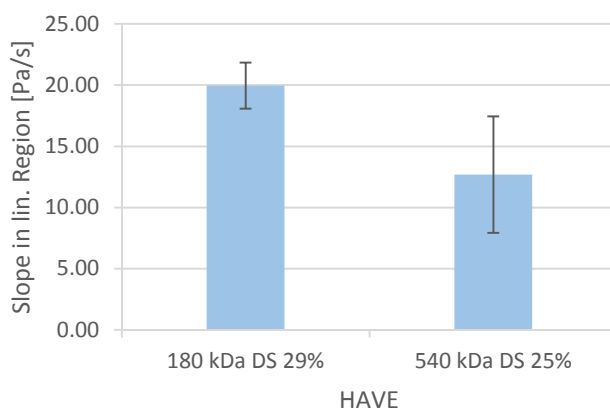


Figure 102: Slope in linear region of the storage modulus for HAVE 180 kDa, DS = 29% and HAVE 540 kDa, DS = 25% with 80 mol% thiol-ene ratio of DTT with a macromer content of 1 wt%

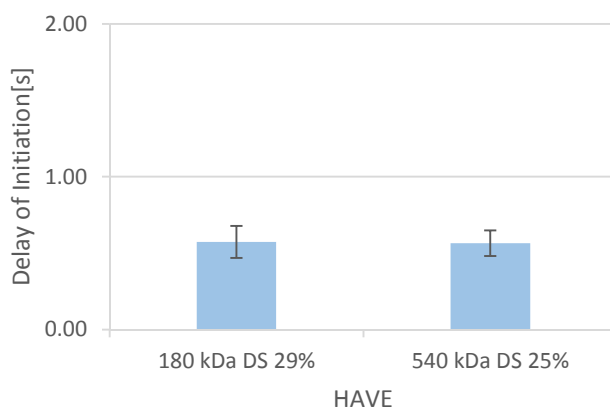


Figure 103: Delay of initiation for HAVE 180 kDa, DS = 29% and HAVE 540 kDa, DS = 25% with 80 mol% thiol-ene ratio of DTT with a macromer content of 1 wt%

Table 38: Values for the maximum storage modulus, the slope in linear region of the storage modulus and the delay of initiation for HAVE 180 kDa, DS = 29% and HAVE 540 kDa, DS = 25% with 80 mol% thiol-ene ratio of DTT with a macromer content of 1 wt%

	HAVE	G'_{max} [Pa]		$\Delta G' \Delta t^{-1}$ [Pa/s]		t_d [s]	
		Avg.	SD	Avg.	SD	Avg.	SD
DTT	180 kDa, DS 29%	193.80	19.08	19.96	1.89	0.58	0.10
	540 kDa DS 25%	160.81	48.34	12.68	4.76	0.57	0.08

3.4 Hydrogel Network considering Vinyl-Groups per Macromer Chain

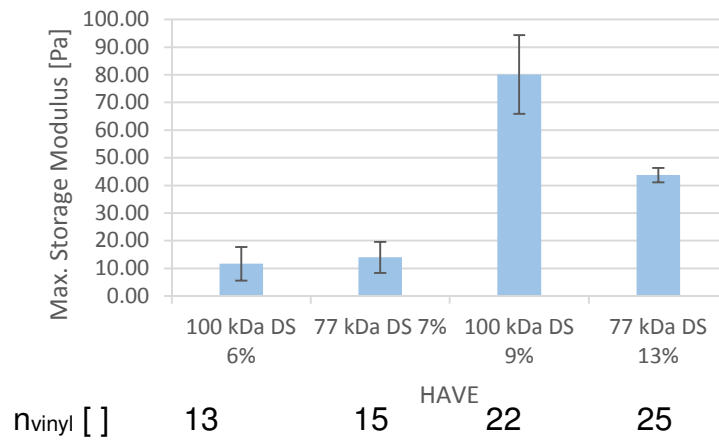


Figure 104: Maximum storage modulus for HAVEs 77 kDa and 100 kDa (macromer content = 3 wt%) ordered by means of increasing number of vinyl functionalities per HA chain with 80 mol% thiol-ene ratio of DTT

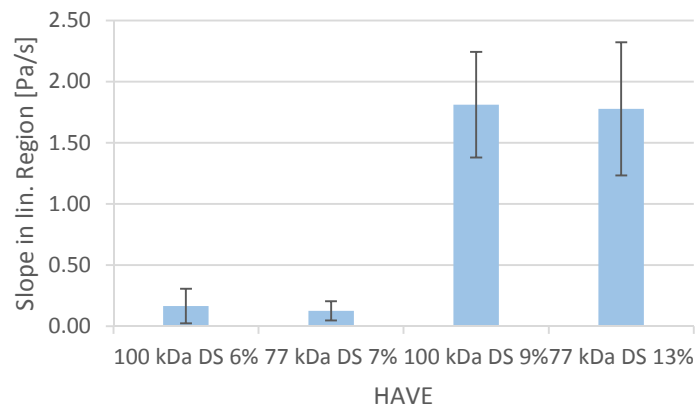


Figure 105: Slope in linear region of the storage modulus for HAVEs 77 kDa and 100 kDa (macromer content = 3 wt%) ordered by means of increasing number of vinyl functionalities per HA chain with 80 mol% thiol-ene ratio of DTT

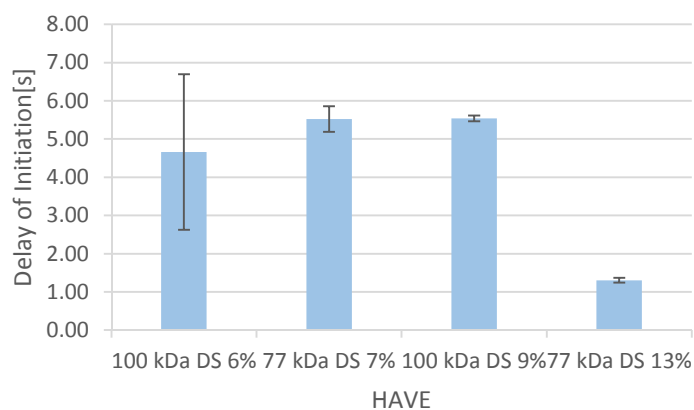


Figure 106: Delay of initiation for for HAVES 77 kDa and 100 kDa (macromer content = 3 wt%) ordered by means of increasing number of vinyl functionalities per HA chain with 80 mol% thiol-ene ratio of DTT

Table 39: Values for the maximum storage modulus, the slope in linear region of the storage modulus and the delay of initiation for HAVES 77 kDa and 100 kDa (macromer content = 3 wt%) ordered by means of increasing number of vinyl functionalities per HA chain with 80 mol% thiol-ene ratio of DTT

	G'_{max} [Pa]		$\Delta G' \Delta t^{-1}$ [Pa/s]		t_d [s]		
	Avg.	SD	Avg.	SD	Avg.	SD	
DTT	HAVE						
	100 kDa, DS 6%	11.66	6.08	0.17	0.14	4.66	2.04
	7 kDa DS 7%	13.96	5.66	0.13	0.08	5.52	0.34
	100 kDa, DS 9%	80.10	14.21	1.81	0.43	5.54	0.08
	7 kDa DS 13%	43.73	2.63	1.78	0.54	1.31	0.06

The Effect of Sonication

Not only pH but also sonication influences the MW of HA. Literature^{120,18} stated that ultrasonic degradation of HA occurs in a different extent depending on the MW of the macromolecule and never leads to complete degradation into HA monomers. An experiment was performed using the macromer with a MW of 22 kDa, a MC of 1 wt% and DS of 95% with DTT as a thiol component. The formulation was prepared and once measured without sonication and once measured after the precursor solution was placed in an ultrasonic bath for 3h. The resulting curves for the Storage Moduli for both measurements which were performed 3 times are depicted in Figure 107.

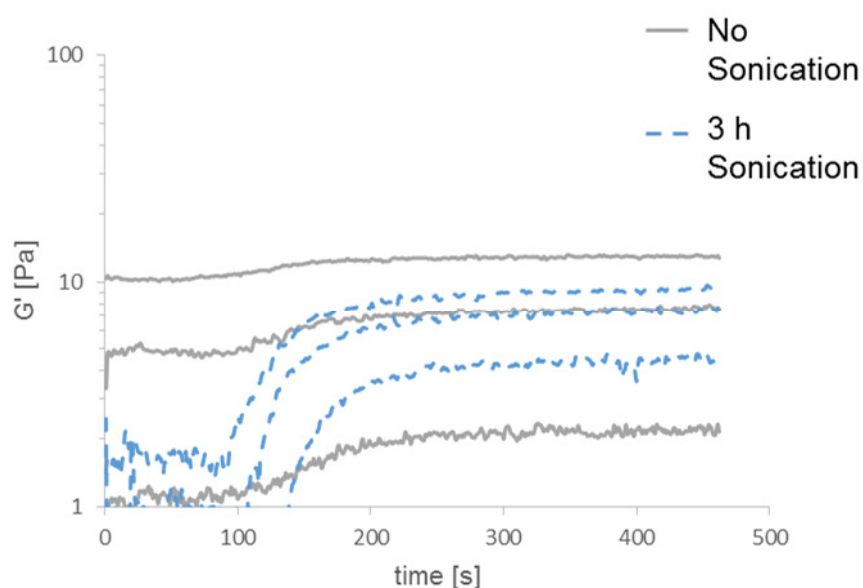


Figure 107: Effect of sonication on HAVE 22 kDa with DS 95 and 1 wt% macromer content DTT

Figure 107 shows that sonication has a tremendous effect on the possibility to polymerize a formulation. The formulation without sonication shows no significant increase of G' after irradiation with light. Additionally, the same formulation shows already quite a high value for G' in the first 60 s of the measurement. This means there is already a quite strong physical gel present before the precursor solution is photopolymerized. It seems that sonication leads to the segregation of the macromer chains by loosening the intermolecular interactions between the molecules. This leads to a better crosslinking possibility because the interaction between the chains increases.

Similar effect can be observed when formulation with MW of 22 kDa, DS of 40% and MC of 2 wt% is measured. First of all, it needs to be mentioned that a MC of 1 wt% for the same formulation did not lead to a polymerization which was detectable by photorheology. The formulation with a MC of 2 wt% led to polymerization even without sonication. Additional influence of sonication was also measured and led to a higher G'_{\max} during the measurement. The effect of segregation of macromer chains and the decrease of G' during the first 60 s of the measurement could only be observed for a few of the measurements. For this formulation, the effect of sonication on G'_{\max} was more significant than the effect of sonication on G' in the beginning of the measurement. The dramatic increase of G'_{\max} after sonication is depicted in Figure 108.

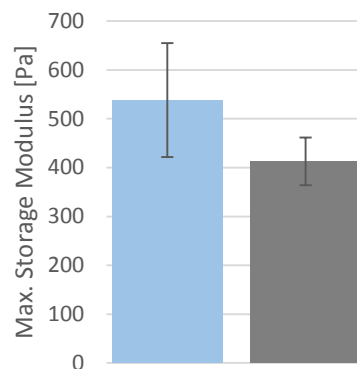


Figure 108: Sonication (blue), without sonication (grey) of HAVE 22kDa, DS = 40%, macromer content = 2 wt% and 80 mol% thiol-ene ratio DTT

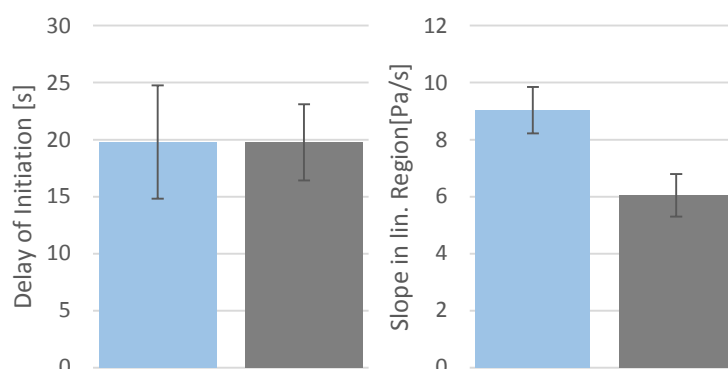


Figure 109: Delay of initiation and slope in the linear region of the storage modulus for HAVE 22kDa, DS = 40%, macromer content = 2 wt% and 80 mol% thiol-ene ratio DTT

This leads to the conclusion that one should consider sonication as a tool to tune sensitivity of a formulation, especially when the formulation is appearing to not being reactive at first.

The same effect was examined for HAVE with MW of 100 kDa, DS of 9%, MC of 2 wt% and the use of ETTMP as thiol component.

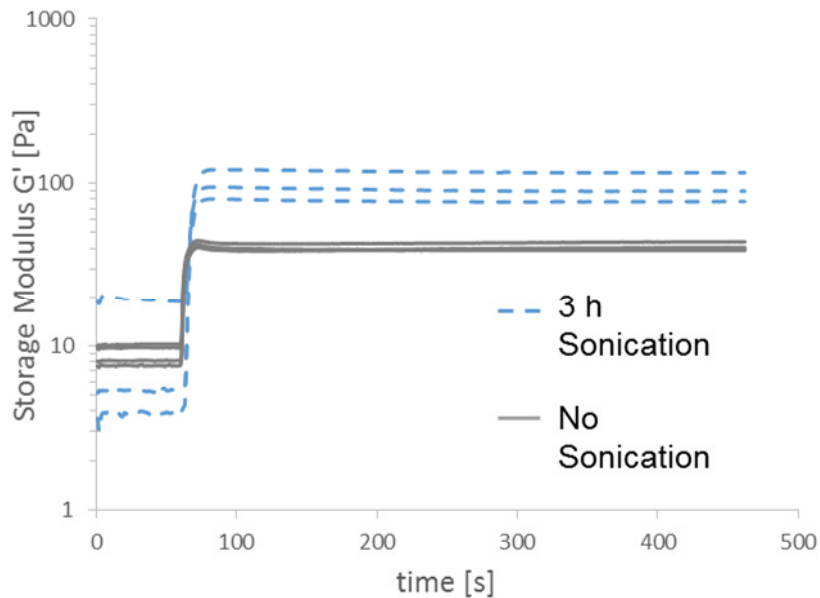


Figure 110: Effect of sonication on HAVE 100 kDa, DS = 9%, macromer content = 2 wt% and 80 mol% thiol-ene ratio ETTMP

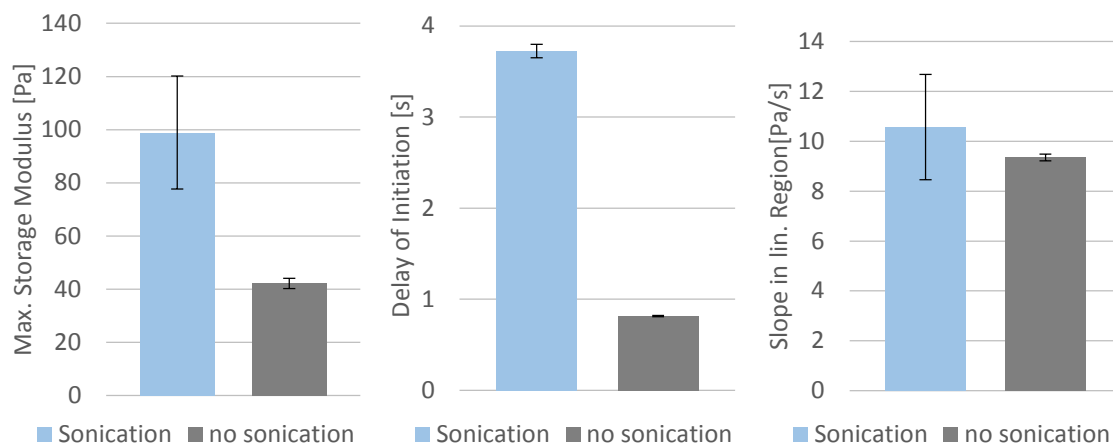


Figure 111: Maximum storage modulus, delay of initiation and slope in the linear region of the storage modulus of HAVE 100 kDa, DS = 9%, macromer content = 2 wt% and 80 mol% thiol-ene ratio ETTMP

On the one side the drastic increase of G' after sonication can be seen but on the other side the deviation of the measurements also increased when sonication is applied to the precursor solution. Interestingly the delay of initiation dramatically increased for the formulations with sonication influence.

For future experiments, sonication can be a tool to be considered for the proper homogenization of the precursor solutions and to adapt the system to desired hydrogel mechanics. On the one hand, physical interactions of macromers can make hydrogel precursor solutions difficult to handle, but on the other hand physical gels can provide already a certain stability of a hydrogel network as described in Section 3.1, which can be advantageous for certain applications.

Mit ETTMP 1 wt%

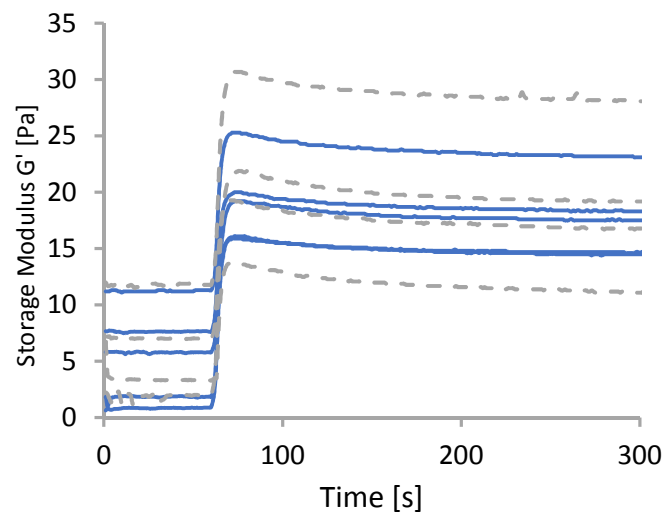


Figure 112: Storage modulus curves of HAVE formulation (77kDa, DS=13%, 1 wt% macromer content, 80 mol% thiol-ene ratio ETTMP) measured directly after mixing (—) and after storage for 48h (---)

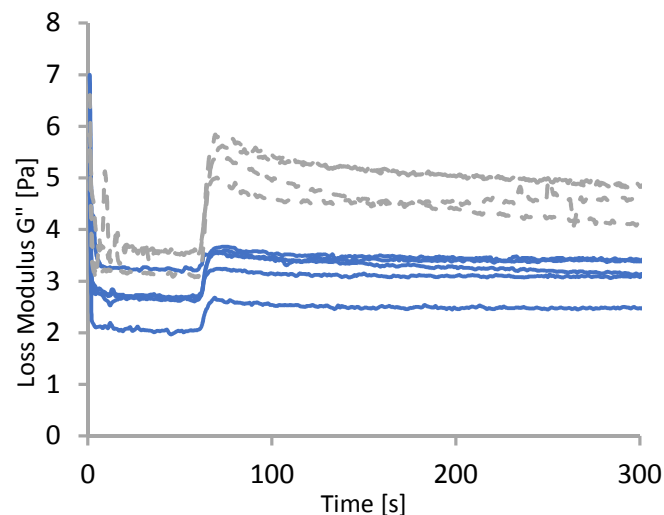


Figure 113: Loss Modulus of HAVE formulation (77kDa, DS=13%, 1 wt% macromer content, 80 mol% thiol-ene ratio ETTMP) measured directly after mixing (—) and after storage for 48h (---)

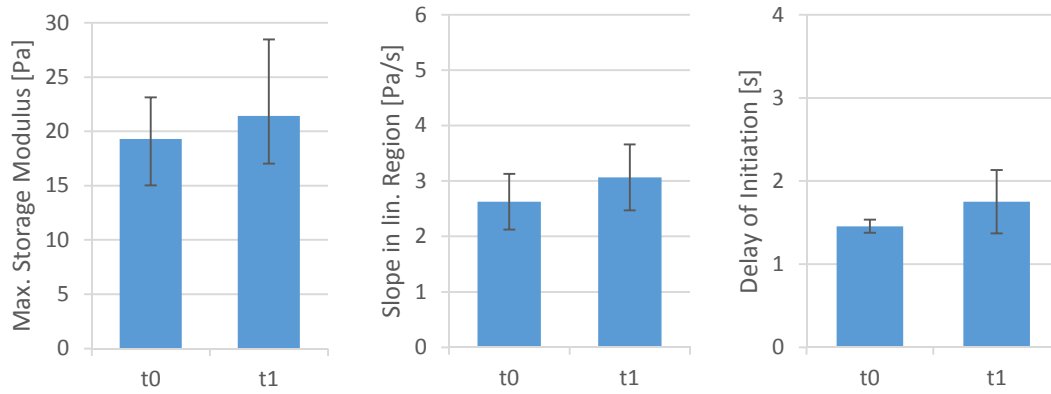


Figure 114: Maximum storage modulus, delay of initiation and slope in the linear region of the storage modulus of HAVE (77kDa, DS=13%, 1 wt% macromer content, 80 mol% thiol-ene ratio ETTMP) measured directly after mixing (t0) and after storage for 48h (t1)

The Effect of Frequency and Strain

Formulations were measured 3 times with 10Hz and 10% strain. (Left-over) formulation was tested with reduced frequency and strain

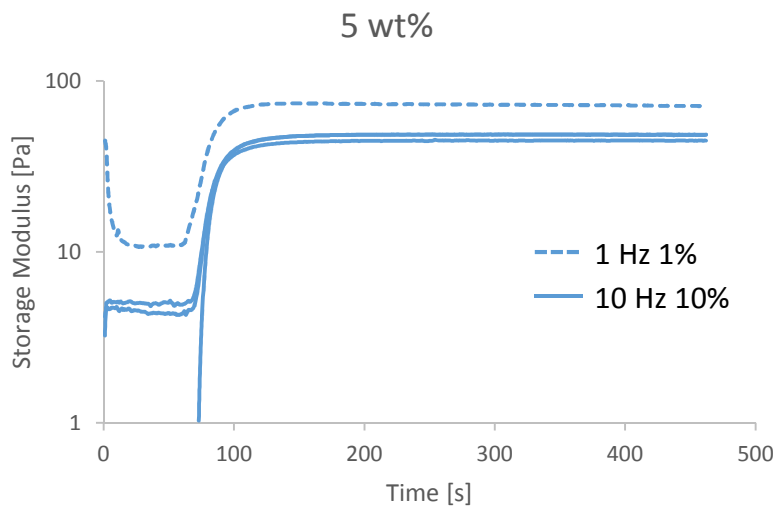


Figure 115: HAVE 22 kDa, DS = 95%, macromer content = 5 wt%, 80 mol% thiol-ene ratio DTT

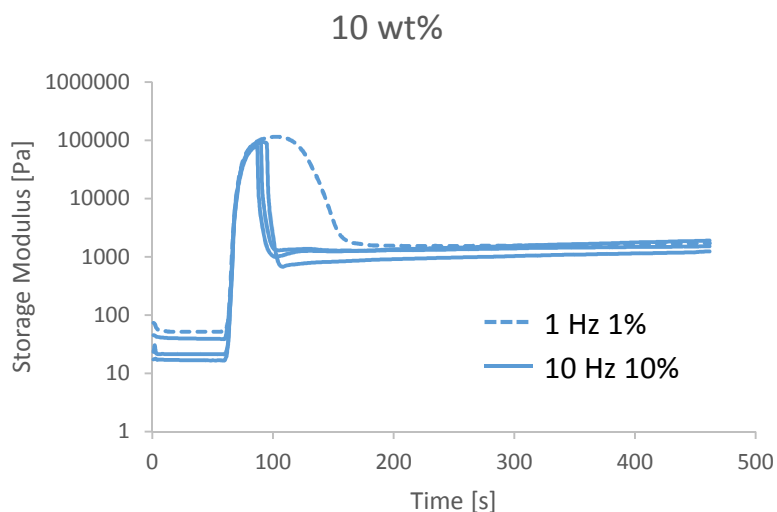


Figure 116: HAVE 22 kDa, DS = 95%, macromer content = 10 wt%, 80 mol% thiol-ene ratio DTT

From rising the macromer content from 5 to 10 wt% exfoliation effect can be observed in Figure 116. For measurements with 1 Hz and 1% strain exfoliation is happening slower.

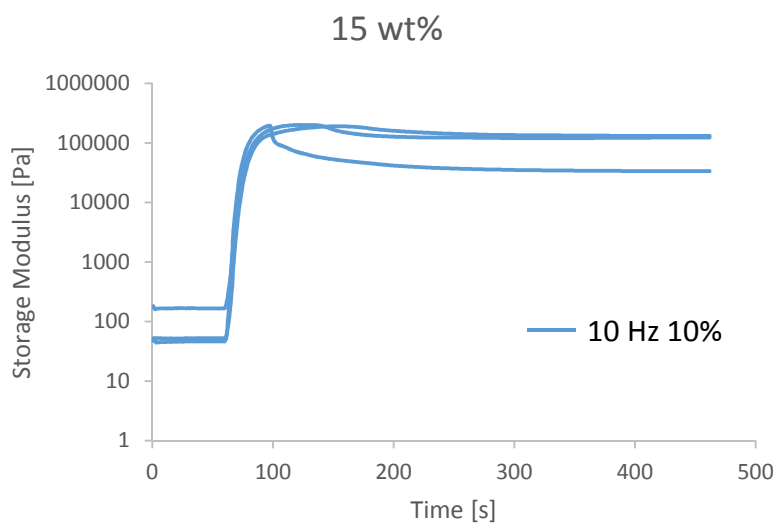


Figure 117: HAVE 22 kDa, DS = 95%, macromer content = 15wt%, 80 mol% thiol-ene ratio DTT

For 10 and 15 wt% exfoliation effect occurs. For 15 wt% there was not enough formulation left to measure formulation with 1 Hz and 1% strain due to too high viscosity and loss of material via pipet tips.

The more the macromer content is increased, the more a physical gel is formed

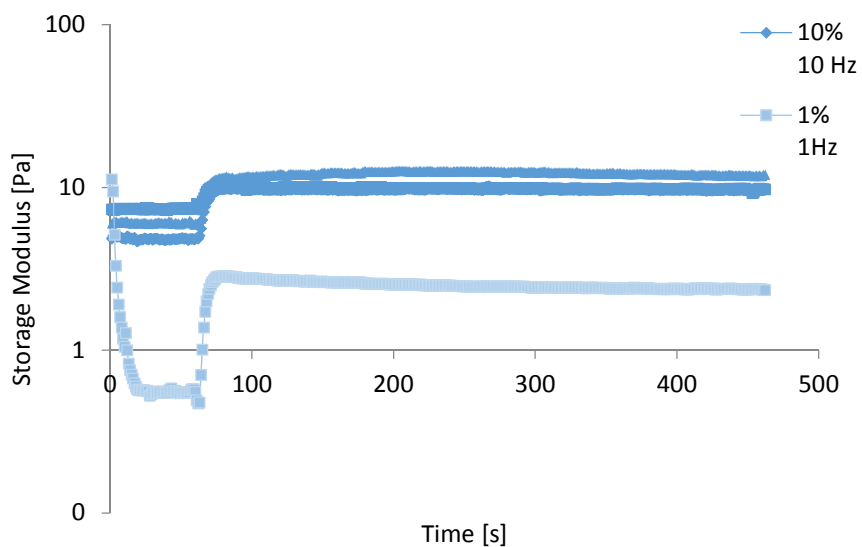


Figure 118: HAVE 100 kDa, DS = 9%, macromer content = 1 wt%, 80 mol% thiol-ene ratio ETTMP

Possibly 10Hz is a frequency which is too high for fragile hydrogels. For future experiments 1Hz may lead to better results

3.5 Collagen as additional Matrix Compound

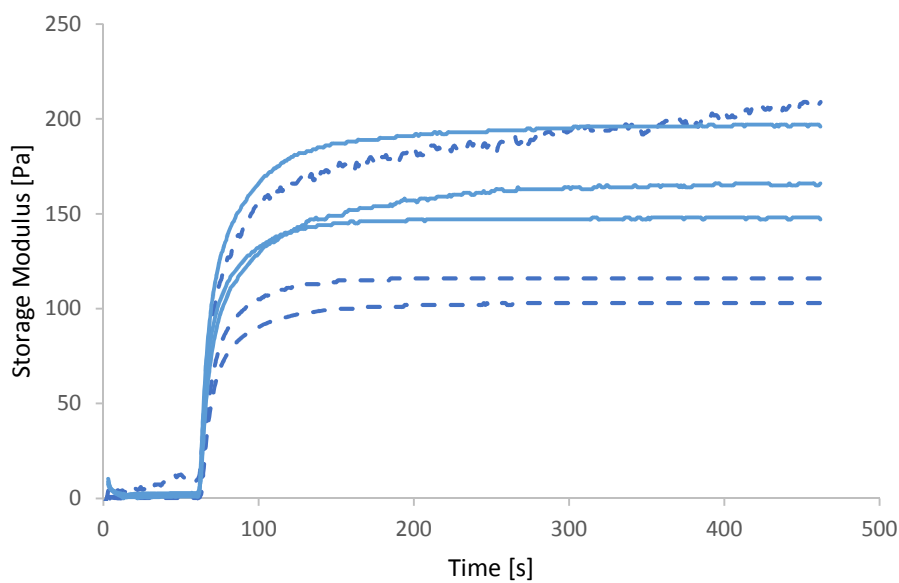


Figure 119: Photopolymerization of HAVE (22kDa, DS = 95%) without the presence of collagen at 25 °C (dotted line) and 5 °C (continuous line) with 80 mol% thiol-ene ratio ETTMP

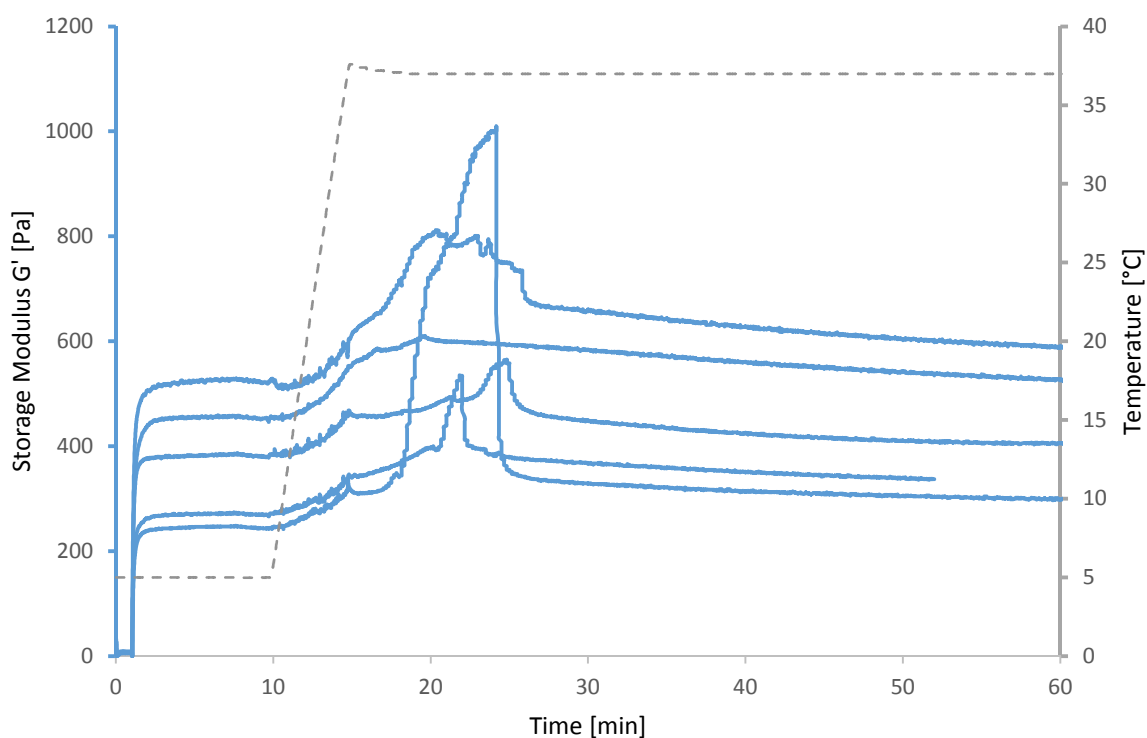


Figure 120: Increase of storage modulus due to collagen gelation after photopolymerization of HAVE (22kDa DS = 95%) with 80 mol% thiol-ene ratio ETTMP

References

- (1) Pawlicki, M., Collins, H. A., Denning, R. G. and Anderson, H. L., *Zweiphotonenabsorption und das Design von Zweiphotonenfarbstoffen*. *Angewandte Chemie*, 2009. **121**(18): p. 3292-3316.
- (2) Vacanti, J. P. and Langer, R., *Tissue engineering: the design and fabrication of living replacement devices for surgical reconstruction and transplantation*. *The Lancet*, 1993. **354**: p. S32-S34.
- (3) Gibas, I. and Janik, H., *Review: Synthetic Polymer Hydrogels for biomedical Applications*. *Chemistry and Chemical Technology* 2010. **4**(4): p. 297-304.
- (4) Viegas, T. X., Bentley, M. D., Harris, J. M., Fang, Z., Yoon, K., Dizman, B., Weimer, R., Mero, A., Pasut, G. and Veronese, F. M., *Polyoxazoline: Chemistry, Properties, and Applications in Drug Delivery*. *Bioconjugate Chemistry*, 2011. **22**(5): p. 976-986.
- (5) Lee, K. Y. and Mooney, D. J., *Hydrogels for tissue engineering*. *Chem Rev*, 2001. **101**(7): p. 1869-79.
- (6) Theocharis, A. D., Skandalis, S. S., Gialeli, C. and Karamanos, N. K., *Extracellular matrix structure*. *Advanced Drug Delivery Reviews*, 2016. **97**: p. 4-27.
- (7) Downloaded on 24.1.2017. Available from: <http://www.swiss-alp-health.ch/science?lang=de>.
- (8) Hutmacher, D. W., *Scaffold design and fabrication technologies for engineering tissues — state of the art and future perspectives*. *Journal of Biomaterials Science, Polymer Edition*, 2001. **12**(1): p. 107-124.
- (9) Hoyle, C. E., Lowe, A. B. and Bowman, C. N., *Thiol-click chemistry: a multifaceted toolbox for small molecule and polymer synthesis*. *Chem. Soc. Rev.*, 2010. **39**(4): p. 1355-1387.
- (10) Tibbitt, M. W. and Anseth, K. S., *Hydrogels as extracellular matrix mimics for 3D cell culture*. *Biotechnology and Bioengineering*, 2009. **103**(4): p. 655-663.
- (11) Van Vlierberghe, S., Dubruel, P. and Schacht, E., *Biopolymer-Based Hydrogels As Scaffolds for Tissue Engineering Applications: A Review*. *Biomacromolecules*, 2011. **12**(5): p. 1387-1408.
- (12) Wichterle, O. and Lim, D., *Hydrophilic Gels for Biological Use*. *Nature*, 1960. **185**(4706): p. 117-118.
- (13) Lanza, R., Langer, R. and Vacanti, J. P., *Principles of tissue engineering*. 2011: Academic press.
- (14) Caliani, S. R. and Burdick, J. A., *A practical guide to hydrogels for cell culture*. *Nat Meth*, 2016. **13**(5): p. 405-414.
- (15) El-Sherbiny, I. M. and Yacoub, M. H., *Hydrogel scaffolds for tissue engineering: Progress and challenges*. *Global Cardiology Science & Practice*, 2013. **2013**(3): p. 316-342.
- (16) Alberts, B., Johnson, A., Lewis, J., Raff, M., Roberts, K. and Walter, P., *The extracellular matrix of animals*. 2002.
- (17) Frantz, C., Stewart, K. M. and Weaver, V. M., *The extracellular matrix at a glance*. *Journal of Cell Science*, 2010. **123**(24): p. 4195-4200.
- (18) Lapčák, L., Lapčák, L., De Smedt, S., Demeester, J. and Chabreček, P., *Hyaluronan: Preparation, Structure, Properties, and Applications*. *Chemical Reviews*, 1998. **98**(8): p. 2663-2684.
- (19) Almond, A., DeAngelis, P. L. and Blundell, C. D., *Hyaluronan: The Local Solution Conformation Determined by NMR and Computer Modeling is Close to*

- a Contracted Left-handed 4-Fold Helix*. Journal of Molecular Biology, 2006. **358**(5): p. 1256-1269.
- (20) Zhang, Z., Ortiz, O., Goyal, R. and Kohn, J., *Chapter 23 - Biodegradable Polymers A2 - Lanza, Robert*, in *Principles of Tissue Engineering (Fourth Edition)*, Langer, R. and Vacanti, J., Editors. 2014, Academic Press: Boston. p. 441-473.
- (21) Weiss, C. and Balazs, E., *Arthroscopic viscosurgery* Arthroscopy 1987. **3**(2): p. 138.
- (22) Zhang, X., Sun, P., Huangshan, L., Hu, B.-H. and Messersmith, P. B., *Improved method for synthesis of cysteine modified hyaluronic acid for in situ hydrogel formation*. Chemical Communications, 2015. **51**(47): p. 9662-9665.
- (23) Highley, C. B., Prestwich, G. D. and Burdick, J. A., *Recent advances in hyaluronic acid hydrogels for biomedical applications*. Current Opinion in Biotechnology, 2016. **40**: p. 35-40.
- (24) Burdick, J. A. and Prestwich, G. D., *Hyaluronic acid hydrogels for biomedical applications*. Adv Mater, 2011. **23**(12): p. H41-56.
- (25) Mena, F., Mena, A. and Mena, B., *Hyaluronic Acid and Derivatives for Tissue Engineering*. J Biotechnol Biomaterial, 2011.
- (26) Fisher, J. P., Mikos, A. G., Bronzino, J. D. and Peterson, D. R., *Tissue Engineering: Principles and Practices*. 2012: CRC Press.
- (27) Zhang, Q., Lu, H., Kawazoe, N. and Chen, G., *Pore size effect of collagen scaffolds on cartilage regeneration*. Acta Biomaterialia, 2014. **10**(5): p. 2005-2013.
- (28) Borzacchiello, A., Mayol, L., Schiavinato, A. and Ambrosio, L., *Effect of hyaluronic acid amide derivative on equine synovial fluid viscoelasticity*. Journal of Biomedical Materials Research Part A, 2010. **92A**(3): p. 1162-1170.
- (29) Pitarresi, G., Palumbo, F. S., Albanese, A., Fiorica, C., Picone, P. and Giammona, G., *Self-assembled amphiphilic hyaluronic acid graft copolymers for targeted release of antitumoral drug*. Journal of Drug Targeting, 2010. **18**(4): p. 264-276.
- (30) Norouzi, M., Nazari, B. and Miller, D. W., *Injectable hydrogel-based drug delivery systems for local cancer therapy*. Drug Discovery Today, 2016. **21**(11): p. 1835-1849.
- (31) Overstreet, D. J., Dutta, D., Stabenfeldt, S. E. and Vernon, B. L., *Injectable hydrogels*. Journal of Polymer Science Part B: Polymer Physics, 2012. **50**(13): p. 881-903.
- (32) Ha, D. I., Lee, S. B., Chong, M. S., Lee, Y. M., Kim, S. Y. and Park, Y. H., *Preparation of thermo-responsive and injectable hydrogels based on hyaluronic acid and poly(N-isopropylacrylamide) and their drug release behaviors*. Macromolecular Research, 2006. **14**(1): p. 87-93.
- (33) Sperling, L. H., *Interpenetrating Polymer Networks and Related Materials*. 2012: Springer US.
- (34) Kim, S. J., Lee, C. K., Lee, Y. M., Kim, I. Y. and Kim, S. I., *Electrical/pH-sensitive swelling behavior of polyelectrolyte hydrogels prepared with hyaluronic acid-poly(vinyl alcohol) interpenetrating polymer networks*. Reactive and Functional Polymers, 2003. **55**(3): p. 291-298.
- (35) Pescosolido, L., Schuurman, W., Malda, J., Matricardi, P., Alhaique, F., Coviello, T., van Weeren, P. R., Dhert, W. J. A., Hennink, W. E. and Vermonden, T., *Hyaluronic Acid and Dextran-Based Semi-IPN Hydrogels as Biomaterials for Bioprinting*. Biomacromolecules, 2011. **12**(5): p. 1831-1838.

- (36) Rodell, C. B., MacArthur, J. W., Dorsey, S. M., Wade, R. J., Wang, L. L., Woo, Y. J. and Burdick, J. A., *Shear-Thinning Supramolecular Hydrogels with Secondary Autonomous Covalent Crosslinking to Modulate Viscoelastic Properties In Vivo*. *Advanced Functional Materials*, 2015. **25**(4): p. 636-644.
- (37) Lee, K. Y., Rowley, J. A., Eiselt, P., Moy, E. M., Bouhadir, K. H. and Mooney, D. J., *Controlling Mechanical and Swelling Properties of Alginate Hydrogels Independently by Cross-Linker Type and Cross-Linking Density*. *Macromolecules*, 2000. **33**(11): p. 4291-4294.
- (38) Kuo, J. W., *Practical Aspects of Hyaluronan Based Medical Products*. 2005, CRC Press.
- (39) Schante, C. E., Zuber, G., Herlin, C. and Vandamme, T. F., *Chemical modifications of hyaluronic acid for the synthesis of derivatives for a broad range of biomedical applications*. *Carbohydr. Polym.*, 2011. **85**(3): p. 469-489.
- (40) Matricardi, P., Alhaique, F. and Coviello, T., *Polysaccharide Hydrogels: Characterization and Biomedical Applications*. 2016: CRC Press.
- (41) Bulpitt, P. and Aeschlimann, D., *New strategy for chemical modification of hyaluronic acid: Preparation of functionalized derivatives and their use in the formation of novel biocompatible hydrogels*. *Journal of Biomedical Materials Research*, 1999. **47**(2): p. 152-169.
- (42) Prestwich, G. D., Marecak, D. M., Marecek, J. F., Vercruyse, K. P. and Ziebell, M. R., *Controlled chemical modification of hyaluronic acid: synthesis, applications, and biodegradation of hydrazide derivatives*. *Journal of Controlled Release*, 1998. **53**(1-3): p. 93-103.
- (43) Luo, Y., Kirker, K. R. and Prestwich, G. D., *Cross-linked hyaluronic acid hydrogel films: new biomaterials for drug delivery*. *Journal of Controlled Release*, 2000. **69**(1): p. 169-184.
- (44) Maitra, J. and Shukla, V. K., *Cross-linking in Hydrogels - A Review*. *American Journal of Polymer Science*, 2014. **4**(2): p. 25-31.
- (45) Hennink, W. E. and van Nostrum, C. F., *Novel crosslinking methods to design hydrogels*. *Advanced Drug Delivery Reviews*, 2012. **64**, **Supplement**: p. 223-236.
- (46) Liang, L. and Astruc, D., *The copper(I)-catalyzed alkyne-azide cycloaddition (CuAAC) "click" reaction and its applications. An overview*. *Coordination Chemistry Reviews*, 2011. **255**(23-24): p. 2933-2945.
- (47) Kolb, H. C., Finn, M. G. and Sharpless, K. B., *Click Chemistry: Diverse Chemical Function from a Few Good Reactions*. *Angewandte Chemie International Edition*, 2001. **40**(11): p. 2004-2021.
- (48) Crescenzi, V., Cornelio, L., Di Meo, C., Nardecchia, S. and Lamanna, R., *Novel Hydrogels via Click Chemistry: Synthesis and Potential Biomedical Applications*. *Biomacromolecules*, 2007. **8**(6): p. 1844-1850.
- (49) Michael, A., *Ueber die Einwirkung von Diazobenzolimid auf Acetylendicarbonsäuremethylester*. *Journal für Praktische Chemie*, 1893. **48**(1): p. 94-95.
- (50) Jewett, J. C. and Bertozzi, C. R., *Cu-free click cycloaddition reactions in chemical biology*. *Chemical Society reviews*, 2010. **39**(4): p. 1272-1279.
- (51) Xu, J., Fillion, T. M., Prifti, F. and Song, J., *Cytocompatible Poly(ethylene glycol)-co-polycarbonate Hydrogels Crosslinked by Copper-free, Strain-promoted "Click" Chemistry*. *Chemistry, an Asian journal*, 2011. **6**(10): p. 2730-2737.
- (52) Takahashi, A., Suzuki, Y., Suhara, T., Omichi, K., Shimizu, A., Hasegawa, K., Kokudo, N., Ohta, S. and Ito, T., *In Situ Cross-Linkable Hydrogel of Hyaluronan*

- Produced via Copper-Free Click Chemistry*. *Biomacromolecules*, 2013. **14**(10): p. 3581-3588.
- (53) Nimmo, C. M., Owen, S. C. and Shoichet, M. S., *Diels–Alder Click Cross-Linked Hyaluronic Acid Hydrogels for Tissue Engineering*. *Biomacromolecules*, 2011. **12**(3): p. 824-830.
- (54) Owen, S. C., Fisher, S. A., Tam, R. Y., Nimmo, C. M. and Shoichet, M. S., *Hyaluronic Acid Click Hydrogels Emulate the Extracellular Matrix*. *Langmuir*, 2013. **29**(24): p. 7393-7400.
- (55) Hoyle, C. E. and Bowman, C. N., *Thiol-Ene Click Chemistry*. *Angew. Chem., Int. Ed.*, 2010. **49**(9): p. 1540-1573.
- (56) Kharkar, P. M., Rehmann, M. S., Skeens, K. M., Maverakis, E. and Kloxin, A. M., *Thiol–ene Click Hydrogels for Therapeutic Delivery*. *ACS Biomaterials Science & Engineering*, 2016. **2**(2): p. 165-179.
- (57) Mather, B. D., Viswanathan, K., Miller, K. M. and Long, T. E., *Michael addition reactions in macromolecular design for emerging technologies*. *Progress in Polymer Science*, 2006. **31**(5): p. 487-531.
- (58) Cai, S., Liu, Y., Zheng Shu, X. and Prestwich, G. D., *Injectable glycosaminoglycan hydrogels for controlled release of human basic fibroblast growth factor*. *Biomaterials*, 2005. **26**(30): p. 6054-6067.
- (59) Zheng Shu, X., Liu, Y., Palumbo, F. S., Luo, Y. and Prestwich, G. D., *In situ crosslinkable hyaluronan hydrogels for tissue engineering*. *Biomaterials*, 2004. **25**(7–8): p. 1339-1348.
- (60) Mautner, A., Qin, X., Wutzel, H., Ligon, S. C., Kapeller, B., Moser, D., Russmueller, G., Stampfl, J. and Liska, R., *Thiol-ene photopolymerization for efficient curing of vinyl esters*. *J. Polym. Sci., Part A: Polym. Chem.*, 2013. **51**(1): p. 203-212, S203/1-S203/6.
- (61) Decker, C., *New developments in UV radiation curing of protective coatings*. *Surface Coatings International Part B: Coatings Transactions*, 2005. **88**(1): p. 9-17.
- (62) Leach, J. B., Bivens, K. A., Patrick, C. W., Jr. and Schmidt, C. E., *Photocrosslinked hyaluronic acid hydrogels: Natural, biodegradable tissue engineering scaffolds*. *Biotechnol. Bioeng.*, 2003. **82**(5): p. 578-589.
- (63) Nguyen, K. T. and West, J. L., *Photopolymerizable hydrogels for tissue engineering applications*. *Biomaterials*, 2002. **23**(22): p. 4307-4314.
- (64) Fouassier, J.-P., *Photoinitiation, photopolymerization, and photocuring: fundamentals and applications*. 1995: Munich: Carl Hanser Verlag.
- (65) Husar, B., Hatzenbichler, M., Mironov, V., Liska, R., Stampfl, J. and Ovsianikov, A., *Photopolymerization-based additive manufacturing for the development of 3D porous scaffolds*. Elsevier Ltd., 2014: p. 149-201.
- (66) Dietliker, K., *Photoinitiators for Free Radical and Cationic Polymerisation*. Vol. 3. 1991, SITA Technology Ltd. London UK.
- (67) Ullrich, G., Burtscher, P., Salz, U., Moszner, N. and Liska, R., *Phenylglycine derivatives as coinitiators for the radical photopolymerization of acidic aqueous formulations*. *Journal of Polymer Science Part A: Polymer Chemistry*, 2006. **44**(1): p. 115-125.
- (68) Liu, M., Li, M.-D., Xue, J. and Phillips, D. L., *Time-Resolved Spectroscopic and Density Functional Theory Study of the Photochemistry of Irgacure-2959 in an Aqueous Solution*. *The Journal of Physical Chemistry A*, 2014. **118**(38): p. 8701-8707.
- (69) Majima, T., Schnabel, W. and Weber, W., *Phenyl-2,4,6-trimethylbenzoylphosphinates as water-soluble photoinitiators. Generation and*

- reactivity of O=P(C6H5)(O-) radical anions.* Die Makromolekulare Chemie, 1991. **192**(10): p. 2307-2315.
- (70) Benedikt, S., Wang, J., Markovic, M., Moszner, N., Dietliker, K., Ovsianikov, A., Grützmacher, H. and Liska, R., *Highly efficient water-soluble visible light photoinitiators.* Journal of Polymer Science Part A: Polymer Chemistry, 2016. **54**(4): p. 473-479.
- (71) Fairbanks, B. D., Schwartz, M. P., Bowman, C. N. and Anseth, K. S., *Photoinitiated polymerization of PEG-diacrylate with lithium phenyl-2,4,6-trimethylbenzoylphosphinate: polymerization rate and cytocompatibility.* Biomaterials, 2009. **30**(35): p. 6702-6707.
- (72) Williams, C. G., Malik, A. N., Kim, T. K., Manson, P. N. and Elisseeff, J. H., *Variable cytocompatibility of six cell lines with photoinitiators used for polymerizing hydrogels and cell encapsulation.* Biomaterials, 2005. **26**(11): p. 1211-1218.
- (73) Bae, M. S., Yang, D. H., Lee, J. B., Heo, D. N., Kwon, Y.-D., Youn, I. C., Choi, K., Hong, J. H., Kim, G. T., Choi, Y. S., Hwang, E. H. and Kwon, I. K., *Photo-cured hyaluronic acid-based hydrogels containing simvastatin as a bone tissue regeneration scaffold.* Biomaterials, 2011. **32**(32): p. 8161-8171.
- (74) Seidi, A., Ramalingam, M., Elloumi-Hannachi, I., Ostrovidov, S. and Khademhosseini, A., *Gradient biomaterials for soft-to-hard interface tissue engineering.* Acta Biomaterialia, 2011. **7**(4): p. 1441-1451.
- (75) Bencherif, S. A., Srinivasan, A., Horkay, F., Hollinger, J. O., Matyjaszewski, K. and Washburn, N. R., *Influence of the degree of methacrylation on hyaluronic acid hydrogels properties.* Biomaterials, 2008. **29**(12): p. 1739-1749.
- (76) Kade, M. J., Burke, D. J. and Hawker, C. J., *The power of thiol-ene chemistry.* Journal of Polymer Science Part A: Polymer Chemistry, 2010. **48**(4): p. 743-750.
- (77) Marklein, R. A., Soranno, D. E. and Burdick, J. A., *Magnitude and presentation of mechanical signals influence adult stem cell behavior in 3-dimensional macroporous hydrogels.* Soft Matter, 2012. **8**(31): p. 8113-8120.
- (78) Park, Y. D., Tirelli, N. and Hubbell, J. A., *Photopolymerized hyaluronic acid-based hydrogels and interpenetrating networks.* Biomaterials, 2003. **24**(6): p. 893-900.
- (79) Gramlich, W. M., Kim, I. L. and Burdick, J. A., *Synthesis and orthogonal photopatterning of hyaluronic acid hydrogels with thiol-norbornene chemistry.* Biomaterials, 2013. **34**(38): p. 9803-9811.
- (80) Husar, B., Heller, C., Schwentenwein, M., Mautner, A., Varga, F., Koch, T., Stampfl, J. and Liska, R., *Biomaterials based on low cytotoxic vinyl esters for bone replacement application.* J. Polym. Sci., Part A: Polym. Chem., 2011. **49**(23): p. 4927-4934.
- (81) Heller, C., Schwentenwein, M., Russmueller, G., Varga, F., Stampfl, J. and Liska, R., *Vinyl esters: Low cytotoxicity monomers for the fabrication of biocompatible 3D scaffolds by lithography based additive manufacturing.* Journal of Polymer Science Part A: Polymer Chemistry, 2009. **47**(24): p. 6941-6954.
- (82) Guvendiren, M., Molde, J., Soares, R. M. D. and Kohn, J., *Designing Biomaterials for 3D Printing.* ACS Biomaterials Science & Engineering, 2016.
- (83) Landers, R., Pfister, A., Hübner, U., John, H., Schmelzeisen, R. and Mülhaupt, R., *Fabrication of soft tissue engineering scaffolds by means of rapid prototyping techniques.* Journal of Materials Science, 2002. **37**(15): p. 3107-3116.

- (84) Hutmacher, D. W., *Scaffolds in tissue engineering bone and cartilage*. Biomaterials, 2000. **21**(24): p. 2529-2543.
- (85) Vandenbroucke, B. and Kruth, J. P., *Selective laser melting of biocompatible metals for rapid manufacturing of medical parts*. Rapid Prototyping Journal, 2007. **13**(4): p. 196-203.
- (86) Tirella, A., Maria, C. D., Criscenti, G., Vozzi, G. and Ahluwalia, A., *The PAM2 system: a multilevel approach for fabrication of complex three-dimensional microstructures*. Rapid Prototyping Journal, 2012. **18**(4): p. 299-307.
- (87) Hutmacher, D. W., Sittinger, M. and Risbud, M. V., *Scaffold-based tissue engineering: rationale for computer-aided design and solid free-form fabrication systems*. Trends in Biotechnology, 2004. **22**(7): p. 354-362.
- (88) Domingos, M., Chiellini, F., Gloria, A., Ambrosio, L., Bartolo, P. and Chiellini, E., *Effect of process parameters on the morphological and mechanical properties of 3D Bioextruded poly(ϵ -caprolactone) scaffolds*. Rapid Prototyping Journal, 2012. **18**(1): p. 56-67.
- (89) Stampfl, J., Baudis, S., Heller, C., Liska, R., Neumeister, A., Kling, R., Ostendorf, A. and Spitzbart, M., *Photopolymers with tunable mechanical properties processed by laser-based high-resolution stereolithography*. Journal of Micromechanics and Microengineering, 2008. **18**(12): p. 125014.
- (90) Hull, C. W., Cohen, A. L., Spence, S. L. and Lewis, C. W., *Apparatus and related method for forming a substantially flat stereolithographic working surface*. 1995, Google Patents.
- (91) O'Brien, A. K., Cramer, N. B. and Bowman, C. N., *Oxygen inhibition in thiol-acrylate photopolymerizations*. Journal of Polymer Science Part A: Polymer Chemistry, 2006. **44**(6): p. 2007-2014.
- (92) Ovsianikov, A., Mironov, V., Stampfl, J. and Liska, R., *Engineering 3D cell-culture matrices: multiphoton processing technologies for biological and tissue engineering applications*. Expert Rev. Med. Devices, 2012. **9**(6): p. 613-633.
- (93) Denk, W. and Svoboda, K., *Photon upmanship: why multiphoton imaging is more than a gimmick*. Neuron, 1997. **18**(3): p. 351-7.
- (94) Lu, Y., Hasegawa, F., Goto, T., Ohkuma, S., Fukuhara, S., Kawazu, Y., Totani, K., Yamashita, T. and Watanabe, T., *Highly sensitive measurement in two-photon absorption cross section and investigation of the mechanism of two-photon-induced polymerization*. Journal of Luminescence, 2004. **110**(1-2): p. 1-10.
- (95) Li, Z., Torgersen, J., Ajami, A., Muhleder, S., Qin, X., Husinsky, W., Holnthoner, W., Ovsianikov, A., Stampfl, J. and Liska, R., *Initiation efficiency and cytotoxicity of novel water-soluble two-photon photoinitiators for direct 3D microfabrication of hydrogels*. RSC Advances, 2013. **3**(36): p. 15939-15946.
- (96) Maruo, S., Nakamura, O. and Kawata, S., *Three-dimensional microfabrication with two-photon-absorbed photopolymerization*. Optics Letters, 1997. **22**(2): p. 132-134.
- (97) Melissinaki, V., Gill, A. A., Ortega, I., Vamvakaki, M., Ranella, A., Haycock, J. W., Fotakis, C., Farsari, M. and Claeysens, F., *Direct laser writing of 3D scaffolds for neural tissue engineering applications*. Biofabrication, 2011. **3**(4): p. 045005.
- (98) Torgersen, J., Ovsianikov, A., Mironov, V., Pucher, N., Qin, X., Li, Z., Cicha, K., Machacek, T., Liska, R., Jantsch, V. and Stampfl, J., *Photo-sensitive hydrogels for three-dimensional laser microfabrication in the presence of whole organisms*. Journal of Biomedical Optics, 2012. **17**(10): p. 105008.

- (99) Kufelt, O., El-Tamer, A., Sehring, C., Schlie-Wolter, S. and Chichkov, B. N., *Hyaluronic Acid Based Materials for Scaffolding via Two-Photon Polymerization*. *Biomacromolecules*, 2014. **15**(2): p. 650-659.
- (100) Qin, X., *3D Construction of Artificial Extracellular Matrix Hydrogels by Two-Photon-Induced Polymerization* 2014: Dissertation, Vienna University of Technology.
- (101) Shu, X. Z., Liu, Y., Luo, Y., Roberts, M. C. and Prestwich, G. D., *Disulfide Cross-Linked Hyaluronan Hydrogels*. *Biomacromolecules*, 2002. **3**(6): p. 1304-1311.
- (102) Uyama, H., Yaguchi, S. and Kobayashi, S., *Lipase-catalyzed polycondensation of dicarboxylic acid-divinyl esters and glycols to aliphatic polyesters*. *Journal of Polymer Science Part A: Polymer Chemistry*, 1999. **37**(15): p. 2737-2745.
- (103) Wang, N., Chen, Z. C., Lu, D. S. and Lin, X. F., *Controllable selective synthesis of a polymerizable prodrug of cytarabine by enzymatic and chemical methods*. *Bioorganic & Medicinal Chemistry Letters*, 2005. **15**(18): p. 4064-4067.
- (104) Dai, S., Xue, L., Zinn, M. and Li, Z., *Enzyme-Catalyzed Polycondensation of Polyester Macrodiols with Divinyl Adipate: A Green Method for the Preparation of Thermoplastic Block Copolyesters*. *Biomacromolecules*, 2009. **10**(12): p. 3176-3181.
- (105) Tomášiková, Z., *Hydrogels for Tissue Engineering*. 2015: Master Thesis, Vienna University of Technology.
- (106) Xiao-Hua Qin, P. G., Marica Markovic, Birgit Plochberger, and Enrico Klotzsch, J. S., Aleksandr Ovsianikov and Robert Liska, *Enzymatic synthesis of hyaluronic acid vinyl esters for two-photon microfabrication of biocompatible and biodegradable hydrogel constructs*. 2014.
- (107) Marklein, R. A. and Burdick, J. A., *Spatially controlled hydrogel mechanics to modulate stem cell interactions*. *Soft Matter*, 2010. **6**(1): p. 136-143.
- (108) Voelcker, V., Gebhardt, C., Averbek, M., Saalbach, A., Wolf, V., Weih, F., Sleeman, J., Anderegg, U. and Simon, J., *Hyaluronan fragments induce cytokine and metalloprotease upregulation in human melanoma cells in part by signalling via TLR4*. *Experimental Dermatology*, 2008. **17**(2): p. 100-107.
- (109) Fraser, J. R. E., Laurent, T. C. and Laurent, U. B. G., *Hyaluronan: its nature, distribution, functions and turnover*. *Journal of Internal Medicine*, 1997. **242**(1): p. 27-33.
- (110) D. Jiang, J. L., and P. W. Noble, *Hyaluronan as an immune regulator in human diseases*. *Physiological Reviews*, 2011. **vol. 91**(no. 1): p. pp. 221–264.
- (111) Day, A. J. and Sheehan, J. K., *Hyaluronan: polysaccharide chaos to protein organisation*. *Current Opinion in Structural Biology*, 2001. **11**(5): p. 617-622.
- (112) Midwood, K., Sacre, S., Piccinini, A. M., Inglis, J., Trebault, A., Chan, E., Drexler, S., Sofat, N., Kashiwagi, M., Orend, G., Brennan, F. and Foxwell, B., *Tenascin-C is an endogenous activator of Toll-like receptor 4 that is essential for maintaining inflammation in arthritic joint disease*. *Nat Med*, 2009. **15**(7): p. 774-780.
- (113) Taylor, K. R., Yamasaki, K., Radek, K. A., Nardo, A. D., Goodarzi, H., Golenbock, D., Beutler, B. and Gallo, R. L., *Recognition of Hyaluronan Released in Sterile Injury Involves a Unique Receptor Complex Dependent on Toll-like Receptor 4, CD44, and MD-2*. *Journal of Biological Chemistry*, 2007. **282**(25): p. 18265-18275.
- (114) Sze, J. H., Brownlie, J. C. and Love, C. A., *Biotechnological production of hyaluronic acid: a mini review*. *3 Biotech*, 2016. **6**(1): p. 67.
- (115) Bothner, H., Waaler, T. and Wik, O., *Limiting viscosity number and weight average molecular weight of hyaluronate samples produced by heat*

- degradation*. International Journal of Biological Macromolecules, 1988. **10**(5): p. 287-291.
- (116) Reháková, M., Bakoš, D., Soldán, M. and Vizárová, K., *Depolymerization reactions of hyaluronic acid in solution*. International Journal of Biological Macromolecules, 1994. **16**(3): p. 121-124.
- (117) Lauwers, A. and Scharpe, S., *Pharmaceutical enzymes*. 1997: Marcel Dekker.
- (118) Scott, J. E., Cummings, C., Greiling, H., Stuhlsatz, H. W., Gregory, J. D. and Damle, S. P., *Examination of corneal proteoglycans and glycosaminoglycans by rotary shadowing and electron microscopy*. International Journal of Biological Macromolecules, 1990. **12**(3): p. 180-184.
- (119) Ghosh, S., Kopal, I., Zanette, D. and Reed, W. F., *Conformational contraction and hydrolysis of hyaluronate in sodium hydroxide solutions*. Macromolecules, 1993. **26**(17): p. 4685-4693.
- (120) Stern, R., Kogan, G., Jedrzejewski, M. J. and Šoltés, L., *The many ways to cleave hyaluronan*. Biotechnology Advances, 2007. **25**(6): p. 537-557.
- (121) Kakizaki, I., Ibori, N., Kojima, K., Yamaguchi, M. and Endo, M., *Mechanism for the hydrolysis of hyaluronan oligosaccharides by bovine testicular hyaluronidase*. FEBS Journal, 2010. **277**(7): p. 1776-1786.
- (122) Gatej, I., Popa, M. and Rinaudo, M., *Role of the pH on Hyaluronan Behavior in Aqueous Solution*. Biomacromolecules, 2005. **6**(1): p. 61-67.
- (123) Khetan, S., Katz, J. S. and Burdick, J. A., *Sequential crosslinking to control cellular spreading in 3-dimensional hydrogels*. Soft Matter, 2009. **5**(8): p. 1601-1606.
- (124) Kirk, O. and Christensen, M. W., *Lipases from Candida antarctica: Unique Biocatalysts from a Unique Origin*. Organic Process Research & Development, 2002. **6**(4): p. 446-451.
- (125) Maleki, A., Kjøniksen, A. L. and Nyström, B. *Effect of pH on the behavior of hyaluronic acid in dilute and semidilute aqueous solutions*. in *Macromolecular symposia*. 2008: Wiley Online Library.
- (126) Winter, H. H., *Can the gel point of a cross-linking polymer be detected by the G' – G'' crossover?* Polymer Engineering & Science, 1987. **27**(22): p. 1698-1702.
- (127) Shah, R., Saha, N., Kitano, T. and Saha, P., *Influence of strain on dynamic viscoelastic properties of swelled (H₂O) and biomineralized (CaCO₃) PVP–CMC hydrogels*. Appl Rheol, 2015. **25**: p. 33979.
- (128) Cowman, M. K., Spagnoli, C., Kudasheva, D., Li, M., Dyal, A., Kanai, S. and Balazs, E. A., *Extended, Relaxed, and Condensed Conformations of Hyaluronan Observed by Atomic Force Microscopy*. Biophysical Journal, 2005. **88**(1): p. 590-602.
- (129) Gloria, A., Borzacchiello, A., Causa, F. and Ambrosio, L., *Rheological Characterization of Hyaluronic Acid Derivatives as Injectable Materials Toward Nucleus Pulposus Regeneration*. Journal of Biomaterials Applications, 2012. **26**(6): p. 745-759.
- (130) Collins, M. N. and Birkinshaw, C., *Hyaluronic acid based scaffolds for tissue engineering—A review*. Carbohydrate Polymers, 2013. **92**(2): p. 1262-1279.
- (131) Zhang, Y., Heher, P., Hilborn, J., Redl, H. and Ossipov, D. A., *Hyaluronic acid-fibrin interpenetrating double network hydrogel prepared in situ by orthogonal disulfide cross-linking reaction for biomedical applications*. Acta Biomaterialia, 2016.
- (132) Guo, Y., Yuan, T., Xiao, Z., Tang, P., Xiao, Y., Fan, Y. and Zhang, X., *Hydrogels of collagen/chondroitin sulfate/hyaluronan interpenetrating polymer network for*

- cartilage tissue engineering*. Journal of Materials Science: Materials in Medicine, 2012. **23**(9): p. 2267-2279.
- (133) Carey, S. P., Kraning-Rush, C. M., Williams, R. M. and Reinhart-King, C. A., *Biophysical control of invasive tumor cell behavior by extracellular matrix microarchitecture*. Biomaterials, 2012. **33**(16): p. 4157-4165.
- (134) Lee, F. and Kurisawa, M., *Formation and stability of interpenetrating polymer network hydrogels consisting of fibrin and hyaluronic acid for tissue engineering*. Acta Biomaterialia, 2013. **9**(2): p. 5143-5152.
- (135) Chen, S., Zhang, Q., Kawazoe, N. and Chen, G., *Effect of high molecular weight hyaluronic acid on chondrocytes cultured in collagen/hyaluronic acid porous scaffolds*. RSC Adv., 2015(5): p. 94405-94410.
- (136) Brigham, M. D., Bick, A., Lo, E., Bendali, A., Burdick, J. A. and Khademhosseini, A., *Mechanically Robust and Bioadhesive Collagen and Photocrosslinkable Hyaluronic Acid Semi-Interpenetrating Networks*. Tissue Engineering. Part A, 2009. **15**(7): p. 1645-1653.
- (137) Connizzo, B. K., Yannascoli, S. M. and Soslowsky, L. J., *Structure–function relationships of postnatal tendon development: A parallel to healing*. Matrix Biology, 2013. **32**(2): p. 106-116.
- (138) Lee, C. H., Singla, A. and Lee, Y., *Biomedical applications of collagen*. International Journal of Pharmaceutics, 2001. **221**(1–2): p. 1-22.
- (139) Bellis, S. L., *Advantages of RGD peptides for directing cell association with biomaterials*. Biomaterials, 2011. **32**(18): p. 4205-4210.
- (140) Drury, J. L. and Mooney, D. J., *Hydrogels for tissue engineering: scaffold design variables and applications*. Biomaterials, 2003. **24**(24): p. 4337-4351.
- (141) Ovsianikov, A. and Chichkov, B. N., *Three-Dimensional Microfabrication by Two-Photon Polymerization Technique*, in *Computer-Aided Tissue Engineering*, Liebschner, A.K.M., Editor. 2012, Humana Press: Totowa, NJ. p. 311-325.
- (142) Torgersen, J., Dissertation, Technische Universität Wien 2013
- (143) Qin, X., Torgersen, J., Robert, S., Mühleder, S., Niklas, P., Ligon, S. C., Holthöner, W., Redl, H., Ovsianikov, A., Stampf, J. and Liska, R., *Three-dimensional microfabrication of protein hydrogels via two-photon-excited thiol-vinyl ester photopolymerization*. Polymer Chemistry, 2013. **51**(22): p. 4799-4810.
- (144) Gruber, P., *Institute of Materials Science and Technology of TU Wien*. 2016. p. Setup for Two Photon Structuring
- (145) Xing, J.-F., Zheng, M.-L. and Duan, X.-M., *Two-photon polymerization microfabrication of hydrogels: an advanced 3D printing technology for tissue engineering and drug delivery*. Chemical Society Reviews, 2015. **44**(15): p. 5031-5039.